Utrecht University

Institute for Theoretical Physics
&
Nikhef Theory Group

Master's Thesis

Complex Mass Scheme and Higgs Phenomenology

Author:
Pedro Cal

Supervisor:
Prof. Dr. Eric Laenen

Second Examiner:
Dr. Enrico Pajer

Thesis submitted for the Master's in Theoretical Physics
Utrecht University

October 9th, 2017

Abstract

This thesis will deal with the phenomenological aspects of calculations involving unstable particles. In the first part we discuss techniques used in the treatment of unstable particles such as the complex mass scheme and the narrow width approximation. We show the complex mass scheme allows us to include finite width effects while providing gauge invariant results, both for a fermionic and a bosonic resonance. In the second part we move towards Higgs phenomenology computations. We present a full calculation of the Higgs production cross section $\sigma(gg \to H)$ through top quark loop as well as for the Higgs decay width $\Gamma(H \to \gamma\gamma)$, which includes fermion and W boson loops. Respectively, these processes correspond to the dominant Higgs production mechanism at hadron colliders and to the decay mode used for the discovery of the Higgs boson at the LHC. Lastly, we write a Monte Carlo C++ event generator which provides the cross section for Higgs production associated with top quark pair $\sigma(qq \to t\bar{t}H)$, and which can be readily modified to output any of the usual desired quantities and plots, as well as unweighted events.

Ackowledgments

First and foremost I would like to thank professor Eric Laenen for his invaluable support in the making of this thesis, as well as for his guidance in my transition to the world of research. I am also very grateful for his assistance and advice regarding my search for a PhD position, which ended up being successful.

I would also like to thank my office mates and everyone at Nikhef's theory group for being as welcoming as they are, in particular to Dr. Andreas Papaefstathiou for his help with kick-starting the Monte Carlo event generator.

For a multitude of reasons that require no explanation I would like to thank the support and friendship of my housemate André Melo. To Tomás Martins, Manuel Santos and Miguel Jaques I would also like to extend a word of appreciation.

Finally, I would like to thank my parents for their unconditional support and enthusiasm, and my nephew for being a stark reminder of what the simple pleasures in life truly are - swimming, doodling and portuguese folk music.

Contents

1 Introduction

Since its development in the 1970s, the Standard Model of particle physics (SM) has become a remarkably successful and well established theory. The SM is summarized in figure 2, where we can see it consists of a bosonic and fermionic sector. The former is related to the three fundamental forces described by the Standard Model: the strong force - mediated by gluons, the weak force- mediated by the W^+, W^- and Z bosons, and the electromagnetic force - mediated by photons. The fermionic sector is composed by six leptons: the electron, muon, tau and respective neutrinos, and corresponding antiparticles and by six quarks:up, down, strange, charm, top and bottom, and their corresponding antiparticles. Finally, a central piece of the puzzle is the only scalar particle of the theory, the Higgs boson.

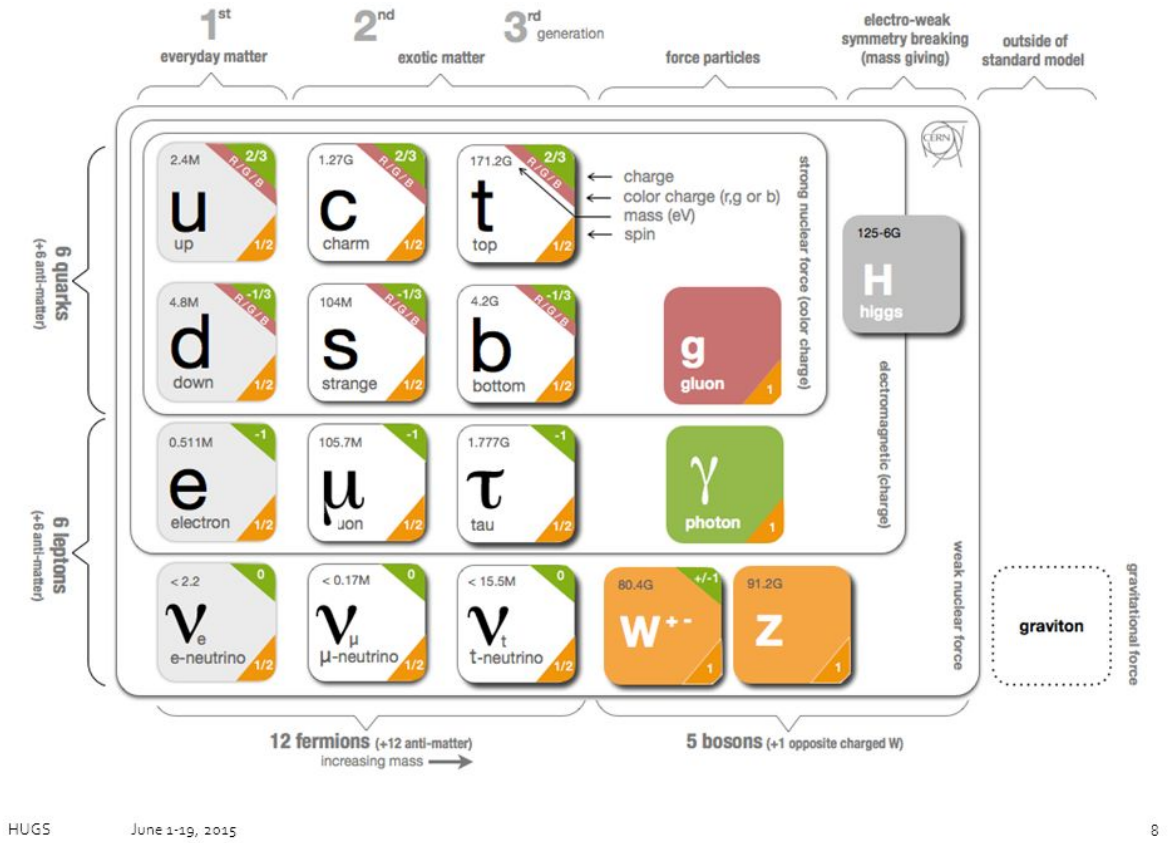

Figure 2: Particles and sectors of the Standard Model

Before stipulating the existence of the Higgs field and the Higgs mechanism, the Standard

Model had no way of explaining how elementary particles obtained their mass. Understanding the process responsible for electroweak symmetry breaking and generating the masses of elementary particles became one of the main goals of the particle physics community since the mechanism was first proposed in the 1960's. The search for the Higgs boson was a long journey that culminated in July of 2012 when the CMS and ATLAS collaborations at CERN announced they had discovered a narrow resonance with mass around 125 GeV, which inferred the existence of a new particle compatible with a Higgs boson. This claim was later updated when in March of 2013 it was reported that the new particle had no spin and even parity, and measurements of the boson's interaction with other particles strongly indicated that the recently discovered particle was in fact the SM Higgs boson.

This thesis will address some of the phenomenological aspects of calculations involving unstable particles. Of the Standard Model particles only the lightest ones are stable since heavier particles can always decay to lighter ones. This means massless particles, like the gluon, photon and neutrinos (which in the SM have zero mass) are necessarily stable, while particles like the top quark, the W and Z bosons, and the Higgs boson are unstable. The first part of the thesis will be concerned with the general properties of unstable particles and what the appropriate techniques are for dealing with them, in particular the application of the *Complex Mass Scheme* (CMS). The second part will approach Higgs phenomenology and the employment of Monte Carlo methods.

In chapter 2 we lay out the foundation of the thesis, introducing the fundamental concepts which play a central role in our discussion of unstable particles, as well as illustrating the importance of the Higgs boson in the Standard Model. Having gone over the necessary relevant concepts, in chapter 3 we focus on mass renormalization and renormalization schemes. We begin by highlighting the differences between stable and unstable particles and describing how one can define their physical mass. These differences turn out to have implications on which renormalization schemes are appropriate when dealing with stable or unstable particles, so we proceed by demonstrating how mass renormalization of a stable particle works in the two most widely used schemes: the On-Shell Scheme and the $\overline{MS}$ scheme.

In chapter 4 we discuss why the resonances of unstable particles pose a problem when dealing with perturbative calculations in one of the before mentioned schemes, since up to a fixed order they do not produce gauge-invariant results. The need for a new renormalization scheme that can effectively deal with unstable particles in the same way the previous schemes took care of stable particles becomes evident. This is where we introduce the complex mass scheme. In this chapter we show how this scheme solves the problem of gauge-invariance both for a bosonic and a fermionic resonance. Lastly, we use the complex mass scheme setting of the event-generator *Madgraph* to study how the CMS affects the cross-section of one of the main Higgs production mechanisms at hadron colliders $pp \to t\bar{t}H$. We take the opportunity to segue into our next topic: Higgs phenomenology.

In chapter 5 we discuss the main Higgs production and decay mechanisms at the LHC. We present a full calculation of the cross section of the dominant production channel - $gg \to H$, also known as *gluon fusion*, as well as for the partial decay width $\Gamma(H \to \gamma\gamma)$, which is precisely the signature that allowed for the discovery of the Higgs boson at the LHC in 2012.

Finally, still in the topic of phenomenology, in chapter 6 we present an introduction to Monte Carlo integration and how it is used in the computation of relevant quantities in collider physics. We use a sequential s-type branching algorithm to write our own MC code for computing the cross-section both for $qq \to t\bar{t}$ and $qq \to t\bar{t}H$, with excellent agreement with *Madgraph* in both cases. In the case of Higgs production associated with a top-quark pair we also adapt our code to produce some of the usual plots relevant when analyzing scattering data.

2 Important Concepts

2.1. Gauge Theories and Gauge Invariance

The most successful theories describing the behavior of elementary particles belong to a particular class known as *gauge theories*. Simply put, a gauge theory is one whose Lagrangian is locally invariant under a certain continuous symmetry group, also known as a Lie group. If the transformations of the symmetry group commute we say the theory is abelian, otherwise it is known as a non-abelian gauge theory. For example, the remarkably successful quantum field theory of electromagnetism - known as Quantum Electrodynamics (QED) - is an abelian gauge theory invariant under transformations of the $U(1)$ local symmetry group. An example of an non-abelian gauge theory is the Standard Model of particle physics, with symmetry $SU(3)_c \times SU(2)_L \times U(1)_Y$, where the $SU(3)_c$ corresponds to the strong sector which gives rise to the eight SM gluons while $SU(2)_L \times U(1)_Y$ is the electroweak sector which after symmetry breaking - a concept we will explain next section - gives rise to the photon and the massive W and Z bosons.

Gauge theories appear to be highly adept at describing three of the four fundamental forces in nature, so it is important to understand exactly what they are and how one can obtain such theories. In this section we will impose a gauge symmetry on a Lagrangian and follow the necessary modifications until one obtains an abelian gauge theory. In particular, we will start with the Dirac Lagrangian, whose equation of motion describes the relativistic behavior of massive spin $\frac{1}{2}$ particles, and obtain the QED Lagrangian. Here we follow chapter 7 of de Wit, Laenen and Smith [1].

To begin, let us then consider the Dirac Lagrangian

$$\mathcal{L}_\psi = i\overline{\psi}\partial\!\!\!/\psi - m\overline{\psi}\psi \ . \tag{2.1}$$

This Lagrangian is invariant under the rigid phase transformations $\psi \to \psi' = e^{iq\xi}\psi$ and $\overline{\psi} \to \overline{\psi}' = e^{-iq\xi}\overline{\psi}$. We note, however, that because of the derivative in the first term it is **not** invariant under *local* phase transformations. To see this let us perform the following transformations to the fields

$$\begin{aligned} \psi &\to \psi' = e^{iq\xi(x)}\psi, \\ \overline{\psi} &\to \overline{\psi}' = e^{-iq\xi(x)}\overline{\psi}, \end{aligned} \tag{2.2}$$

which implies the following transformation of the Lagrangian

$$\begin{aligned}\mathcal{L}_\psi \to \mathcal{L}'_\psi =& i\overline{\psi}e^{-iq\xi(x)}\not{\partial}\left(e^{iq\xi(x)}\psi\right) - m\overline{\psi}\psi \\ =& i\overline{\psi}(iq\not{\partial}\xi\psi + \not{\partial}\psi) - m\overline{\psi}\psi \\ =& i\overline{\psi}\not{\partial}\psi - m\overline{\psi}\psi - q\overline{\psi}\not{\partial}\xi\psi \neq \mathcal{L}_\psi.\end{aligned} \tag{2.3}$$

In doing this calculation we see that the problem lies in the fact that the derivative does not transform in the same way as the field, but instead as

$$\begin{aligned}\partial_\mu\psi(x) \to (\partial_\mu\psi(x))' =& \partial_\mu\left(e^{iq\xi(x)}\psi(x)\right) \\ =& e^{iq\xi(x)}(\partial_\mu\psi(x) + iq\partial_\mu\left(\xi(x)\right)\psi(x)).\end{aligned} \tag{2.4}$$

We can solve this by devising a modified derivative that transforms in a manner identical to the field. If we substitute the regular derivative in the original Lagrangian by this new *covariant* derivative we ensure the Lagrangian remains invariant under local phase transformations. Thus, we construct the covariant derivative first by defining

$$D_\mu\psi(x) = (\partial_\mu - iqA_\mu)\psi(x), \tag{2.5}$$

which transforms as

$$\begin{aligned}D_\mu\psi(x) \to (D_\mu\psi(x))' =& (\partial_\mu\psi(x))' - iqA'_\mu\psi(x) \\ =& \partial_\mu\psi(x) + iq\partial_\mu\xi(x)\psi(x) - iqA'_\mu\psi(x).\end{aligned} \tag{2.6}$$

We note that in our definition of the covariant derivative we introduced a new field A_μ, whose transformation $A_\mu \to A'_\mu$ is as of yet unspecified. Since our goal is to have $D_\mu\psi(x) \to (D_\mu\psi(x))' = e^{iq\xi(x)}D_\mu\psi(x)$, we can set a transformation rule for A_μ that ensures this. Indeed, we impose

$$A_\mu \to A'_\mu = A_\mu + \partial_\mu\xi \tag{2.7}$$

which cancels the extra term coming from the regular derivative, ensuring the desired transformation property of $D_\mu\psi$. Then, the Lagrangian

$$\begin{aligned}\mathcal{L}_\psi =& i\overline{\psi}\not{D}\psi - m\overline{\psi}\psi \\ =& i\overline{\psi}\not{\partial}\psi - m\overline{\psi}\psi - iqA_\mu\overline{\psi}\gamma^\mu\psi\end{aligned} \tag{2.8}$$

is invariant under the simultaneous transformations (2.2) and (2.7). Thus, this Lagrangian satisfies U(1) symmetry since it is invariant under the multiplication of the fields by a 1x1 unitary matrix, i.e. a local phase transformation. In sum, we started with a Lagrangian containing only a kinetic and a mass term for field ψ and our requirement that this theory be *gauge invariant* under U(1) led us to introduce a *gauge field* whose transformations properties assured this would be the case.

By definition the successive application of covariant derivatives also yields a covariant

object. This allows us to to define a gauge covariant object depending only on the gauge fields, as we now show.

Let us compute

$$[D_\mu, D_\nu]\psi = D_\mu(D_\nu\psi) - D_\nu(D_\mu\psi). \tag{2.9}$$

We start by writing the explicit expression for $D_\mu(D_\nu\psi)$ resorting to the definition of the covariant derivative (2.5)

$$\begin{aligned} D_\mu(D_\nu\psi) =& D_\mu\left(\partial_\nu\psi - iqA_\nu\psi\right) \\ =& \partial_\mu\left(\partial_\nu\psi - iqA_\nu\psi\right) - iqA_\mu\left(\partial_\nu\psi - iqA_\nu\psi\right) \\ =& \partial_\mu\partial_\nu\psi - iq(\partial_\mu A_\nu)\psi - iqA_\nu\partial_\mu - iqA_\mu\partial_\nu\psi - q^2A_\mu A_\nu\psi. \end{aligned} \tag{2.10}$$

By interchanging the indices $\mu \leftrightarrow \nu$ we also obtain the expression for $D_\nu D_\mu\psi$. Since partial derivatives commute we obtain

$$[D_\mu, D_\nu]\psi = -iqF_{\mu\nu}\psi, \tag{2.11}$$

where we have defined the field strength tensor $F_{\mu\nu} = \partial_\mu A_\nu - \partial_\nu A_\mu$. It is easy to see $F_{\mu\nu}$ is a gauge invariant object under (2.7)

$$\begin{aligned} F_{\mu\nu} \to F'_{\mu\nu} =& \partial_\mu A'_\nu - \partial_\nu A'_\mu \\ =& \partial_\mu A_\nu - \partial_\mu\partial_\nu\xi + \partial_\nu A_\nu - \partial_\nu\partial_\mu\xi \\ =& \partial_\nu A_\mu - \partial_\mu A_\nu \\ =& F_{\mu\nu}, \end{aligned} \tag{2.12}$$

meaning $-iqF_{\mu\nu}\psi$ is indeed covariant, as we predicted. We can use the field strength tensor to construct a Lagrangian for the gauge field

$$\mathcal{L}_A = -\frac{1}{4}F_{\mu\nu}F^{\mu\nu}, \tag{2.13}$$

which is clearly gauge invariant. Adding $\mathcal{L}_A$ to our gauge invariant Lagrangian for the field ψ (2.8) we obtain

$$\begin{aligned} \mathcal{L}_{QED} =& \mathcal{L}_A + \mathcal{L}_\psi \\ =& -\frac{1}{4}F_{\mu\nu}F^{\mu\nu} + i\overline{\psi}\partial\!\!\!/\psi - m\overline{\psi}\psi - iqA_\mu\overline{\psi}\gamma^\mu\psi \end{aligned} \tag{2.14}$$

which is the Lagrangian for Quantum Electrodynamics with A_μ being the photon field and $q = -e$ being the charge of the electron.

A point of vital importance to our discussion is that we cannot include a mass term for the gauge field. A term of the form $\frac{1}{2}m^2A_\mu A^\mu$ is not invariant under (2.7) since

$$\begin{aligned}\frac{1}{2}m^2 A_\mu A^\mu \rightarrow &\frac{1}{2}m^2 A'_\mu A'^\mu \\ =&\frac{1}{2}m^2(A_\mu + \partial_\mu \xi)(A^\mu + \partial^\mu \xi) \\ =&\frac{1}{2}m^2 A_\mu A^\mu + m^2 A_\mu \partial^\mu \xi + \frac{1}{2}m^2 \partial_\mu \xi \partial^\mu \xi \\ \neq&\frac{1}{2}m^2 A_\mu A^\mu\end{aligned} \tag{2.15}$$

and would consequently spoil the gauge invariance of the theory. In the case of QED this is no cause for concern - the photon happens to be massless so there is no need for a mass term in the Lagrangian. In the Standard Model however, this is not so. The W^+, W^-, and Z are massive gauge-bosons. Their mass cannot be accounted for by explicitly writing down a mass term since - just as in the case of U(1) - these terms would spoil the gauge-invariance of the theory.

Thus, we must find a way of providing mass to the gauge bosons we know are massive in the real world without spoiling the gauge-invariance of the theory. Luckily, such a procedure exists. The mechanism responsible for atributing mass to gauge bosons is called the *Brout-Englert-Higgs mechanism*, or often times simply the *Higgs mechanism*, which we will explain in the following section.

2.2. Brout-Englert-Higgs Mechanism

2.2.1 Spontaneous Symmetry Breaking

In the previous section we saw why one cannot simply insert mass terms for gauge bosons in the Lagrangian and claimed this setback is solved by the Higgs mechanism. A key ingredient to understand this procedure is the concept of *spontaneous symmetry breaking*, which we will now illustrate. Consider the following Lagrangian for a complex scalar field ϕ

$$\mathcal{L} = |\partial_\mu \phi|^2 - V(|\phi|^2), \quad \text{with} \quad V(|\phi|^2) = \mu^2|\phi|^2 + \lambda|\phi|^4. \tag{2.16}$$

We note that this is symmetric under **global** phase transformations. To make the degrees of freedom explicit we can rewrite this Lagrangian by decomposing $\phi = \frac{1}{\sqrt{2}}(\phi_R + i\phi_I)$. We obtain

$$\mathcal{L} = \frac{1}{2}(\partial_\mu \phi_R)^2 + \frac{1}{2}(\partial_\mu \phi_I)^2 - \frac{\mu^2}{2}(\phi_R + \phi_I)^2 - \frac{\lambda}{4}(\phi_R + \phi_I)^4. \tag{2.17}$$

Let us first consider the case when $\mu^2 > 0$, for which the potential is plotted in figure 3a. The classical minimum of this potential - also called the vacuum - occurs quite clearly at $\phi(x) = \phi_0 = 0$. In order to investigate the particle spectrum we need to expand the fields around this vacuum. In this case, since the vacuum occurs at the origin, the expression for the field perturbations coincides with the original expression. We then see that we are in the presence of two massive particles ϕ_R and ϕ_I both with mass μ, which interact with one another. Thus, we call the case $\mu^2 > 0$ the manifest realization of the symmetry.

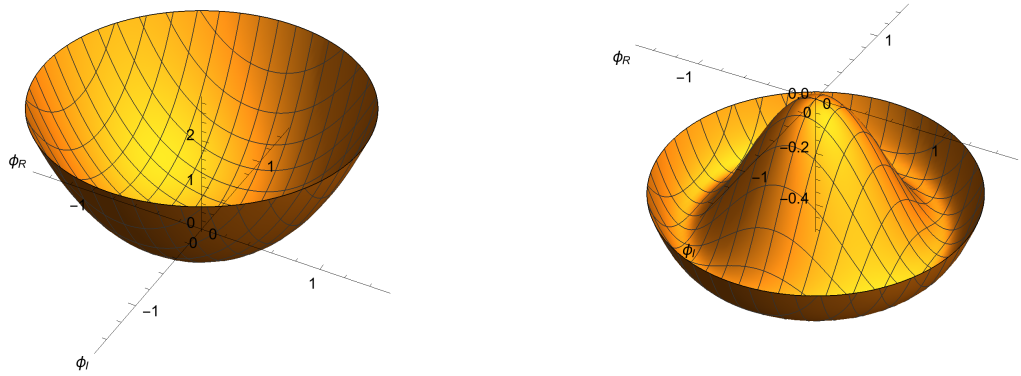

(a) $V(|\phi|^2)$ for $\mu^2 > 0$ **(b)** $V(|\phi|^2)$ for $\mu^2 < 0$

Figure 3: Higgs potential before and after symmetry breaking

Let us now consider the case $\mu^2 < 0$, for which the potential is plotted in figure 3b. In this case it is clear that we no longer have a single vacuum but a ring of vacua satisfying

$$\left.\frac{\partial V(|\phi|^2)}{\partial|\phi|}\right|_{|\phi|=|\phi_0|} = 0, \quad \text{which leads to} \quad \sqrt{-\frac{\mu^2}{\lambda}} = |\phi_0| \equiv v. \tag{2.18}$$

We see that we can no longer consider a vanishing vacuum expectation value, so the $U(1)$ symmetry is no longer manifest since rotations in the complex plane would lead to a different ground state. We say the symmetry has been *spontaneously broken* and call this the spontaneously broken realization of the symmetry.

Out of this infinite number of minima we choose to expand around $\phi_R = v$ and $\phi_I = 0$ such that ϕ becomes

$$\phi = \frac{1}{\sqrt{2}}(v + \widetilde{\phi}_R + i\widetilde{\phi}_I), \tag{2.19}$$

with $\widetilde{\phi}_R$ and $\widetilde{\phi}_I$ being the fluctuations around the vacuum of ϕ_R and ϕ_I, respectively. We now substitute expression (2.19) in the Lagrangian in order to rewrite it in terms of the fluctuations. For the kinetic term we obtain

$$|\partial_\mu \phi|^2 = \frac{1}{2}|\partial_\mu \widetilde{\phi}_R + i\partial_\mu \widetilde{\phi}_I|^2 = \frac{1}{2}(\partial_\mu \widetilde{\phi}_R)^2 + \frac{1}{2}(\partial_\mu \widetilde{\phi}_I)^2. \tag{2.20}$$

To obtain $V(|\phi|^2)$ we first write

$$\begin{aligned} |\phi|^2 =& \frac{1}{2}\left[(v + \widetilde{\phi}_R)^2 + \widetilde{\phi}_I^2)\right] \\ =& \frac{1}{2}v^2 + v\widetilde{\phi}_R + \frac{1}{2}\widetilde{\phi}_R^2 + \frac{1}{2}\widetilde{\phi}_I^2, \end{aligned} \tag{2.21}$$

and

$$|\phi|^4 = \left(|\phi|^2\right)^2 = \frac{1}{4}v^2 + v^2\widetilde{\phi}_R^2 + \frac{1}{4}\widetilde{\phi}_R^4 + \frac{1}{4}\widetilde{\phi}_I^4 + v^3\widetilde{\phi}_R + \frac{1}{2}v^2\widetilde{\phi}_R^2 + \\ + \frac{1}{2}v^2\widetilde{\phi}_I + v\widetilde{\phi}_R^3 + v\widetilde{\phi}_R\widetilde{\phi}_I^2 + \frac{1}{2}\widetilde{\phi}_R^2\widetilde{\phi}_I^2. \tag{2.22}$$

From (2.18) we have $\mu^2 = -2\lambda$ so we write the potential as

$$V(|\phi|^2) = -\frac{1}{4}\lambda v^4 + \lambda v^2\widetilde{\phi}_R^2 + \lambda v\widetilde{\phi}_R^3 + \lambda v\widetilde{\phi}_R\widetilde{\phi}_I^2 + \frac{1}{4}\lambda\widetilde{\phi}_R^4 + \frac{1}{4}\lambda\widetilde{\phi}_I^4 + \frac{1}{2}\lambda\widetilde{\phi}_R^2\widetilde{\phi}_I^2. \tag{2.23}$$

The Lagrangian then becomes

$$\mathcal{L} = \frac{1}{2}(\partial_\mu\widetilde{\phi}_R)^2 + \frac{1}{2}(\partial_\mu\widetilde{\phi}_I)^2 - \lambda v^2\widetilde{\phi}_R^2 \ + \text{ interaction terms} \quad . \tag{2.24}$$

This time we see that we have one massive particle $\widetilde{\phi}_R$ with mass $m^2 = 2\lambda v^2$, and one *massless* particle $\widetilde{\phi}_I$. The fact that the $\widetilde{\phi}_I$ field is massless can be understood by noting that it describes the angular excitations (we chose our ground state on the ϕ_R axis), direction in which the potential is constant. This is a direct consequence of the so-called *Goldstone theorem*, so $\widetilde{\phi}_I$ is what is known as a Goldstone boson.

The Goldstone theorem states that for every generator of the symmetry group that is spontaneously broken by the vacuum expectation value (or in other words for each generator that connects the different vacuum states) there will appear a massless particle called the Goldstone particle. In this case the symmetry is generated by a scalar parameter, thus the Goldstone particle is also a scalar. However this is not always the case. In some supersymmetric models for example, spontaneously broken fermionic symmetries occur - which leads to Goldstone fermions, instead of scalars. We see that in the manifest realization of the theory there is no Goldstone boson since no generator of the symmetry has been broken. On the other hand, in the spontaneously broken realization -also called the *Goldstone realization* - the degeneracy of the groundstate is due to the broken symmetry. According to the theorem this gives rise to a massless particle, which we confirmed.

Now that we have seen how spontaneous symmetry breaking works, we can apply it to a gauge theory by adding the covariant version of Lagrangian (2.16) to our original gauge-invariant Lagrangian. As previously mentioned, this is the procedure known as the *Brout-Englert-Higgs mechanism*, which will give rise to mass terms for the gauge fields without spoiling the gauge-invariance of the theory, as we will see. Next section we will apply the Higgs mechanism to a $U(1)$ gauge theory with the intention of afterwards building on that example and subsequently apply it to $SU(2)_L \times U(1)_Y$, i.e. the electroweak sector of the Standard Model.

2.2.2 Abelian Case

To apply the Higgs mechanism to a $U(1)$ gauge theory we take Lagrangian (2.16) and substitute the regular derivative by the $U(1)$ covariant derivative, which we have already established is

given by expression (2.5). We get

$$\begin{aligned}\mathcal{L} =&|D_\mu\phi|^2 - \mu^2|\phi|^2 - \lambda|\phi|^4 - \frac{1}{4}F_{\mu\nu}^2 \\ =&|\partial_\mu\phi + ieA_\mu\phi|^2 - \mu^2|\phi|^2 - \lambda|\phi|^4 - \frac{1}{4}F_{\mu\nu}^2 \ .\end{aligned} \tag{2.25}$$

Now we choose $\mu^2 < 0$ such that we are in the spontaneously broken realization of the theory. Let us evaluate the first term of the Lagrangian by again performing decomposition (2.19). For the first term, after a little algebra we obtain

$$\begin{aligned}|\partial_\mu\phi + ieA_\mu\phi|^2 =&|\partial_\mu\phi|^2 + e^2A_\mu^2|\phi|^2 + 2eA_\mu Re[i(\partial_\mu\phi)\phi] \\ =&\frac{1}{2}(\partial_\mu\tilde{\phi}_R)^2 + \frac{1}{2}(\partial_\mu\tilde{\phi}_R)^2 + \frac{1}{2}e^2v^2A_\mu^2 - evA_\mu(\partial^\mu\tilde{\phi}_I) + \text{interaction terms.}\end{aligned} \tag{2.26}$$

The term $+\frac{1}{2}e^2v^2A_\mu^2$ does indeed have the form of a mass term for the photon field so one might think we have fulfilled our goal. However there are two problems we need to deal with. First we note that the original Lagrangian contained four degrees of freedom - two coming from the complex scalar and the other two being the possible spin polarizations for the massless gauge field, whereas in (2.26) the gauge boson is massive so we have five overall degrees of freedom. The second problem is the presence of the $-evA_\mu(\partial^\mu\tilde{\phi}_I)$ term, representing the coupling between the Golstone boson and the gauge field which appears to transform a spin-1 particle into a spin-0 particle. This parametrization of the fields is then obviously unphysical.

We can exploit our gauge freedom to eliminate the Goldstone boson $\tilde{\phi}_I$ from the Lagrangian entirely. This would change the number of degrees of freedom back to four and would rid us from the undesired coupling term thus solving the two issues we mentioned. We do this by writing

$$\frac{1}{2}(\partial_\mu\tilde{\phi}_I)^2 - evA_\mu\partial^\mu\tilde{\phi}_I + \frac{1}{2}e^2v^2A_\mu^2 = \frac{1}{2}e^2v^2[A_\mu - \frac{1}{ev}(\partial\tilde{\phi}_I)]^2, \tag{2.27}$$

and subsquently applying he gauge transformation

$$A_\mu(x) \to A'_\mu(x) = A_\mu + \frac{1}{ev}\partial_\mu\phi_I. \tag{2.28}$$

Usually we say that the Goldstone boson is *eaten* by the gauge boson, which in doing so obtains one extra degree of freedom corresponding to the longitudinal polarization. The gauge in which the Goldstone particle no longer appears explicitely in the Lagrangian is called the *unitary* gauge. It is important to note that while physical predictions do not depend on the choice of gauge the unitary gauge allows us to work with fields that correspond to physical particles and avoid unwanted mixing terms. The gauge tranformation 2.28 on the original field ϕ would be

$$\phi \to \phi' = e^{-ie\tilde{\phi}_I/ev}\phi = e^{-i\tilde{\phi}_I/v}, \tag{2.29}$$

and since up to first order we can write

$$\phi = \frac{1}{\sqrt{2}}(v + \tilde{\phi}_R + i\tilde{\phi}_I) = \frac{1}{\sqrt{2}}(v + \tilde{\phi}_R)e^{i\tilde{\phi}_I/v} \tag{2.30}$$

we see that the effect of the gauge transformation (2.29) is to make the field ϕ purely real. We see that a shortcut to obtain the Lagrangian in the unitary gauge is setting $\tilde{\phi} = 0$ from the beginning.

Now that we know we are working with the physical fields we rename $\tilde{\phi}_R = h$, and write the full Lagrangian as

$$\mathcal{L} = \frac{1}{2}(\partial_\mu h)^2 - \lambda v^2 h^2 - \frac{1}{4}F_{\mu\nu}^2 + \frac{1}{2}e^2 v^2 A_\mu^2 + \text{interaction terms}, \tag{2.31}$$

where we dropped the prime in A_μ. The field h is the so-called *Higgs field*, whose mass is $m_h = \sqrt{2\lambda v^2}$. We see that the A_μ field has a mass $m_A = ev$, so we have attained our goal of having a gauge invariant theory with a massive gauge boson.

2.2.3 Standard Model

In the previous section we have sketched how we can have a U(1) gauge theory with a massive photon by making use of the Higgs mechanism. However in the real world the massive gauge bosons are the W^+, W^- and the Z, not the photon. In this section we will apply the Higgs mechanism to the electroweak sector of the Standard Model, which posesses $SU(2)_L \times U(1)_Y$ local gauge symmetry.

Analogously to the abelian example, we expect there to be three Goldstone bosons which will provide the longitudinal degrees of freedom of the massive W^+, W^- and the Z. We also expect there to be a massive scalar particle - the Standard Model Higgs boson - corresponding to the field excitation in the direction radial direction.

Since we want the Higgs mechanism to provide the masses of the eleectroweak gauge bosons we introduce a $SU(2)_L \times U(1)_Y$ doublet of scalars, one neutral - ϕ^0- and the other charged ϕ^+

$$\phi = \begin{pmatrix} \phi^+ \\ \phi^0 \end{pmatrix} = \frac{1}{\sqrt{2}} \begin{pmatrix} \phi_1 + i\phi_2 \\ \phi_3 + i\phi_4 \end{pmatrix}. \tag{2.32}$$

Choosing the unitary gauge in this case amounts to setting $\phi_1 = \phi_2 = \phi_4 = 0$ and $\phi_3 = v + h$, just like setting $\tilde{\phi}_I = 0$ would lead to the unitary gauge in the abelian example. So we have

$$\phi(x) = \begin{pmatrix} 0 \\ v + h(x) \end{pmatrix}. \tag{2.33}$$

We again want to consider the Lagrangian

$$\mathcal{L} = (\partial_\mu \phi)^\dagger (\partial^\mu \phi) - V(|\phi|^2), \quad \text{with} \quad V(|\phi|^2) = \mu^2 \phi^\dagger \phi + \lambda(\phi^\dagger \phi)^2 \tag{2.34}$$

We see that after spontaneous symmetry breaking this potential has an infinite set of minima with $(\phi^\dagger \phi) = -\frac{\mu^2}{2\lambda}$. To have a $SU(2) \times U(1)$ gauge theory we have to introduce its covariant

derivative, just like we introduced the $U(1)$ covariant derivative in the abelian case. The electroweak covariant derivative is the 2×2 matrix given by

$$D_\mu \phi = \left[\partial_\mu + \frac{1}{2} g' B_\mu Y + g W_\mu^a T_a \right], \tag{2.35}$$

where Y is the so-called weak hypercharge serving as the $U(1)_Y$ generator and $T_a = \frac{1}{2}\sigma_a$ being the $SU(2)_L$ generator, where σ^a denote the Pauli matrices. Also, B_μ is the gauge field associated with the $U(1)$ group whereas W_μ^a denotes the three gauge fields associated with $SU(2)_L$. In explicit matrix form the covariant derivative is

$$\begin{aligned} D_\mu \phi =& \frac{1}{\sqrt{2}} \begin{bmatrix} \partial_\mu + i\frac{g}{2} W_\mu^3 + i\frac{g'}{2} B_\mu & i\frac{g}{2}(W_\mu^1 - iW_\mu^2) \\ i\frac{g}{2}(W_\mu^1 + iW_\mu^2) & \partial_\mu - i\frac{g}{2} W_\mu^3 + i\frac{g'}{2} B_\mu \end{bmatrix} \begin{bmatrix} 0 \\ v + h \end{bmatrix} \\ =& \frac{1}{\sqrt{2}} \begin{bmatrix} i\frac{g}{2}(W_\mu^1 - iW_\mu^2) \\ \partial_\mu - \frac{i}{2}\left(g W_\mu^3 - i g' B_\mu \right) \end{bmatrix} (v + h). \end{aligned} \tag{2.36}$$

Now we evaluate $|D_\mu \phi|^2$

$$(D_\mu \phi)^\dagger (D_\mu \phi) = \frac{1}{2}(\partial_\mu h)^2 + \frac{1}{8} g' (W_\mu^1 + iW_\mu^2)(W^{1\mu} - iW^{2\mu})(v + h)^2 + \frac{1}{8}(g W_\mu^3 - g' B_\mu)(v + h)^2. \tag{2.37}$$

Let us focus on the quadratic part in the W^a and B fields, which is

$$\frac{v^2}{8} g^2 (W_\mu^1 + iW_\mu^2)(W^{1\mu} - iW^{2\mu}) + \frac{v^2}{8}(g W_\mu^3 - g' B_\mu)^2. \tag{2.38}$$

Regarding the first term, it is convenient to recombine the charged fields W_μ^1 and W_μ^2 into a complex field W_μ, such that

$$W_\mu = \frac{1}{\sqrt{2}}(W_\mu^1 - iW_\mu^2). \tag{2.39}$$

This means that

$$\frac{1}{8} g^2 (W_\mu^1 + iW_\mu^2)(W^{1\mu} - iW^{2\mu}) v^2 = \frac{1}{4} g^2 v^2 \overline{W}_\mu W^\mu \tag{2.40}$$

This has the form of a mass term so we see that the W^+ and W^- bosons are associated with the W_μ and $\overline{W}_\mu$ fields with their mass dependeing on the $SU(2)_L$ coupling constant and on the Higgs field vacuum expectation value. The terms quadratic in W_μ^3 and B_μ can be written as

$$\begin{aligned} \frac{v^2}{8}(g W_\mu^3 - g' B_\mu)^2 =& \frac{v^2}{8} \begin{pmatrix} W_\mu^3 & B_\mu \end{pmatrix} \begin{pmatrix} g^2 & -gg' \\ -gg' & g'^2 \end{pmatrix} \begin{pmatrix} W^{3\mu} \\ B^\mu \end{pmatrix} \\ =& \frac{v^2}{8} \begin{pmatrix} W_\mu^3 & B_\mu \end{pmatrix} M^2 \begin{pmatrix} W^{3\mu} \\ B^\mu \end{pmatrix}. \end{aligned} \tag{2.41}$$

We intend to diagonalize the mass matrix M^2 so that we can lose all the mixing terms and thus

be able to write the Lagrangian in terms of the physical fields. Their masses are given by the eigenvalues of M^2, i.e. the solutions to the characteristic equation

$$(g^2-\lambda)(g'^2-\lambda)-g'^2g^2=0, \quad \text{which yields} \quad \lambda=0, \;\; \lambda=g^2+g'^2. \tag{2.42}$$

By computing the eigenvectors we obtain the change-of-basis matrix S

$$S=\frac{1}{\sqrt{g^2+g'^2}}\begin{bmatrix} g' & g \\ g & -g' \end{bmatrix}, \tag{2.43}$$

such that (2.41) becomes

$$\frac{v^2}{8}\begin{pmatrix} W_\mu^3 & B_\mu \end{pmatrix} S^{-1}\begin{pmatrix} 0 & 0 \\ 0 & g^2+g'^2 \end{pmatrix} S\begin{pmatrix} W^{3\mu} \\ B^\mu \end{pmatrix} \tag{2.44}$$

So now we define the photon field A_μ and the Z field Z_μ such that they correspond to the basis that diagonalizes the mass matrix M

$$\begin{bmatrix} A_\mu \\ Z_\mu \end{bmatrix}=\frac{1}{\sqrt{g'^2+g^2}}\begin{bmatrix} g' & g \\ g & -g' \end{bmatrix}\begin{bmatrix} W_\mu^3 & B_\mu \end{bmatrix}, \tag{2.45}$$

yielding,

$$\begin{aligned} A_\mu &= \sin\theta_W W_\mu^3+\cos\theta_W B_\mu \\ Z_\mu &= \cos\theta_W W_\mu^3-\sin\theta_W B_\mu, \end{aligned} \tag{2.46}$$

where we defined the weak mixing angle as $\tan\theta_W=\frac{g'}{g}$. So by applying the Higgs mechanism in the electroweak sector of the Standard Model we see that the photon has remained massless, while the W and Z bosons have acquired a mass

$$\begin{aligned} m_W &= \frac{1}{2}gv \\ m_Z &= \frac{1}{2}\sqrt{g^2+g'^2}v=\frac{1}{2}\frac{gv}{\cos\theta_W}. \end{aligned} \tag{2.47}$$

The relation

$$\cos\theta_W=\frac{m_W^2}{m_Z^2} \quad \text{or} \quad \rho\equiv\frac{m_W^2}{m_Z^2\cos\theta_W}=1 \tag{2.48}$$

is an important experimental check on the Higgs mechanism. Another experimental test is to determine whether the couplings of the Higgs to other particles are the ones predicted by the Standard Model. We can summarize the SM Higgs couplings to gauge bosons and fermions, as well as to the Higgs boson itself in the following Lagrangian [16].

$$\mathcal{L}=-g_{Hf\bar{f}}f\bar{f}H+\frac{g_{HHH}}{6}H^3+\frac{g_{HHHH}}{24}H^4+\delta_V V_\mu V^\mu\left(g_{HVV}H+\frac{g_{HHVV}}{2}H^2\right), \tag{2.49}$$

with

$$g_{Hf\overline{f}} = \frac{m_f}{v}, \quad g_{HVV} = \frac{2m_V^2}{v}, \quad g_{HHVV} = \frac{2m_V^2}{v^2}, \quad g_{HHH} = \frac{3m_H^2}{v}, \quad g_{HHHH} = \frac{3m_H^2}{v^2}, \tag{2.50}$$

where $V = W^+, W^-, Z$ bosons and $\delta_W = 1$, $\delta_Z = \frac{1}{2}$.

2.2.4 Fermion Masses

Besides providing the procedure for having massive gauge bosons without spoling the symmetries of the theory, in the Standard Model the Higgs mechanism is also responsible for explaining the masses of elementary fermions. To see why this is so, we take a fermion mass term $-m\overline{\psi}\psi$ and decompose it into chiral fields such that

$$m\overline{\psi}\psi = m(\overline{\psi}_L\psi_R + \overline{\psi}_R\psi_L), \tag{2.51}$$

where we have defined

$$\begin{aligned} \psi_L &= P_L\psi \\ \psi_R &= P_R\psi, \end{aligned} \tag{2.52}$$

with $\psi_L = \frac{1-\gamma_5}{2}$ and $\psi_R = \frac{1+\gamma_5}{2}$ being the chiral projectors. We call ψ_R the right-handed field and ψ_L the left-handed field. The issue is that in the Standard Model left-handed fermions belong to the doublet representation of $SU(2)$, while right-handed fermions are $SU(2)$ singlets. This means that both the right- and left-handed fields transform under $U(1)_Y$ but only left-handed fields transform under $SU(2)$.

Consequently, the mass term (2.51) is not gauge invariant under $SU(2)_L \times U(1)_Y$, the symmetry group of the electroweak sector of the Standard Model. This is one of the defining characteristics of the Standard Model and the reason why we cannot directly include mass terms in the Lagrangian. Fortunately, we can once again employ the Higgs mechanism to circumvent the fact that mass terms are not gauge invariant, just as before.

Let us call ψ_L the $SU(2)$ doublet, and u_R and d_R the $SU(2)$ singlets, such that

$$\psi_L = \begin{pmatrix} u_L \\ d_L \end{pmatrix}, \tag{2.53}$$

where the u field can represent any up-like quark or neutrino and the d field any down-type quark or charged lepton.

What we would like to do is take the two $SU(2)$ doublets at our disposal - ψ_L and the Higgs doublet ϕ - and combine them to construct an $SU(2)$ singlet which we can then couple to the right handed fields in a gauge invariant manner. Under $SU(2)$, ϕ and ψ_L transform as

$$\begin{aligned} \phi &\to \phi' = U\phi \\ \psi_L &\to \psi'_L = U\psi_L, \end{aligned} \tag{2.54}$$

where U is an unitary 2×2 matrix with unit determinant. We immediately see that $\overline{\psi}\phi$ is then

an $SU(2)$ singlet.

We can construct yet another singlet $\psi_L(-i\sigma_2\phi^*)$. To show this we use the most general parametrization of an $SU(2)$ matrix

$$U = \begin{pmatrix} a & b \\ -b^* & a^* \end{pmatrix}. \tag{2.55}$$

Now we note that

$$-i\sigma_2 U^* = \begin{pmatrix} 0 & -1 \\ 1 & 0 \end{pmatrix} \begin{pmatrix} a^* & b^* \\ -b & a \end{pmatrix} = \begin{pmatrix} b & -a \\ a* & b^* \end{pmatrix}, \tag{2.56}$$

and also

$$U(-i\sigma_2) = \begin{pmatrix} a & b \\ -b^* & a^* \end{pmatrix} \begin{pmatrix} 0 & -1 \\ 1 & 0 \end{pmatrix} = \begin{pmatrix} b & -a \\ a* & b^* \end{pmatrix}, \tag{2.57}$$

such that $-i\sigma_2 U^* = -iU\sigma_2$. Now we can verify that $\psi_L(-i\sigma_2\phi^*)$ is indeed a singlet

$$\overline{\psi}_L(-i\sigma_2\phi^*) \to \overline{\psi}_L U^\dagger(-i\sigma_2)U^*\phi^* = \overline{\psi}_L U^\dagger(-i\sigma_2)U^*\phi^* = \overline{\psi}_L(-i\sigma_2\phi^*). \tag{2.58}$$

We also need to make sure that the term is invariant under $U(1)_Y$ so first we write how the fields transform under this symmetry, the doublets transform as

$$\begin{aligned} \phi \to \phi' &= e^{\frac{i}{2}q\xi} \\ \psi_L \to \psi'_L &= e^{\frac{i}{2}q_1\xi} \end{aligned} \tag{2.59}$$

and the singlets as

$$\begin{aligned} u_R =& e^{\frac{1}{2}q_2\xi}u_R \\ d_R =& e^{\frac{1}{2}q_3\xi}d_R, \end{aligned} \tag{2.60}$$

where ξ is the generator of the $U(1)$ transformations and for now q, q_1, q_2, q_3 are just arbitrary numbers. We see that the $SU(2)$ singlets $\psi_1 \equiv \overline{\psi}_L\phi$ and $\psi_2 \equiv \overline{\psi}_L(-i\sigma_2\phi^*)$ transform under $U(1)$ as

$$\begin{aligned} \psi_1 \to \psi'_1 =& e^{\frac{i}{2}(q-q_1)}\psi_1 \\ \psi_2 \to \psi'_2 =& e^{-\frac{i}{2}(q+q_1)}\psi_2, \end{aligned} \tag{2.61}$$

so we set $q_3 = q_1 - q$ and $q_2 = q + q_1$ since this will ultimately lead to a mass terms also invariant under $U(1)_Y$ transformations, as we will see below.

Now we set the Higgs doublet to the unitary gauge, such that

$$\phi = \frac{1}{\sqrt{2}} \begin{pmatrix} 0 \\ v + h(x) \end{pmatrix}. \tag{2.62}$$

We will only keep the terms proportional to the vacuum expectation value since we are interested

in the mass terms, however we note that the perturbation $h(x)$ gives rise to interaction terms between the fermions and the Higgs field. We are finally able to construct gauge invariant mass terms. For the down- and up-type quark respectively we have

$$\begin{aligned}\mathcal{L}_d =&\lambda_d \left(\overline{\psi}_L \phi d_R + \overline{d}_R \phi^\dagger \psi_L\right) \\ =&\frac{\lambda_d v}{\sqrt{2}}[\overline{d}_L d_R + \overline{d}_R d_L]\end{aligned} \tag{2.63}$$

and

$$\begin{aligned}\mathcal{L}_u =&\lambda_u \left(\overline{\psi}_L (-i\sigma_2 \phi^*) d_R + \overline{d}_R (-i\sigma_2 \phi^*)^\dagger \psi_L\right) \\ =&\frac{\lambda_u v}{\sqrt{2}}[\overline{u}_L u_R + \overline{u}_R u_L]\end{aligned} \tag{2.64}$$

We were once again able to obtain mass terms in the Lagrangian in a way that does not spoil gauge invariance by resorting to the Higgs mechanism. We should make a brief note here. While this mechanism is responsible for providing masses to elementary fermions, it does not provide the mass of what we commonly think of as matter. This is because only 1% of the mass of the proton comes from the rest masses of the quarks. The remaining contributions to the mass come from QCD binding energy, which comes from the kinetic energy of the quarks and gluon fields that bind the quarks together. This is also true for the neutron.

2.3. Particles and Propagators

In this section we aim to understand the effect a time-dependent external disturbance has on a field, including what happens to such field once that disturbance is switched off. We follow section 2.2 from de Wit, Laenen and Smith [1].

To do this, let us consider the Lagrangian for a relativistic scalar field in the presence of a source $J(x)$

$$\mathcal{L} = \frac{1}{2}(\partial_\mu \phi)^2 - \frac{1}{2}m^2\phi^2 + J\phi. \tag{2.65}$$

The equation of motion reads

$$(\Box^2 + m^2)\phi(x) = J(x), \tag{2.66}$$

which is just the Klein-Gordon equation in the presence of a source. We solve this equation through the Green's function method by introducing $\Delta(x)$ which must satisfy

$$(\Box^2 + m^2)\Delta(x) = -i\delta^{(4)}(x). \tag{2.67}$$

Using the definition for the Fourier transform as well as the definition of the Dirac delta

$$\Delta(x) = \int \frac{d^4k}{(2\pi)^4} e^{ik\cdot x}\Delta(k)\ , \qquad \delta^{(4)}(x) = \int \frac{d^4k}{(2\pi)^4} e^{ik\cdot x} \tag{2.68}$$

we see equation (2.67) in momentum space yields

$$\Delta(k) = \frac{i}{k^2 - m^2}, \tag{2.69}$$

such that

$$\Delta(x) = \int \frac{d^4k}{(2\pi)^4} \frac{i}{k^2 - m^2} e^{ik\cdot x}. \tag{2.70}$$

Now we can solve the differential equation through the Green's function method

$$\phi(x) = \phi_0(x) + \delta\phi(x), \tag{2.71}$$

where ϕ_0 is the solution to the free (homogeneous) Klein-Gordon equation and

$$\delta\phi(x) = \int d^4y \Delta(x - y) J(y). \tag{2.72}$$

We can make the time dependence of (2.72) clearer by writing

$$\delta\phi(x) = \int d^3k e^{-i\mathbf{k}\cdot\mathbf{x}} \int dk^0 e^{ik^0 t} \frac{J(\mathbf{k}, k^0)}{(k^0)^2 - \mathbf{k}^2 - m^2}. \tag{2.73}$$

Now we see that for large values of $|t|$ the exponential $e^{ik^0 t}$ oscillates very quickly so we expect (2.73) to vanish. More precisely we can resort to the Riemann-Lebesgue theorem which states

$$\lim_{t\to\infty} \int_{-\infty}^{+\infty} \mathrm{d}x f(x) e^{\pm itx} = 0, \quad \text{when} \quad \int_{-\infty}^{+\infty} |f(x)| \mathrm{d}x \quad \text{is finite.} \tag{2.74}$$

However we see that this latter condition is not satisfied, since our integrand has two poles located at $k^0 = \pm\omega(\mathbf{k})$, with $\omega(\mathbf{k}) = \sqrt{\mathbf{k}^2 + m^2}$. Due to these poles, $\delta\phi(x)$ will not vanish. Even when $J(\mathbf{k}, k^0)$ is integrable there will always be contributions corresponding to plane waves whose four-momenta satisfy the relativistic dispersion equation $E = \sqrt{\mathbf{k}^2 + m^2}$. These contributions can then be identified with physical particles associated with field ϕ, since they survive at assymptotically large times. The contributions that do not satisfy $E = \sqrt{\mathbf{k}^2 + m^2}$ correspond to virtual particles, since they cannot survive at times substantially larger than the time scale over which the source varies.

Let us focus on the following integration over k^0

$$I(t) = \int_{-\infty}^{+\infty} dk^0 e^{ik^0 t} f(k^0) \quad \text{, with} \qquad f(k^0) = \frac{i}{(k^0)^2 - \mathbf{k}^2 - m^2} \tag{2.75}$$

This integral can be evaluated by contour integration. For $t > 0$ we can choose the contour seen in figure 4. For large values of k^0 we see $f(k^0) \to 0$, so we can safely assume that the contributions coming from the vertical pieces of the contour vanish.

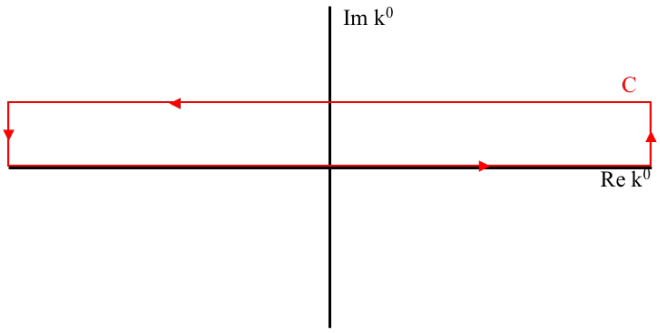

Figure 4: Contour chosen to perform integral (2.75)

We then have

$$\begin{aligned}\oint_C \mathrm{d}k^0 e^{ik^0 t} f(k^0) &= \int \mathrm{d}k^0 e^{ik^0 t} f(k^0) + \int \mathrm{d}k^0 e^{i(k^0+ia)t} f(k^0+ia) \\ &= \int \mathrm{d}k^0 e^{ik^0} f(k^0) + e^{-at} \int \mathrm{d}k^0 e^{ik^0} f(k^0+ia)\end{aligned} \tag{2.76}$$

We see that the second term is exponentially supressed and vanishes for large values of t. Thus, by Cauchy's residue theorem we have

$$I(t) = \oint_C \mathrm{d}k^0 e^{-ik^0} f(k^0) = -2\pi i \sum_n e^{i\omega_n t} \mathrm{Res} f(\omega_n), \tag{2.77}$$

where ω_n are the poles of $f(k^0)$. As it stands, the poles of $f(k^0)$ lie on the real axis. How one chooses the contour to circumvent the poles will lead to different forms of the field propagator, namely the retarded, the advanced and the Feynman propagators.

Figure 5: Contour choice for the retarded propagator

The retarded propagator amounts to choosing contour seen in figure 5 and it is given by the Green's function

$$\Delta_R(x-y) = \lim_{\epsilon\to 0} \int \frac{d^4k}{(2\pi)^4} \frac{e^{ik(x-y)}}{(k^0+i\epsilon)^2 - \omega_k^2}. \tag{2.78}$$

As we can see from this expression, this choice of contour is equivalent to shifting the poles above the real axis by an infinitesimal amount $i\epsilon$ and taking the integral on the real axis.

Figure 6: Contour choice for the advanced propagator

Similarly, the advanced propagator amounts to choosing the contour in figure 6 and its

expression is

$$\Delta_A(x-y) = \lim_{\epsilon\to 0}\int \frac{d^4k}{(2\pi)^4}\frac{e^{ik(x-y)}}{(k^0-i\epsilon)^2-\omega_k^2}. \tag{2.79}$$

Figure 7: Contour choice for the Feynman propagator

Lastly, we have the Feynman propagator, which amounts to choosing contour in figure 7 or shifting the left pole above the real axis and the right pole below the real axis. Its expression is the famous Lorentz invariant object

$$\Delta_F(x-y) = \lim_{\epsilon\to 0}\int \frac{d^4k}{(2\pi)^4}\frac{e^{ik(x-y)}}{k^2-m^2+i\epsilon}. \tag{2.80}$$

This propagator can also be derived as the vacuum expectation value of the time-ordered product of the free fields ϕ_0

$$\Delta_F(x-y) = \langle|T\{\phi_0(x)\phi_0(y)\}|\rangle. \tag{2.81}$$

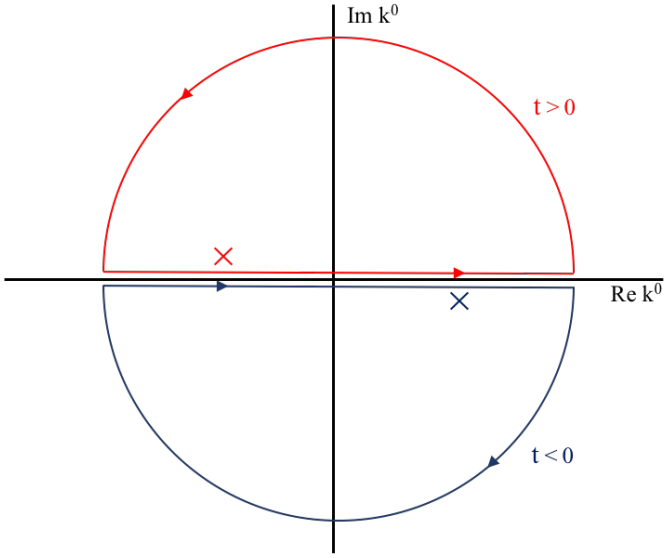

Figure 8: Appropriate contour choices for the Feynman propagator for $t > 0$ and $t < 0$

In this section we only explicitly evaluated the integral for $t > 0$ but the procedure for $t < 0$ is essentially the same, the only difference being that we close the contour in the lower half-plane instead of closing it from above. The summary of how we choose the contour for the Feynman propagator can be seen in figure 8. In most calculations in this thesis we will use the Feynman propagator but leave the $i\epsilon$ implicit unless we are directly dealing with its consequences.

Unstable particles will play a vital role in this thesis so one last remark is in order. In chapter

3 we will show that due to quantum corrections to the two-point Green's function, the pole of the propagator of unstable particles is shifted into the complex plane. Exactly how this comes about will be explained later; for now it suffices to consider the propagator with a complex valued pole

$$\Delta(x) = \int \frac{d^4k}{(2\pi)^4} \frac{i}{k^2 - m^2 + i\gamma} e^{ik\cdot x}. \tag{2.82}$$

Once again, at very large times only the modes associated with the pole of the propagator survive, however now we have the pole located at $(k^0)^2 = \omega^2(k) + i\gamma$. If we assume $\gamma << \omega^2(k)$ then the location of the pole can be written as $k^0 = \omega(\mathbf{k})\sqrt{1 + i\frac{\gamma}{\omega^2(\mathbf{k})}} \approx \omega(\mathbf{k}) + i\frac{\gamma}{2\omega(\mathbf{k})}$. The leading contribution to the propagator at large times will then be proportional to

$$e^{ik^0 t}\Big|_{k^0 pole} = e^{i\left(\omega(k) + i\frac{\gamma}{2\omega(\mathbf{k})}\right)t} = e^{i\omega(\mathbf{k})t} e^{-\frac{\gamma}{2\omega(\mathbf{k})}}. \tag{2.83}$$

We see the inclusion of an imaginary part in the denominator leads to a damping of the usual plane wave solution. Thus, the probability of detecting an unstable particle decreases exponentially with a characteristic time

$$\tau(\mathbf{k}) = \frac{\omega(\mathbf{k})}{\gamma} \equiv \Gamma^{-1}(\mathbf{k}), \tag{2.84}$$

where we have defined the decay width $\Gamma(\mathbf{k})$ of a particle as the inverse of its mean life time $\tau(\mathbf{k})$. We can recover the plane wave solution for stable particles by taking the limit $\Gamma(\mathbf{k}) \to 0$ since by definition they have infinite decay times.

2.4. Unitarity

2.4.1 Optical Theorem

Unitarity is a fundamental property of any quantum field theory which simply put means that probabilities add up to one. In order to have a probabilistic interpretation of a theory it is required that it be unitary.

Let $|i\rangle$ denote our initial state at $t = -\infty$ and $|f\rangle$ our final state at $t = +\infty$. We will assume that interactions occur in a finite interval, so that at $t = \pm\infty$ these states are free states at infinite times *assymptotic states*. This is closely related to our discussion about real and virtual particles in the previous section. Now we define the scattering matrix or the S-matrix as

$$\langle f|S|i\rangle = \langle f|U(t = +\infty, t = -\infty)|i\rangle, \tag{2.85}$$

where U is the time evolution operator in the Schrodinger picture. We can easily check why this S-matrix must be unitary. In the Schrodinger picture the norm of a state is constant in time, which implies that for any value of t

$$\langle \Psi; t|\Psi; t\rangle = \langle \Psi; 0|\Psi; 0\rangle. \tag{2.86}$$

Now, since we have

$$|\Psi;t\rangle = e^{-iHt}|\Psi;0\rangle \equiv S|\Psi\rangle, \tag{2.87}$$

then

$$\langle\Psi;t|\Psi;t\rangle = \langle\Psi;0|S^\dagger S|\Psi;0\rangle = \langle\Psi;0|\Psi;0\rangle, \tag{2.88}$$

which together with equation (2.86) implies $S^\dagger S = 1$, meaning S must be unitary. This apparently simple result has remarkable consequences. We note that the amplitudes we are used to computing through Feynman rules are related to the S-matrix elements by

$$\langle f|\mathcal{T}|i\rangle = (2\pi)^4\delta^{(4)}(p_i - p_f)\mathcal{M}(i \to f), \tag{2.89}$$

where $\mathcal{T}$ is known as the transfer matrix and is defined as the non trivial part of the S-matrix

$$S = \mathbb{1} + i\mathcal{T}. \tag{2.90}$$

Unitarity of the S-matrix implies that

$$(1 - \mathcal{T}^\dagger)(1 + i\mathcal{T}) = 1 \Rightarrow i(\mathcal{T}^\dagger - \mathcal{T}) = \mathcal{T}^\dagger\mathcal{T}. \tag{2.91}$$

If we now apply $|i\rangle$ from the right and $\langle f|$ from the left this yields

$$\begin{aligned}\langle i(\mathcal{T}^\dagger - \mathcal{T})|i\rangle =& i(\langle i|\mathcal{T}|\rangle^* - \langle f|\mathcal{T}|i\rangle \\ =& i(2\pi)^4\delta^{(4)}(p_i - p_f)\left(\mathcal{M}^*(f \to i) - \mathcal{M}(i \to f)\right).\end{aligned} \tag{2.92}$$

Now we use the completeness relation

$$\mathbb{1} = \sum_X \int d\Pi_x |X\rangle\langle X|, \tag{2.93}$$

with $d\Pi_X = \prod_{i\in X} \frac{d^3p_i}{(2\pi)^3}\frac{1}{2E_i}$ and the sum being over single and multiparticle states, and we insert it in the right hand side of equation (2.91)

$$\langle f|\mathcal{T}^\dagger\mathcal{T}|i\rangle = \sum_X \int d\Pi_X \langle f|\mathcal{T}^\dagger|X\rangle\langle X|\mathcal{T}|i\rangle. \tag{2.94}$$

Now since

$$\langle f|\mathcal{T}^\dagger|X\rangle = (\langle X|\mathcal{T}|f\rangle) = (2\pi)^4\delta^{(4)}(p_f - p_X)\mathcal{M}^x(f \to X), \tag{2.95}$$

and

$$\langle X|\mathcal{T}|i\rangle = (2\pi)^4\delta^{(4)}(p_X - p_i)\mathcal{M}(i \to X), \tag{2.96}$$

we then have

$$\langle f|\mathcal{T}^\dagger\mathcal{T}|i\rangle = \sum_x \int d\Pi_x (2\pi)^4\delta^{(4)}(p_X - p_i)(2\pi)^4\delta^{(4)}(p_X - p_f)\mathcal{M}^*\left(f \to X\right)\mathcal{M}(i \to X). \quad (2.97)$$

Equating the right and left hand sinde of equation (2.91) and using that $\delta^{(4)}(p_X - p_i)\delta^{(4)}(p_X - p_f) = \delta^{(4)}(p_X - p_i)\delta^{(4)}(p_i - p_f)$ we obtain an important result

$$\mathcal{M}(i \to f) - \mathcal{M}^*(f \to i) = i\sum_X \int d\Pi_X (2\pi)^4\delta^{(4)}(p_i - p_X)\mathcal{M}^*(f \to X)\mathcal{M}(i \to X). \quad (2.98)$$

We call this result the generalized optical theorem. We see the left-hand side is proportional to g if $\mathcal{M} \sim g$, while the right-hand side goes with g^2 since it has a squared amplitude. However this result must hold order by order in perturbation theory. The only way to reconcile this is by concluding the amplitude on the LHS must contain loops and therefore be of the same order as the product of the tree-level amplitudes on the RHS. We see then that the imaginary part of the loops (noting that $a - a^* = 2\Im(a)$) can be computed resorting to tree-level amplitudes. When the initial and final states are the same, for example in self energy amplitudes, we see equation (2.98) becomes

$$\begin{aligned} \Im\mathcal{M}(A \to A) =& m_A \sum_X \Gamma(A \to X) \\ =& m_A \Gamma_{total}, \end{aligned} \quad (2.99)$$

where we used the definition of the partial width

$$\Gamma(A \to X) = \frac{1}{2m_A}\int d\Pi_X (2\pi)^4\delta^{(4)}(p_A - p_X)|\mathcal{M}(A \to X)|^2, \quad (2.100)$$

and defined Γ_{total} as the total width of the particle, equal to the inverse of the particles lifetime. We take this opportunity to note that the self-energy of stable particles- which as we previously saw have infinite decay times and therefore zero width- do not have an imaginary part. This will be relevant for our discussion in later chapters.

2.4.2 Cutkosky Cutting Rules

In section 2.3 we described how one had to perform the $i\epsilon$ prescription to the scalar propagator in order to choose the appropriate contour to our integration. In this section we will introduce another consequence of unitarity which will be very useful later in the thesis. We start by evaluating the imaginary part of the Feynman propagator

$$\begin{aligned} \Im\left[\frac{1}{p^2 - m^2 + i\epsilon}\right] =& \frac{1}{2i}\left(\frac{1}{p^2 - m^2 + i\epsilon} - \frac{1}{p^2 - m^2 - i\epsilon}\right) \\ =& -\frac{\epsilon}{p^2 - m^2 + \epsilon^2} \end{aligned} \quad (2.101)$$

Now we use the following definition of the Dirac delta

$$\delta(x) = \lim_{\epsilon \to 0} \frac{\epsilon}{x^2 + \epsilon^2} = \pi \delta(x), \tag{2.102}$$

to write

$$\Im \left(\frac{1}{p^2 - m^2 + i\epsilon} \right) = -\pi \delta(p^2 - m^2). \tag{2.103}$$

This tells us that only when the particle goes on-shell does $1/(p^2 - m^2 + i\epsilon)$ have an imaginary part. In particular, this means that in the computation of loop-amplitudes the contributions to the imaginary part come when the intermediate particles in the loop go on-shell. We will demonstrate this by computing the imaginary part of a one-loop amplitude in a scalar ϕ^3 theory

$$\mathcal{L} = \frac{1}{2}(\partial_\mu \phi)^2 - \frac{1}{2} m^2 \phi^2 + \lambda \phi^3. \tag{2.104}$$

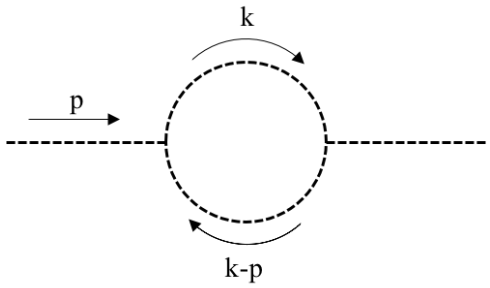

Figure 9: Loop diagram for ϕ^3

This diagram can be seen in figure 9 and its amplitude is given by

$$\mathcal{M} = -\frac{\lambda^2}{2} \int \frac{d^4k}{(2\pi)^4} \frac{i}{k^2 - m^2 + i\epsilon} \frac{i}{(k-p)^2 - m^2 + i\epsilon}. \tag{2.105}$$

We can rewrite the Feynman propagator as

$$\frac{i}{2\omega_k} \left[\frac{1}{k_0 - \omega_k + i\epsilon} - \frac{1}{k_0 + \omega_k - i\epsilon} \right] = \frac{i}{(k^0)^2 - \omega_k^2 + i\epsilon} = \frac{i}{k^2 - m^2 + i\epsilon} = \Delta_F(k^2), \tag{2.106}$$

where as usual $\omega_k = \mathbf{k}^2 + m^2$. Now we note that

$$\frac{1}{k_0 - \omega_k + i\epsilon} - \frac{1}{k_0 - \omega_k - i\epsilon} = \frac{-2i\epsilon}{(k_0 - \omega_k)^2 + \epsilon^2} = -2i\pi \delta(k_0 - \omega_k), \tag{2.107}$$

where again we used (2.102). The Feynman propagator then is

$$\begin{aligned}\Delta_F(k) =& \frac{i}{2\omega_k}\left[\frac{1}{k_0^2-\omega_k^2+i\epsilon}-\frac{1}{k_0^2+\omega_k-i\epsilon}\right]\\ =& \frac{i}{2\omega_k}\left[\frac{1}{k_0-\omega_k+i\epsilon}-\frac{1}{k_0-\omega_k-i\epsilon}+\frac{1}{k_0-\omega_k-i\epsilon}-\frac{1}{k_0+\omega_k-i\epsilon}\right]\\ =& \frac{\pi}{\omega_k}\delta(k_0-\omega_k)+\Delta_R(k),\end{aligned} \tag{2.108}$$

where $\Delta_R(k)$ is the retarded propagator we introduced in section 2.3

$$\Delta_R(k) = \frac{i}{2\omega_k}\left[\frac{1}{k_0-\omega_k-i\epsilon}-\frac{1}{k_0+\omega_k-i\epsilon}\right] = \frac{i}{(k_0-i\epsilon)^2-\omega_k^2}. \tag{2.109}$$

Unlike the Feynman propagator, which has one pole above and one pole below the real axis, the retarded propagator has both poles above the real axis, namely at $k_0 = \pm\omega_k + i\epsilon$. We can insert this in our expression for the amplitude

$$i\mathcal{M} = -\frac{\lambda^2}{2}\int\frac{d^4k}{(2\pi)^4}\left[\Delta_R(k)+\frac{\pi}{\omega_k}\delta(k_0-\omega_k)\right]\left[\Delta_R(k-p)+\frac{\pi}{\omega_{k-p}}\delta(k_0-p_0-\omega_k)\right]. \tag{2.110}$$

Now the term $\Delta_R(k-p)\Delta_R(p)$ only has poles above the real axis, so we can close the contour from below to see that this integral is zero. The integral over $\delta(k_0-p_0-\omega_{k-p})\delta(k_0-\omega_k)$ is also zero since we cannot satisfy both delta functions simultaneously. This is easily seen by going to the frame where $\mathbf{p}=0$, such that k_0 must satisfy $k_0=\omega_k$ and $k_0 = p_0+\omega_k$, which it cannot. We are left with the integral

$$i\mathcal{M} = -\frac{\lambda^2}{2}\int\frac{d^4k}{(2\pi)^4}\left[\Delta_R(k-p)\frac{\pi}{\omega_k}\delta(k_0-\omega_k)+\Delta_R(k)\frac{\pi}{\omega_{k-p}}\delta(k_0-p_0-\omega_k)\right]. \tag{2.111}$$

We can turn the retarded propagators back to Feynman propagators since according to (2.108) we have $\Delta_R(k) = \Delta_F(k) - \frac{\pi}{\omega_k}\delta(k_0-\omega_k)$, but once again the terms proportional to the delta functions drop out for the same reasons as before. We are left with

$$i\mathcal{M} = -\frac{\lambda^2}{2}\int\frac{d^4k}{(2\pi)^4}\left[\Delta_F(k-p)\frac{\pi}{\omega_k}\delta(k_0-\omega_k)+\Delta_F(k)\frac{\pi}{\omega_{k-p}}\delta(k_0-p_0-\omega_k)\right]. \tag{2.112}$$

Now we turn to the evaluation of the imaginary part of this amplitude, which must come from the Feynman propagators since the delta functions are real. We have

$$\begin{aligned}\Im\mathcal{M} =& -\frac{\lambda^2}{2}\int\frac{d^4k}{(2\pi)^2}\left(\Im\left[-i\Delta_F(k-p)\right]\frac{\pi}{\omega_k}\delta(k_0-\omega_k)+\Im\left[-i\Delta_F(k)\right]\frac{\pi}{\omega_{k-p}}\delta(k_0-p_0-\omega_{k-p})\right)\\ =& \frac{\lambda^2}{2}\int\frac{d^4k}{(2\pi)^2}\left(\pi\delta\left((k-p)^2-m^2\right)\frac{\pi}{\omega_k}\delta(k_0-\omega_k)+\pi\delta\left(k^2-m^2\right)\frac{\pi}{\omega_{k-p}}\delta(k_0-p_0-\omega_{k-p})\right),\end{aligned} \tag{2.113}$$

where the second term is zero for the usual reasons. Now we use

$$\frac{1}{2\omega_k}\delta(k_0-\omega_k)=\delta(k^2-m^2)-\frac{1}{2\omega_k}\delta(k_0+\omega_k), \tag{2.114}$$

as well as $\int dk_0\delta((p-k)^2-m^2)\delta(k_0+\omega_k)=0$ to find

$$2\Im\mathcal{M}=-\frac{\lambda^2}{2}\int\frac{d^4k}{(2\pi)^4}(-2\pi i)\delta((p-k)^2-m^2)(-2\pi i)\delta(k^2-m^2). \tag{2.115}$$

This means one can compute the imaginary part of the amplitude by setting intermediate particles on-shell.

This procedure can be generalized and performed for any amplitude, in which case it can be achieved by applying the so called *Cutkosky cutting rules*. These rules form an algorithm that allows us to compute the imaginary part of an amplitude. In this context the word *cut* simply means a specific way of putting intermediate particles on-shell. A usual representation of a cut in a Feynman diagram can be seen in figure 10.

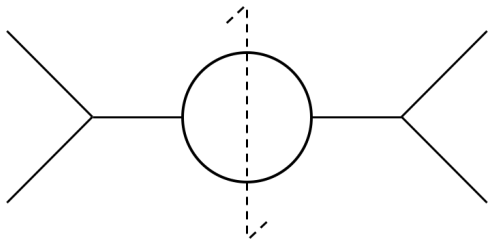

Figure 10: Representation of a cut

The algorithm goes as follows: First one cuts in all possible ways of putting intermediate particles on-shell while still respecting momentum conservation. Then for each cut one substitutes the cut propagators by $-2\pi i\delta(k^2-m^2)\theta(k_0)$, meaning they are put on-shell. We then sum over all possible cuts and the result is precisely $-2\Im\mathcal{M}$, i.e. the discontinuity of the diagram.

As an example of an application of this powerful tool we will confirm the optical theorem by following the recipe explained above. Let us change the term $\lambda\phi^3$ in Lagrangian (2.104) to $\lambda\phi\chi^2$ and add the kinetic terms for a scalar χ with mass m_χ. We assume that $m_\phi>2m_\chi$ so the decay $\phi\to\chi\chi$ is kinematically allowed.

We want to compute the same diagram as before but with particle χ in the loop, as opposed to ϕ. It is easy to see the expression for the amplitude will remain the same. We make the cut over the loop and make the replacements according to the cutting rules to get

$$2\Im\mathcal{M}=-\frac{\lambda^2}{2}\int\frac{d^4k}{(2\pi)^4}(-2\pi i)\delta((p-k)^2-m^2)(-2\pi i)\delta(k^2-m^2). \tag{2.116}$$

Now we make the change of variables $k=q_2$ and $p-k=q_1$ and insert $1=\int d^4q_1\delta^{(4)}(p-q_1-q_2)$ to get

$$2\Im\mathcal{M}=\frac{\lambda^2}{2}\int\frac{d^4q_1}{(2\pi)^4}\int\frac{d^4q_2}{(2\pi)^4}(2\pi)^2\delta(q_1^2-m^2)\delta(q_2^2-m^2)(2\pi)^4\delta^{(4)}(p-q_1-q_2) \tag{2.117}$$

Since $p^0 > 0$ we must also have $q_1^0, q_2^0 > 0$. Then we can use

$$\int \frac{d^4k}{(2\pi)^4} 2\pi\delta(k^2 - m^2) = \int \frac{d^3k}{(2\pi)^3} \frac{1}{2\omega_k}, \tag{2.118}$$

which leaves us with

$$\begin{aligned} \Im\mathcal{M} =& \frac{1}{2}\frac{\lambda^2}{2} \int \frac{d^3q_1}{(2\pi)^3} \frac{1}{2\omega_{q_1}} \frac{d^3q_2}{(2\pi)^3} \frac{1}{2\omega_{q_2}} (2\pi)^4 \delta(p - q_1 - q_2) \\ =& M\Gamma(\phi \to \chi\chi), \end{aligned} \tag{2.119}$$

where we used the definition of the partial width (2.100). We see this is exactly the same result one gets from applying the optical theorem to a self-energy diagram.

3 Particle Masses and Renormalization Schemes

3.1. Stable and Unstable Particles

We know that tree-level diagrams are associated with a perturbative expansion of the classical theory, e.g. QED cross sections computed at tree level are identical to those of the scattering of classical point-like charges. One can easily verify this by reintroducing $\hbar$ (which is usually set to unity in QFT calculations, as is the case with this thesis) and noting that particle loops in QFT are proportional to $\hbar$, indicating we are considering quantum effects. Since tree-level amplitudes are usually not sufficient for our purposes we are forced to take into account these quantum corrections in our theoretical results.

As we saw in chapter 2 only the modes that obey the dispersion relation $E = \sqrt{\mathbf{k}^2 + m^2}$ survive after an infinite amount of time, since they are related to the pole of the propagator. On the other hand this also means we can define the physical mass of the particle as the pole position of k^2 in the two-point Green's function, since propagation at infinite times is what we associate with physical particles. At tree-level this pole corresponds to the bare parameter m appearing in the Lagrangian, but this ceases to be the case when we include quantum corrections. To see this let us consider all *one particle irreducible* diagrams, that is, all the diagrams that cannot be divided into two by cutting only one internal line. Since we are considering these diagrams in the context of the two-point Green's function they are also *self-energy* diagrams and we denote their overall sum by $i\Sigma(p)$. So to obtain the so called *full-propagator* which corresponds to the physical propagation of a particle, we have to add up all the possible diagrams contributing to the two-point function, that is, we want to compute the sum:

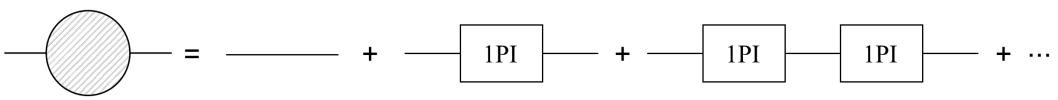

Figure 11: Representation of the series of 1P1 insertions

We denote the bare propagator of the theory $\Delta_0(p)$ and the full propagator by $\Delta(p)$ we see that this sum corresponds to

$$\begin{aligned}\Delta(p) =&\Delta_0(p) + \Delta_0(p)\Sigma(p)\Delta_0(p) + \Delta_0(p)\Sigma(p)\Delta_0(p)\Sigma(p)\Delta_0(p) + ... \\ =&\Delta_0(p)\left[\sum_{n=0}\left(\Sigma(p)\Delta_0(p)\right)^n\right] \\ =&\frac{\Delta_0(p)}{1-\Sigma(p)\Delta_0(p)},\end{aligned} \tag{3.1}$$

where we used the result for an infinite geometric series $\sum_{n=0} x^n = \frac{1}{1-x}$, for $|x| < 1$.

We have assumed that $|\Sigma(p)\Delta_0(p)| < 1$ in order to satisfy d'Alembert's convergence criterion. If this is not the case then we say perturbation theory *breaks down* since for every insertion of $1PI$ diagrams the terms become more dominant and as such it makes no sense to truncate the series up to a certain order. What one can do in this situation will be a main point of discussion of chapter 4, as well as the problems arising from following that procedure. For a scalar, whose bare propagator equals $\Delta_0(p) = i[p^2 - m^2]^{-1}$, equation (3.1) becomes

$$\Delta(p) = \frac{i}{p^2 - m^2 + \Sigma(p)}. \tag{3.2}$$

The definition of the physical mass M_p is then the solution to the equation

$$M_p^2 - m^2 + \Sigma(M_p) = 0. \tag{3.3}$$

Until now we have made no considerations about the stability of the particle in question but this becomes an important aspect from now on. In chapter 2 we presented the Cutkosky cutting rules and derived the generalized optical theorem, valid for S-matrix elements as well as for any amplitudes $\mathcal{M}$. This is particularly convenient since unstable particles do not occur as assymptotic states. As we for described in chapter 2, for the special case where the final and initial state are the same the imaginary part of the amplitude is given by

$$\Im\mathcal{M}(A \to A) = \frac{1}{2}\sum_X \int d\Pi_X (2\pi)^4 \delta^{(4)}(p_A - p_X)|\mathcal{M}(A \to X)|^2 \tag{3.4}$$

and then from the definition of partial width (2.100), the imaginary part of the self-energy becomes

$$\Im\mathcal{M}(A \to A) = m_A \Gamma_{total}. \tag{3.5}$$

This illustrates a significant difference between stable and unstable particles. Stable particles by definition do not decay, which means their width Γ is 0, as we explained in chapter 2. Hence the self energy of a stable particle is purely real. For particles that have width, i.e. unstable particles, the self energy does have an imaginary component. An important consequence of this is that for unstable particles the pole of the Dyson propagator will be complex, and so will the solution of equation (3.3). Obviously the physical mass of a particle cannot be complex so we

must slightly amend its definition be the solution of the equation

$$M_p^2 - m^2 + \Re\Sigma(M_p^2) = 0, \tag{3.6}$$

which is valid for both stable and unstable particles. We call this definition of mass the *real pole mass*, which is physical and does not depend on the renormalization scheme used. Near the pole the full propagator (3.2) takes the form

$$\Delta(p) = \frac{i}{p^2 - M_p^2 + i\Im\Sigma(M_p^2)} \tag{3.7}$$

$$= \frac{i}{p^2 - M_p^2 + iM_p\Gamma_{total}} \tag{3.8}$$

When this propagator appears in the s-channel of an amplitude then the cross section in a region close to the pole takes the form

$$\sigma \propto \left| \frac{i}{p^2 - M_p^2 + iM_p\Gamma_{total}} \right|^2 = \frac{1}{(p^2 - M_p^2)^2 + (M_p\Gamma_{total})^2}, \tag{3.9}$$

which is the so-called Breit-Wigner distribution and is usually a good description of a resonance occurring at M_p. When the width of the resonant particle is small compared to its mass there is very useful and widely applied approximation one can make, dubbed the *narrow-width approximation*, which we presently address.

3.1.1 Narrow Width Approximation

Although most elementary particles are unstable only the W, the Z and the top quark are considered to have large widths, or more rigorously, widths that are not sufficiently small compared to their mass. For all other unstable particles we can take the limit $\frac{\Gamma}{M} \to 0$ as a reasonable approximation. We can make use of the definition of the Dirac delta in equation (2.102) and apply it to the Breit-Wigner distribution (3.9)

$$\left|\Delta_{NWA}(p^2)\right|^2 = \frac{1}{\Gamma_{total}M_p^3} \frac{\Gamma_{total}/M_p}{\left(\frac{p^2-M_p^2}{M_p^2}\right)^2 + \left(\frac{\Gamma_{total}}{M_p}\right)^2} = \frac{\pi}{\Gamma_{total}M_p^3}\delta\left(\frac{p^2 - M_p^2}{M_p^2}\right) = \frac{\pi}{\Gamma_{total}M_p}\delta(p^2 - M_p^2), \tag{3.10}$$

meaning that near a resonance we can treat the particle as being on-shell. Another important aspect of the narrow width approximation is that production and decay of a resonance can be treated as seperate processes because the overall cross section factorizes into an on-shell production cross section and subsequent decay. For a scalar field this is easily shown by writing

the cross section for the generic process present in figure 12 as

$$\begin{aligned}\sigma(A \to B + C) =& \frac{1}{2s} \int d\Pi_p \, d\Pi_q |\mathcal{M}(A \to B + C)|^2 (2\pi)^4 \delta^{(4)} \left(\sum k - \sum p - \sum q \right) \\ =& \frac{1}{2s} \int d\Pi_p \, d\Pi_q \left| \mathcal{M}_{prod} \left(p_i^2, \left[\sum q_i \right]^2 \right) \right|^2 \left| \Delta_{NWA} \left(\left[\sum q_i \right]^2 \right) \right|^2 \\ & \left| \mathcal{M}_{decay} \left(\left[\sum q_i \right]^2 \right) \right|^2 (2\pi)^4 \delta^{(4)} \left(\sum k - \sum p - \sum q \right)\end{aligned} \tag{3.11}$$

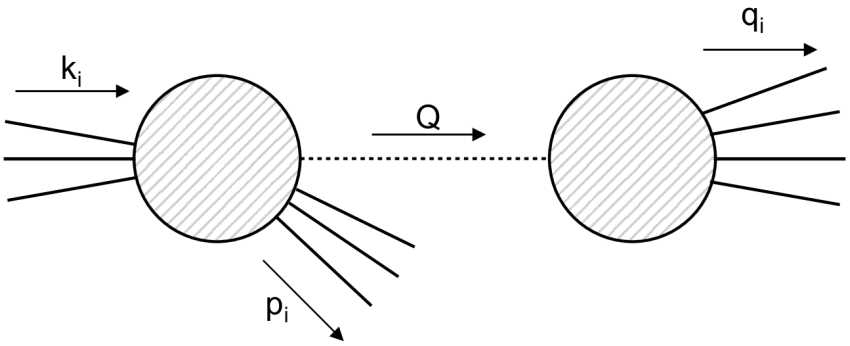

Figure 12: Generic process with production and decay process with a single scalar ocurring in the s channel

Now we introduce the unit factor $1 = \int \frac{d^4Q}{(2\pi)^4} (2\pi)^4 \delta^{(4)}(Q - \sum q_i)$ and also plug (3.10) which allows us to write

$$\begin{aligned}\sigma(A \to B + C) =& \frac{1}{2s} \int d\Pi_p \frac{d^4Q}{(2\pi)^4} 2\pi \delta(Q^2 - M_p^2) \left| \mathcal{M}_{prod} \left(p_i^2, Q^2 \right]^2 \right) (2\pi)^4 \delta^{(4)} \left(\sum k_i - \sum p_i - Q \right) \\ & \frac{1}{2M_p} \int d\Pi_q \left| \mathcal{M}_{decay} \left(\left[\sum q_i \right]^2 \right) \right|^2 (2\pi) \delta^{(4)} \left(\sum k_i - \sum p_i - \sum q_i \right)\end{aligned} \tag{3.12}$$

Noting that $\frac{d^4Q}{(2\pi)^4} 2\pi \delta(Q^2 - M_p^2) = d\Pi_Q$ and using our definitions for the cross section and the width (2.100) we see this becomes

$$\sigma(A \to B + C) = \sigma(A \to B + X) \frac{\Gamma(X \to C)}{\Gamma_{total}}. \tag{3.13}$$

So we have proven that in the NWA the total cross section decouples into the product of the production cross section and of the branching ratio $\frac{\Gamma(X \to C)}{\Gamma_{total}}$. Since resonant regions are dominant, the NWA provides a consistent theoretical method to extract the relevant part of the amplitude since it allows us to neglect non-resonant and non-factorizable contributions to the cross section. This makes computations considerably simpler. Applying the NWA to non-scalar particles is not as straightforward since there are correlation effects between the production and decay processes. However one can still choose to neglect the correlation between spins, in which case one gets back the standard factorization of the NWA. More specifically, for the

schematic production and decay of a vector-boson seen in figure 12 one chooses to approximate

$$\left|\mathcal{M}^{\mu}_{prod}\left(\eta_{\mu\nu}-\frac{Q_\mu Q_\nu}{m_V^2}\right)\mathcal{M}^{\nu}_{decay}\right|^2=\left|\sum_{\lambda}\mathcal{M}^{\mu}_{prod}\bar{\epsilon}^{\lambda}_{\mu}\epsilon^{\lambda}_{\nu}\mathcal{M}^{\nu}_{decay}\right|^2 \tag{3.14}$$

by

$$\frac{1}{3}\sum_{\lambda_1,\lambda_2}\left|\mathcal{M}^{\mu}_{prod}\bar{\epsilon}^{\lambda_1}_{\mu}\epsilon^{\lambda_2}_{\nu}\mathcal{M}^{\nu}_{decay}\right|^2, \tag{3.15}$$

where we made use of the polarization sum identity

$$\sum_{\lambda}\bar{\epsilon}^{\lambda}_{\mu}\epsilon^{\lambda}_{\nu}=-\eta_{\mu\nu}+\frac{k_\mu k_\nu}{m_V^2}. \tag{3.16}$$

Analogously for fermions, neglecting spin correlation effects in the generic production and decay process of figure 12 means approximating

$$|\mathcal{M}_{prod}(\not{Q}+m_f)\mathcal{M}_{decay}|^2=\left|\sum_{s}\mathcal{M}_{prod}u^s(q)\overline{u}^s(q)\mathcal{M}_{decay}\right|^2 \tag{3.17}$$

by

$$\frac{1}{2}\sum_{s,r}\left|\mathcal{M}_{prod}u^s(q)\right|^2\left|\overline{u}^r(q)\mathcal{M}_{decay}\right|^2, \tag{3.18}$$

where we used the result for the sum over particle spinors

$$\sum_{s}u(p)\overline{u}(p)=\not{p}+m_f. \tag{3.19}$$

As we mentioned before, making the above approximations leads to the standard NWA factorization σ_{prod} times the branching ratio. There are of course drawbacks of employing the NWA , such as neglecting off-shell effects. For a detailed discussion of the accuracy of the NWA we refer the reader to [7].

In the following sections we will introduce two renormalization schemes in the pedagogical context of QED mass renormalization. Ultimately our main interest lies in the Complex Mass Scheme (CMS), but first we introduce two standard schemes - On-shell renormalization and $\overline{MS}$ - which will serve as an introduction and a good reference point to the CMS.

3.2. On-Shell Renormalization Scheme

We have seen how radiative corrections displace the pole of the propagator of a field and therefore influence the physical mass of such field. It is therefore useful to study mass renormalization, which is what we will do in this section in the context of QED. This will allow us to introduce and discuss the notion of *renormalization schemes* and pave the way to our discussion about the Complex Mass Scheme. Before we delve into the details of any particular scheme

we have to compute the electron self-energy diagram - seen in figure 13- which corrects the electron tree level propagator.

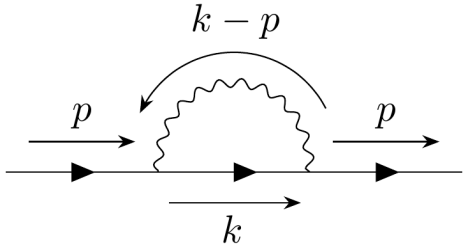

Figure 13: QED fermion self-energy diagram

In the Feynman-'t Hooft gauge this diagram equals

$$i\Sigma(\not{p}) = -e^2 \int \frac{d^n k}{(2\pi)^n} \gamma_\mu \frac{i(\not{k}+m)}{k^2-m^2} \gamma^\mu \frac{-i}{(p-k)^2}. \tag{3.20}$$

To evaluate this we use that $\gamma^\mu \gamma_\rho \gamma_\mu = (2-n)\gamma_\rho$ and recall the Feynman trick

$$\frac{1}{AB} = \int_0^1 dx \frac{1}{[Ax + B(1-x)]^2}, \tag{3.21}$$

so that we get

$$i\Sigma(\not{p}) = -e^2 \int \frac{d^n k}{(2\pi)^n} \frac{(n-2)\not{k} - nm^2}{[(p-k)^2 x + (1-x)(k^2-m^2)]^2}. \tag{3.22}$$

We see that the denominator becomes $(k-xp)+(1-x)[xp^2-m^2]$ so we make the shift $k \to k+xp$ and drop the term in the numerator proportional to k, since the denominator is symmetric under $k \to -k$ and the integral is over all space. The result then is

$$i\Sigma(\not{p}) = -e^2 \int_0^1 dx \int \frac{d^n k}{(2\pi)^n} \frac{(n-2)x\not{p} - nm^2}{[k^2-\Delta^2]^2}, \tag{3.23}$$

with $\Delta^2 = (1-x)[m^2 - xp^2]$. We see that for large k the integral goes with k^{-1} so this diagram is logarithmically divergent. In order to regulate this divergence we will use dimensional regularization, which consists in taking $n = 4-2\epsilon$. Now we make use of the formula for this type of integral

$$\int \frac{d^n k}{(2\pi)^n} \frac{1}{[k^2-\Delta^2]^\alpha} = i \frac{(-1)^\alpha}{(4\pi)^{\frac{n}{2}-\alpha}} \frac{\Gamma(\alpha - \frac{n}{2})}{\Gamma(\alpha)} (\Delta^2)^{\frac{n}{2}-\alpha}. \tag{3.24}$$

In our case $\alpha = 2$, which yields

$$i\Sigma(\not{p}) = 2e^2 \frac{\mu^{2\epsilon}}{16\pi^2} \Gamma(\epsilon)(4\pi)^\epsilon \int_0^1 dx (x\not{p} - 2m)[\Delta^2(x)]^{-\epsilon} \tag{3.25}$$

Now we use that $\Gamma(\epsilon) = \frac{1}{\epsilon}\Gamma(1+\epsilon)$ and $\Gamma(1+\epsilon) \sim e^{-\epsilon\gamma_E}$ to write

$$\begin{aligned} i\Sigma(\not{p}) =& 2ie^2 \frac{1}{16\pi^2}\frac{1}{\epsilon}\int_0^1 dx(x\not{p} - 2m)\left(\frac{4\pi e^{\gamma_E}\mu^2}{\Delta^2(x)}\right)^{\epsilon} \\ =& 2ie^2 \frac{1}{16\pi^2}\frac{1}{\epsilon}\int_0^1 dx(x\not{p} - 2m)\left(1 + \epsilon\ln\left(\frac{\tilde{\mu}^2}{\Delta^2(x)}\right)\right), \end{aligned} \tag{3.26}$$

where we defined $\tilde{\mu}^2 = 4\pi e^{\gamma_E}\mu^2$, and used that $a^{\epsilon} = e^{\epsilon \ln a} = 1 + \epsilon \ln a + \mathcal{O}(\epsilon^2)$. Finally we get that

$$\Sigma(\not{p}) = \frac{\alpha}{4\pi}\frac{1}{\epsilon}(\not{p} - 4m) + \frac{\alpha}{2\pi}\int_0^1 dx\left(\ln\left(\frac{\tilde{\mu}}{\Delta^2(x)}\right)\right), \tag{3.27}$$

with the first term being divergent when $\epsilon \to 0$. Now we are ready to begin the renormalization procedure. We note that since there are divergences proportional to the mass and to $\not{p}$ we will have two quantities to renormalize. The infinity proportional to the mass will naturally be absorbed by the mass parameter, whereas the divergence proportional to $\not{p}$ will be absorbed by the field ψ. The QED Lagrangian written in terms of bare quantities is

$$\mathcal{L}_{QED} = -F_{\mu\nu}^2 + i\overline{\psi}_0\not{\partial}\psi_0 - m_0\overline{\psi}_0\psi + eA_\mu\overline{\psi}_0\gamma^\mu\psi_0. \tag{3.28}$$

Now we renormalize the bare mass and the field ψ

$$\begin{aligned} m_0 =& Z_m m_R \\ \psi_0 =& \sqrt{Z_\psi}\psi. \end{aligned} \tag{3.29}$$

and write $Z_\psi = 1 + \delta_\psi$ and $Z_m = 1 + \delta_m$, where δ_ψ and δ_m are the coefficients of the so called *counterterms*, which we will choose strategically in order to cancel the divergences coming from the self energy diagram. In terms of the renormalized quantities the QED Lagrangian then reads

$$\begin{aligned} \mathcal{L}_{QED} =& -F_{\mu\nu}^2 + iZ_\psi\overline{\psi}\not{\partial}\psi - m_R Z_\psi Z_m\overline{\psi}\psi + eA_\mu\overline{\psi}\gamma^\mu\psi \\ =& -F_{\mu\nu}^2 + i\overline{\psi}\not{\partial}\psi - m_R\overline{\psi}\psi + eA_\mu\overline{\psi}\gamma^\mu\psi + \Delta\mathcal{L}_m + \Delta\mathcal{L}_{\not{p}}, \end{aligned} \tag{3.30}$$

where $\Delta\mathcal{L}_m$ and $\Delta\mathcal{L}_{\not{p}}$ are the counterterms given by

$$\begin{aligned} \Delta\mathcal{L}_{\not{p}} =& \delta_\psi\overline{\psi}\not{p}\psi \\ \Delta\mathcal{L}_m =& (\delta_\psi + \delta_m)m_R\overline{\psi}\psi, \end{aligned} \tag{3.31}$$

where we note that since we expect $\delta_m, \delta_\psi \sim \alpha$ we only kept terms proportional to α such that $(1+\delta_m)(1+\delta_\psi) = 1 + \delta_m + \delta_\psi + \mathcal{O}(\alpha^2)$. We treat the counterterms as interactions so if we now compute the self energy in terms of the renormalized parameters - which we denote by $\Sigma_R(\not{p})$- we have to add these interaction terms to previously calculated expression for the self energy.

We then get

$$\begin{aligned}\Sigma_R(\not{p}) =&\Sigma(\not{p}) + \delta_\psi \not{p} - (\delta_\psi + \delta_m) m_R \\ =&\frac{\alpha}{4\pi}\frac{\not{p}}{\epsilon} - \frac{\alpha}{\pi}\frac{m_R}{\epsilon} + \delta_\psi \not{p} - (\delta_\psi + \delta_m) m_R + \text{ finite terms.}\end{aligned} \tag{3.32}$$

We see that by choosing

$$\delta_\psi = -\frac{\alpha}{\pi}\frac{1}{4\epsilon} \qquad \text{and} \qquad \delta_m = -\frac{3\alpha}{4\pi}\frac{1}{\epsilon} \tag{3.33}$$

one cancels the divergent part in the renormalized self-energy $\Sigma_R(\not{p})$. We can of course also include finite terms in our counterterms (3.33) and they would still cancel the divergence. There is then a certain ambiguity in choosing such finite terms and which ones we end up choosing define the *renormalization scheme*. Although physical results should of course be independent of the renormalization scheme used, depending on the circunstances some are much more convenient than others. The two most used schemes are the On-Shell Renormalization scheme (OSRS), which we will address in a moment, and the $\overline{MS}$ which we will discuss in the following section.

To begin our discussion of the on-shell scheme we recall from expression (3.1) that after we perform the Dyson sum the full propagator (in this case for the electron) is

$$\Delta(\not{p}) = \frac{i}{\not{p} - m_R + \Sigma_R(\not{p})}, \tag{3.34}$$

with the renormalized self energy given by (3.32). We know the physical mass is defined by the real pole of the propagator. In this case, since the electron is a stable particle definitions (3.3) and (3.6) are equivalent. In order to have a pole when $\not{p} = M_p$ we see that the renormalized self-energy must satisfy

$$\Sigma_R(M_p) = m_R - M_p. \tag{3.35}$$

This pole must also have residue i, which means

$$\lim_{\not{p}\to M_p} [\not{p} - M_p] \frac{i}{\not{p} - m_R + \Sigma_R(\not{p})} = \lim_{\not{p}\to M_p} \frac{i}{1 + \frac{d}{d\not{p}}\Sigma_R(\not{p})} = i \quad \Rightarrow \frac{d\Sigma_R}{d\not{p}}(M_p) = 0, \tag{3.36}$$

where we used l'Hopital's rule in the last step. As of yet we have not specified any renormalization scheme, these are still two general conditions that define the pole mass independently of the scheme.

We are now in the condition to introduce the OSRS. The point of the on-shell scheme is that the *renormalized mass equal the physical mass*, i.e. $m_R = M_p$. Thus, in this scheme we have what are called the on-shell renormalization conditions

$$\boxed{\Sigma_R(M_p) = 0 \qquad \text{and} \qquad \frac{d\Sigma_R}{d\not{p}}(M_p) = 0} \tag{3.37}$$

By applying these conditions to the expression of the renormalized self-energy (3.32) we get

$$\begin{aligned} 0 =& \Sigma(M_p) - \delta_m M_p \\ 0 =& \frac{d\Sigma}{d\not{p}}(M_p) + \delta_\psi, \end{aligned} \tag{3.38}$$

yielding

$$\begin{aligned} \delta_\psi =& -\frac{d\Sigma}{d\not{p}}(M_p) \\ \delta_m =& \frac{\Sigma(M_p)}{M_p}. \end{aligned} \tag{3.39}$$

We use expression (3.26) to compute $\frac{d}{d\not{p}}\Sigma(\not{p})$ and obtain

$$\frac{d}{d\not{p}}\Sigma(\not{p}) = \frac{\alpha}{2\pi}\frac{1}{\epsilon}\int_0^1 dx x\left[1 + \epsilon \ln\left(\frac{\tilde{\mu}}{\Delta^2(x)}\right)\right] + 2\epsilon x \frac{(x\not{p} - 2M_p)}{M_p^2 - xp^2}, \tag{3.40}$$

where we recall that $\Delta^2(x) = (1-x)[m^2 - xp^2]$. This integral has a infrared divergence at $x = 1$, so we introduce a photon mass m_γ to regulate this divergence. One need not worry since physical observables are IR finite and the dependence on m_γ drops out. Thus, we rewrite the self energy as

$$i\Sigma(\not{p}) = 2ie^2 \frac{1}{16\pi^2}\frac{1}{\epsilon}\int_0^1 dx (x\not{p} - 2m)\left[1 + \epsilon \ln\left(\frac{\tilde{\mu}}{\Delta^2(x) + xm_\gamma^2}\right)\right] \tag{3.41}$$

to obtain

$$\frac{d\Sigma}{d\not{p}}(M_p) = \frac{\alpha}{4\pi}\left(\frac{1}{\epsilon} + \ln\left(\frac{\tilde{\mu}}{M_p^2}\right) + 2\ln\left(\frac{m_\gamma^2}{M_p^2}\right)\right). \tag{3.42}$$

This leads to the following results for the counterterms δ_ψ and δ_m

$$\begin{aligned} \delta_\psi =& -\frac{\alpha}{4\pi}\left(\frac{1}{\epsilon} + \ln\left(\frac{\tilde{\mu}}{M_p^2}\right) + 2\ln\left(\frac{m_\gamma^2}{M_p^2}\right) + 5\right) \\ \delta_m =& \frac{\alpha}{4\pi}\left[-\frac{3}{\epsilon} - 3\ln\left(\frac{\tilde{\mu}}{m_P^2}\right) - 5\right] \end{aligned} \tag{3.43}$$

3.3. $\overline{MS}$ Scheme

In the scheme known as minimal subtraction (MS) the only requirement is that the counterterms have no finite parts. This we have already done when we first explained how chosing the countermens would cancel the divergence. The counterterms provided in this scheme are thus the ones from equation (3.33). However usually one uses a modified version of this scheme called *modified minimal subtraction* ($\overline{MS}$), the only difference being that one also subtracts the finite terms γ_E and $\ln(4\pi)$ coming from $\tilde{\mu}^2 = \mu e^{\gamma_E} 4\pi$, which turns $\tilde{\mu}$ into μ in dimensionally regularized amplitudes. To see how this works we recall from expression (3.26) that the

unrenormalized self energy is given by

$$\begin{aligned}\Sigma(\not{p}) =&\frac{\alpha}{2\pi}\int_0^1 dx(x\not{p}-2m_R)\left[\frac{1}{\epsilon}+\ln\left(\frac{4\pi e^{-\gamma_E}\mu^2}{\Delta^2(x)}\right)\right]\\ =&\frac{\alpha}{2\pi}\int_0^1 dx(x\not{p}-2m_R)\left[\frac{1}{\epsilon}-\gamma_E+\ln(4\pi)+\ln\left(\frac{\mu^2}{\Delta^2(x)}\right)\right]\\ =&\frac{\alpha}{4\pi}\left[\frac{1}{\epsilon}+\gamma_E+\ln(4\pi)\right]\not{p}-\frac{\alpha}{\pi}\left[\frac{1}{\epsilon}-\gamma_E+\ln(4\pi)\right]m_R+\frac{\alpha}{2\pi}\int_0^1 dx(x\not{p}-2m)\ln\left(\frac{\mu^2}{\Delta^2(x)}\right)\end{aligned} \tag{3.44}$$

Now again we use that after renormalizing the fields and mass the renormalized seld energy is given by $\Sigma_R(\not{p}) = \Sigma(\not{p}) + \delta_\psi \not{p} - (\delta_\psi + \delta_m)m_R$, but this time we choose the counterterms such that the terms $\ln(4\pi)$ and γ_E also vanish. This yields

$$\begin{aligned}\delta_\psi =&-\frac{\alpha}{4\pi}\left[\frac{1}{\epsilon}+\gamma_E+\ln(4\pi)\right]\\ \delta_m =&-\frac{3\alpha}{4\pi}\left[\frac{1}{\epsilon}+\gamma_E+\ln(4\pi)\right],\end{aligned} \tag{3.45}$$

which makes $\Sigma_R(\not{p})$ equal

$$\Sigma_R(\not{p}) = \frac{\alpha}{2\pi}\int_0^1 dx(x\not{p}-2m_R)\ln\left(\frac{\mu^2}{\Delta^2(x)}\right). \tag{3.46}$$

This last expression is UV finite and depends on μ instead of $\tilde{\mu}$, as we claimed it would. When using this scheme the renormalized mass m_R is called the $\overline{MS}$ mass, which contrary to the on-shell scheme does not coincide with the pole-mass M_p. The full electron propagator in this scheme is

$$\Delta(\not{p}) = \frac{i}{\not{p} - m_R + \Sigma_R(\not{p})}, \tag{3.47}$$

so we see that by requiring that the pole be at M_p we can relate the on-shell scheme mass with the $\overline{MS}$ mass. We want

$$M_p - m_R + \Sigma_R(M_p) = 0 \tag{3.48}$$

Now we use that m_R and M_p only differ in terms of order α, since they are both related to the bare mass by $M_p + M_p\,\delta_{OSS} = m_0 = m_R + m_R\,\delta_{MS}$ and $\delta_{OSS},\ \delta_{MS} \sim \alpha$. Now we evaluate the integral

$$\int_0^1 dx(x-2)M_p\ln\left(\frac{\mu^2}{M_p^2(1-x)^2}\right) = -\frac{3}{2}M_p\ln\left(\frac{\mu^2}{M_P^2}\right) - \frac{5}{2}. \tag{3.49}$$

So we finally obtain the relation between the $\overline{MS}$ mass and the physical mass

$$m_R = M_p\left[1-\frac{\alpha}{4\pi}\left(3\ln\left(\frac{\mu^2}{M_p^2}\right)+5\right)\right]+\mathcal{O}(\alpha). \tag{3.50}$$

We see in expression (3.50) that the $\overline{MS}$ mass m_R (which is often represented as $\overline{m}(\mu)$ in the literature) depends on the renormalization scale μ. The fact that physical observables cannot depend on this parameter is what leads us to the renormalization group equation $\frac{d\mathcal{O}}{d(\ln \mu)} = 0$, which is an important constraint appearing in many contexts. The reason why this seemingly arbitrary mass is important is because the $\overline{MS}$ scheme is much simpler to use when performing calculations than the on-shell scheme. When computing loop-amplitudes it is easier to use the $\overline{MS}$, and make the conversion to the physical mass afterwards, than to use the on shell scheme mass every step of the way. Moreover, numerically speaking the physical and the $\overline{MS}$ mass are quite close when μ is chosen to be close to M_p - the notable exception being the top quark since $M_p \sim 173$ GeV but $m_R \sim 163$ GeV. Also, since quarks are subject to color confinement they do not appear as assymptotic states. This means that they do not have a well defined pole-mass so the $\overline{MS}$ mass is usually preferred for quarks. The quark masses are displayed in the appropriate scheme in table 1. We note that for the light-quarks the $\overline{MS}$ mass is taken at $\mu = 2$ GeV, while for the heavy quarks the renormalization scale is set at the value of the running mass. This can be achieved by plotting $\overline{m}(\mu)$ and μ - the intersection point of the two curves is precisely the value $\overline{m}(\overline{m})$.

Quark type	Quark mass	Scheme
u	$\overline{m}_u(2\text{ GeV}) = 2.49^{+0.81}_{-0.79}$ MeV	$\overline{MS}$
d	$\overline{m}_d(2\text{ GeV}) = 5.05^{+0.75}_{-0.95}$ MeV	$\overline{MS}$
s	$\overline{m}_s(2\text{ GeV}) = 101^{+29}_{-21}$ MeV	$\overline{MS}$
c	$\overline{m}_c(\overline{m}_c) = 1.27^{+0.07}_{-0.09}$ GeV	$\overline{MS}$
b	$\overline{m}_b(\overline{m}_b) = 4.19^{+0.18}_{-0.06}$ GeV	$\overline{MS}$
t	$m_t = 172 \pm 1.6$ GeV	On-shell

Table 1: Values for the quark masses in the appropriate scheme taken from [17]

.

On a final note, contrary to the on-shell scheme in which we claimed that - by definition - the propagator did not get radiative corrections, in the $\overline{MS}$ it does, since the renormalized self-energy is no longer set to be equal to zero.

4 Complex Mass Scheme and Gauge Invariance

4.1. Resonances and spoiled Gauge Invariance

Let us consider a generic $n_{in} \to n_{out}$ scattering process occurring through the s-channel like the one in figure 14, where n_{in} particles combine to form an unstable particle with mass M_A, which then decays. We use the on-shell scheme, such that the renormalized mass equals the physical mass M_A. Now let's say we want to compute quantum corrections up to a certain order to the internal tree level propagator of the unstable particle, which goes as $\Delta_0(p) \sim \frac{1}{p^2 - M_A^2}$.

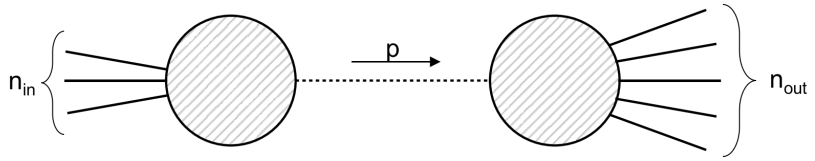

Figure 14: Generic process with n_{in} particles creating a resonant particle which then decay into n_{out} particles

As we mentioned before, this would amount to computing the series of 1PI insertions as in figure 11 up to the desired order. However a problem arises in the region where the center of mass energy comes close to the mass of the particle. We recall that for every 1PI insertion one includes a factor of

$$i\Sigma(p^2)\Delta_0(p^2) \sim i\Sigma(p^2)\frac{1}{p^2 - M_A^2}, \tag{4.1}$$

so in the region where $s \sim M_A^2$ we see that this factor diverges. This means that as we increase the order in α in our corrections, those terms become **more** dominant, as opposed to less, so truncating the series at a given order would give unreliable results. Hence in this region - called the resonance region - we say that perturbation theory **breaks down**. Resonances are then an intrinsically non-perturbative object and need to be taken care of by a non-perturbative procedure. One such procedure is precisely the Dyson summation we saw in (3.1), which in the on-shell scheme takes the form

$$\Delta(p) \sim \frac{1}{p^2 - M^2 + i\Im\Sigma_R(p^2)}. \tag{4.2}$$

One might be worried that when using the result for a geometric series to obtain (4.2) we assumed that it satisfied d'Alemberts criterium of convergence, which clearly is not the case in the resonance region. We can circumvent this formality by introducing an effective action

such that the tree-level propagator corresponds to (4.2). The point here is that we are going to assume the full propagator takes the form (4.2) over all phase-space, including the resonance region.

Now we arrive at the heart of this discussion. Results for physical observables must be gauge independent, and this independence is guaranteed order by order in perturbation theory. When computing a scattering amplitude, individual diagrams are usually gauge dependent and the overall gauge independence at a given order comes from delicate cancellations between diagrams when all the processes ocurring at that order are considered. The issue, then, is the following: when using (4.2) the expression for $\Sigma_R(p^2)$ is usually only known to a certain order in α. If we use $\Delta(p)$ in a given finite order - let's say α^n - then expanding (4.2) will produce diagrams of order α^{n+1} and higher. In order to cancel the gauge dependence we would have to add all other diagrams of order α^{n+1}, which we by definition are not. Consequently the result will be gauge dependent, which is an indicator that the renormalization scheme is incomplete.

In most cases we can use the narrow-width approximation to deal with the presence of unstable particles in perturbative calculations. As we explained in section 3.1.1 the NWA consists of approximating the resonant resummed propagator by a delta function divided by the width. In this case the troublesome denominater no longer exists so no mixing of perturbative orders occurs, meaning that the NWA provides a gauge-invariant results. However we also saw the limitations of the NWA. When one intends to study either the production of broad resonances or kinematical regions where the unstable particle is considerably off-shell one often needs to go beyond NWA. In this situation it becomes necessary to perform a complete calculation that considers off-shell effects, spin correlations as well as the interference with non resonant backgrounds. At leading order (LO) several ways have been introduced to circumvent this problem, one of which we will tackle in the upcoming sections. At next-to-leading order (NLO) one could perform a pole expansion, which does provides a gauge-invariant answer but unfortunately is only valid in the resonance region.

The modern and most widely-used procedure to treat unstable particles is called the Complex Mass Scheme (CMS), which we will introduce and discuss in detail in the next section. In short, it amounts to performing an analytical continuation in the complex plane of the Standard Model parameters that depend on the masses of the unstable particles.

4.2. Complex Mass Scheme

In the previous section we described that the appropriate treatment of resonances requires one performs a Dyson resummation of the propagator, which leads to the mixing of perturbative orders resulting in the loss of gauge invariance.

We would like to have a consistent scheme that would be valid throughout phase space and would produce gauge invariant results. We claimed that the most pragmatic way to handle this issue can be accomplished by the *Complex Mass Scheme* (CMS) [8] [10] [12] , which is a generalization of the on-shell scheme in the sense that it is an analytical continuation of the masses to the complex plane. As the name suggests, we will define the renormalized masses of the unstable particles complex in such a way that we can consider finite-width effects while

obtaining a gauge invariant result.

To do so, it is a necessary condition that no mixing of perturbative orders occurs. This can be achieved defining the renormalized mass $\hat{\mu}$ to be the complex valued pole of the resummed propagator. We perform the Dyson resummation

$$\Delta(p^2) \sim \frac{1}{p^2 - \hat{\mu}^2 + i\Sigma_R(p^2)}, \tag{4.3}$$

with $\Sigma_R(p^2)$ now being the (complex) renormalized self-energy depending on $\hat{\mu}$. To have a pole at $p^2 = \hat{\mu}^2$ implies $\Sigma_R(\hat{\mu}^2) = 0$. Analogously to what we did for the on-shell scheme,if we impose that the residue of the full propagator be equal to i we have the CMS renormalization conditions:

$$\boxed{\Sigma_R(\hat{\mu}^2) = 0 \qquad \text{and} \qquad \frac{d\Sigma_R}{dp^2}(\hat{\mu}^2) = 0} \tag{4.4}$$

these differ from the on-shell scheme conditions, which were only valid for the real part of the self energy. The CMS mass $\hat{\mu}$ is related to the on-shell scheme mass M by

$$\hat{\mu}^2 = M^2 - iM\Gamma, \tag{4.5}$$

such that $\hat{\mu}$ is the complex valued pole of (4.3), and M its real valued pole.

The way one applies this renormalization scheme is simple and quite analogous to the procedure we followed for the on-shell scheme. In fact one can start by performing the on-shell renormalization and then add and subtract an imaginary part

$$\begin{aligned} m_0^2 =& M^2 + \delta M^2 \\ =& M^2 - iM\Gamma + \delta M^2 + iM\Gamma \\ \equiv& \hat{\mu}^2 + \delta\hat{\mu}^2. \end{aligned} \tag{4.6}$$

Since the bare mass is real this implies $\Im[\hat{\mu}^2] = -\Im[\delta\hat{\mu}^2]$. Now we choose the finite parts of $\delta\hat{\mu}^2$ and of the field counterterm such that the complex self-energy satisfies the renormalization conditions (4.4).

By resumming the CMS tree level propagator one obtains the full CMS propagator. However, thanks to the renormalization conditions (4.4) the resummed propagator is the same as the tree level propagator

$$\Delta_0(p^2) \sim \frac{1}{p^2 - \hat{\mu}^2} \quad \xrightarrow[\text{Dyson}]{} \quad \Delta(p^2) \sim \frac{1}{p^2 - \hat{\mu}^2 + \Sigma_R(p^2)} = \frac{1}{p^2 - \hat{\mu}^2 + \Sigma_R(\hat{\mu}^2)} = \frac{1}{p^2 - \hat{\mu}^2} \sim \Delta_0(p^2). \tag{4.7}$$

Since $\hat{\mu}$ is a renormalized mass it must appear everywhere in the Feynman rules. This means that in the Standard Model in particular the Weinberg mixing angle must be modified to

$$\cos(\theta_W) = \frac{\hat{\mu}_W}{\hat{\mu}_Z}, \tag{4.8}$$

with $\hat{\mu}_Z^2 = M_Z^2 - iM_Z\Gamma$ and $\hat{\mu}_W^2 = M^2 - iM_W\Gamma$. From what we have seen, computing an amplitude with a resonant propagator in the CMS is formally equivalent to computing the tree-level amplitude in the bare theory, since the resummed CMS propagator has the form of a tree-level propagator. It is easy to see why we expect the results to be gauge invariant. We also see that the CMS is for unstable particles what the on-shell scheme was for stable particles. In both cases the resummed propagator has the form of the tree-level propagator, and in both cases the propagators do not receive radiative corrections since any 1P1 insertion is proportional to the renormalized self-energy which vanishes.

There are a few thing one needs to point out about the CMS. Once we have consistently introduced the complex masses everywhere in the Feynman rules gauge invariance is preserved. All relations that do not involve complex conjugation also remain valid like the Ward Identity (which is directly related to gauge invariance) and the Slavnov-Taylor identity, since the masses are only modified by analytic continuation. Then at tree-level when computing the matrix elements, independence and unitarity cancellations hold order by order in perturbation theory, even though some higher order contributions are incorporated in the complex masses.

The CMS has also been shown to maintain gauge invariance and unitarity at least at NLO. The generalization of the CMS at one-loop goes as follows. First, as we showed, the complex masses are introduced in the Lagrangian by splitting the bare masses into the CMS complex masses and complex counterterms. The former became part of the free propagator while the latter are treated as an interaction. In the SM, the complex masses are introduced for all unstable particles such as the Higgs, W and Z bosons, and the top. Independently of the imaginary part added and subtracted this does not spoil gauge invariance and unitarity cancellations are respected order by order [8]. Performing a $\mathcal{O}(\alpha)$ calculation in the CMS yields $\mathcal{O}(\alpha)$ accuracy everwhere in phase space provided the width used in the resonant propagators through the complex mass is itself computed at $\mathcal{O}(\alpha)$. This is easy to see away from resonances where expanding the propagator provides the usual perturbative expansion. At first sight the complex masses and couplings seem to violate unitarity since the Cutkosky rules used to prove unitarity order by order are no longer valid, as they assumed real masses. However since we do not change the bare Lagrangian unitarity of the overall theory is guaranteed, and unitarity violating terms are of order $\mathcal{O}(\alpha)$ in a $\mathcal{O}(\alpha^2)$ calculation. We note that this unitarity violation cannot be enhanced because the Ward and Slavnov-Taylor identities are exactly preserved. Lastly, as was pointed out by Veltmann unstable particles should be excluded as external states and only the S-matrix connecting stable particle needs to be unitary.

4.3. Vector boson resonance

Bearing in mind our previous discussion, in this section we will address vector boson resonance, namely $q\overline{q}' \to W \to l^-\overline{\nu}_l\gamma$ which is $q\overline{q}' \to W \to l^-\overline{\nu}_l$ with an external photon attached at all possible places. We will compute it in a gauge invariant manner in two ways: first a correction to the $WW\gamma$ vertex, in which we closely follow the article by Baur and Zeppenfeld [13], and second through the complex mass scheme, which we have claimed produces gauge-invariant amplitudes but have not explicitly observed it yet.

4.3.1 $WW\gamma$ Vertex Correction

As we said, our goal in this section is to calculate the amplitude of the process seen in the figure below in a gauge invariant manner

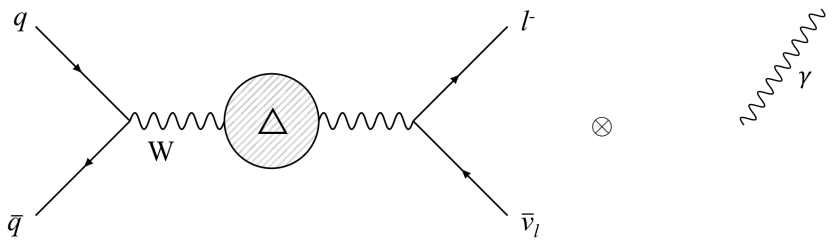

where the $\otimes$ means we want to attach a photon in all possible ways to the diagram. The first step is to obtain the explicit form of the resummed W propagator. The tree-level propagator in the unitary gauge is given by

$$\begin{aligned}
\Delta^0_{\mu\nu}(p^2) &= \frac{-i}{p^2 - m_W^2}\left(\eta_{\mu\nu} - \frac{p_\mu p_\nu}{m_W^2}\right) \\
&= \frac{-i}{p^2 - m_W^2}\left(\left[\eta_{\mu\nu} - \frac{p_\mu p_\nu}{p^2}\right] + p_\mu p_\nu\left[\frac{1}{p^2} - \frac{1}{m_W^2}\right]\right) \\
&= \frac{1}{p^2 - m_W^2}\left(\eta_{\mu\nu} - \frac{p_m up_\nu}{p^2} - \frac{1}{m_W^2}[p^2 - m_W^2]\frac{p_\mu p_\nu}{p^2}\right) \\
&= \frac{1}{p^2 - m_W^2}T_{\mu\nu} - \frac{1}{m_W^2}L_{\mu\nu}
\end{aligned} \tag{4.9}$$

where $T^{\mu\nu} := \left(\eta^{\mu\nu} - \frac{p^\mu p^\nu}{p^2}\right)$ acts as a transverse projection operator and $L^{\mu\nu} := \frac{p_\mu p_\nu}{p^2}$ acts as a longitudinal projection operator. This can be easily checked by verifying that

$$\begin{aligned}
T_\mu^{\ \alpha} T_{\alpha\nu} &= T_{\mu\nu} \\
L_\mu^{\ \alpha} L_{\alpha\nu} &= L_{\mu\nu} \\
T_\mu^{\ \alpha} L_{\alpha\nu} &= L_\mu^\alpha T_{\alpha\nu} = 0 \ .
\end{aligned} \tag{4.10}$$

Now we perform the Dyson sum by first noticing that we can decompose the 1PI amplitudes $\Pi_{\mu\nu}$ into longitudinal and tranverse components

$$\Pi_{\mu\nu}(p^2) = \Pi^T(p^2)T_{\mu\nu} + \Pi^L(p^2)L_{\mu\nu}, \tag{4.11}$$

so for every 1PI insertion we get a factor of

$$\begin{aligned}
\Pi_\mu^{\ \alpha}(p^2)\Delta^0_{\alpha\nu} &= \left(\Pi_T T_\mu^\alpha \ + \Pi_L L_\mu^{\ \alpha}\right)\left(\frac{1}{p^2 - m_W^2}T_{\alpha\nu} - \frac{1}{m_W^2}L_{\alpha\nu}\right) \\
&= \frac{\Pi_T}{p^2 - m_W^2}T_{\mu\nu} - \frac{\Pi_L}{m_W^2}L_{\mu\nu}.
\end{aligned} \tag{4.12}$$

The resummed propagator then is

$$\begin{aligned}\Delta(p^2)_{\mu\nu} &= \Delta^0_{\mu\nu} + \Delta^{0\,\alpha}_{\mu}[\Pi(p^2)\Delta^0]_{\alpha\nu} + \Delta^{0\,\alpha}_{\mu}[\Pi(p^2)\Delta^0]^{\beta}_{\alpha}\,[\Pi(p^2)\Delta^0]_{\beta\nu} + ... \\ &= \Delta^{0\,\alpha}_{\mu}\left(\sum_{n=0}^{\infty}(\Pi(p^2)\Delta^0)^n\right)_{\alpha\nu} \\ &= \Delta^{0\,\alpha}_{\mu}\left[\sum_{n=0}^{\infty}\left(\frac{\Pi_T}{p^2-m_W^2}\right)^n T_{\alpha\nu} + \sum_{n=0}^{\infty}\left(\frac{\Pi_L}{m_W^2}\right)^n L_{\mu\nu}\right] \\ &= -i\left(\frac{1}{p^2-m_W^2}T_{\mu}^{\ \alpha} - \frac{1}{m_W^2}L_{\mu}^{\ \alpha}\right)\left[\frac{1}{1-\frac{\Pi_T}{p^2-m_W^2}}T_{\alpha\nu} + \frac{1}{1-\frac{\Pi_L}{m_W^2}}L_{\alpha\nu}\right],\end{aligned} \tag{4.13}$$

where as usual we used the result for a geometric series. So finally we get that the full W propagator is

$$\Delta(p^2)_{\mu\nu} = \frac{-i}{p^2-m_W^2-\Pi_T}T_{\mu\nu} + \frac{i}{m_W^2-\Pi_L}L_{\mu\nu}. \tag{4.14}$$

Up until now we have been using the *fixed width approximation*, which means that we approximate the self energy to a constant equal to its resonance value $\Sigma(p^2) \sim \Sigma(M^2)$. In this case however we will use the so called *running width approximation* which approximates the self energy as $\Im\Sigma(p^2) = \frac{p^2}{m_W}\Gamma_W\theta(p^2)$, which we note still satisfies the optical theorem $\Sigma(m_W^2) = m_W\Gamma_W$. We are using the on-shell renormalization scheme, so m_W corresponds to the real pole mass and from the renormalization conditions we have $\Re\Pi_L(p^2) = 0$ and $\Re\Pi_T(p^2) = 0$.

Explicit calculation of the imaginary part of the self energy by cutting the fermion loop and making use of the Cutkosky cutting rules leads us to the results

$$\begin{aligned}\Im\Pi_L(p^2) &= 0 \\ \Im\Pi_T(p^2) &= \sum_{generations}\frac{g^2}{48\pi}p^2 \equiv p^2\frac{\Gamma_W}{m_W},\end{aligned} \tag{4.15}$$

where we dropped the theta function from (4.15) because we are only interested in virtual W decays. Having done this we can finally write the resummed W propagator as

$$D_W^{\mu\nu}(p) = \frac{-i}{p^2-m_W^2+ip^2\gamma_W}\left(\eta^{\mu\nu} - \frac{p^\mu p^\nu}{m_W^2}(1+i\gamma_W)\right), \tag{4.16}$$

where we defined $\gamma_W = \Gamma_W/m_W$. Now, a gauge invariant expression is obtained by attaching a photon in all possible ways to the charged particles in the diagram provided we include corrections to the $WW\gamma$ vertex. These corrections are the attachment of the photon to the charged fermion loops in the W boson self energy. Otherwise the amplitude will not be gauge invariant, as we will see. The resulting diagrams can be seen in figure 15

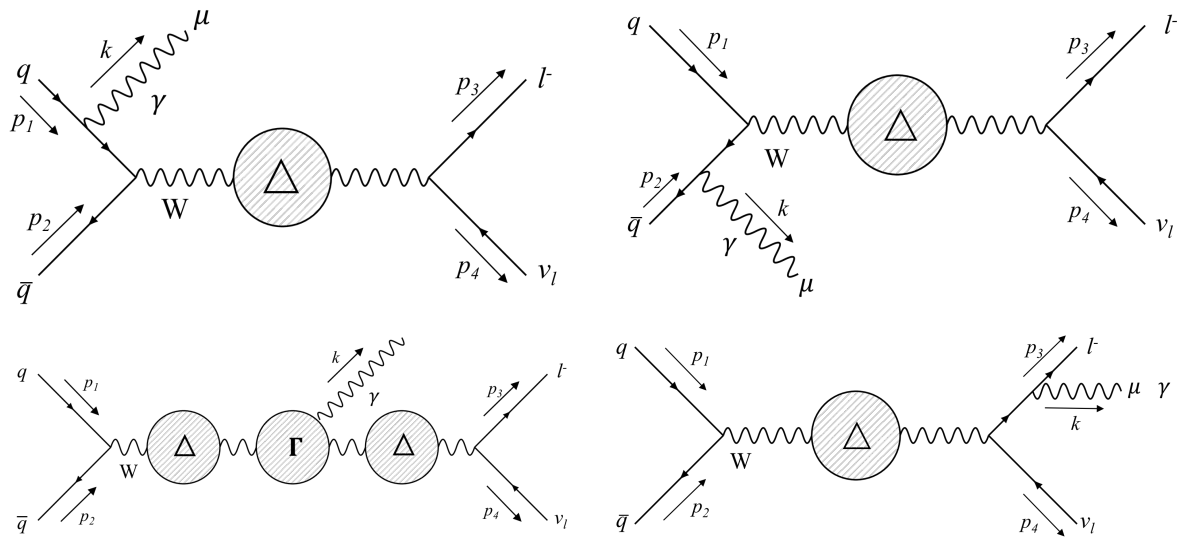

Figure 15: Diagrams contributing to $q\overline{q} \to l^{-}\overline{\nu}_{l}\gamma$

In the third diagram the photon can be attached to the lowest order vertex as well as to the charged fermion loops, as we have mentioned before, meaning that the vertex blob represents the following diagrams

Since we are only keeping the imaginary part of the self energy we must do the same for the triangle diagrams for consistency. As we explained in chapter 2 we can use the Cutkosky cutting rules to obtain the imaginary part of a loop diagram by cutting said diagram in all possible ways. The first diagram is the familiar lowest order vertex for three gauge bosons, given by the expression

$$-ie\Gamma_{0}^{\alpha\beta\mu} = -ie\left(((q_1+q_2)^{\mu})\eta^{\alpha\beta} - (q_1+k)^{\beta}\eta^{\mu\alpha} + (k-q_2)^{\alpha}\eta^{\mu\beta}\right) \tag{4.17}$$

If we neglect the masses of the fermions in the triangle diagrams and drop the terms proportional to k^{μ} which will later contract with the polarization $\overline{\epsilon}_{\mu}(k)$ and vanish, the contribution from the four ways to cut the triangle diagram reduces to a simple expression. Each quark doublet contributes with $i(g^2/48^{\pi})\Gamma_0$ to the lowest order vertex. Thus the vertex becomes

$$\Gamma^{\alpha\beta\mu} = \Gamma_{0}^{\alpha\beta\mu}\left(1 + \sum_{generations}\frac{ig^2}{48\pi}\right) = \Gamma_{0}^{\alpha\beta\mu}(1+i\gamma_W) \tag{4.18}$$

To prove that the full amplitude $q\overline{q}' \to l\overline{\nu}\gamma$ is gauge invariant it suffices to prove that the

electromagnetic Ward identity for the vertex $\Gamma^{\alpha\beta\mu}$ (4.19) is satisfied.

$$k_\mu \Gamma^\mu_{\alpha\beta} = (iD_W)^{-1}_{\alpha\beta}(q_1) - (iD_w)^{-1}_{\alpha\beta}(q_2) \tag{4.19}$$

To see this, we compute the left hand side by writing $k = q_1 - q_2$

$$\begin{aligned} k_\mu \Gamma^\mu_{\alpha\beta} &= [(q_1+q_2)\cdot(q_1-q_2)\eta_{\alpha\beta} - (2q_1-q_2)_\beta(q_1-q_2)_\alpha + (q_1-2q_2)_\alpha(q_1-q_2)_\beta] \\ &= [(q_1^2\eta_{\alpha\beta} - q_{1\alpha}q_{1\beta}) - (q_2\eta_{\alpha\beta} - q_{2\alpha}q_{2\beta})](1+i\gamma_W). \end{aligned} \tag{4.20}$$

It can be easily checked that the expression for the inverse W propagator is given by

$$(iD_W)^{-1}_{\alpha\beta}(p) = (p^2 - m_W^2 + ip^2\gamma_W)T_{\mu\nu} - m_W^2 L_{\mu\nu} \tag{4.21}$$

by verifying that

$$D^\alpha_\mu D^{-1}_{\alpha\nu} = T_{\mu\nu} + L_{\mu\nu} = \eta_{\mu\nu} \tag{4.22}$$

If we compute the right hand side of (4.19) we get

$$\begin{aligned} (iD_W)^{-1}(q_1) - (iD_w)^{-1}_{\alpha\beta}(q_2) &= (q_1^2\eta_{\alpha\beta} - q_{1\alpha}q_{1\beta}) + i\gamma_W(\eta_{\alpha\beta}q_1^2 - q_{1\alpha}q_{1\beta}) \\ &\quad - (q_2^2\eta_{\alpha\beta} - q_{2\alpha}q_{2\beta}) - i\gamma_W(\eta_{\alpha\beta}q_2^2 - q_{1\alpha}q_{2\beta}) \\ &= [(q_1^2\eta_{\alpha\beta} - q_{1\alpha}q_{1\beta}) - (q_2\eta_{\alpha\beta} - q_{2\alpha}q_{2\beta})](1+i\gamma_W), \end{aligned} \tag{4.23}$$

which is indeed equal to the left hand side. The electromagnetic Ward identity is satisfied and we have proven that the inclusion of an imaginary part in the $WW\gamma$ vertex leads to a gauge invariant full amplitude. We note that had we not included such corrections to the $WW\gamma$ vertex, then the term proportional to $i\gamma_W$ would not appear in (4.20) so it would no longer equal (4.23) so the amplitude would not be gauge invariant. This procedure, albeit ad-hoc, delivers a gauge invariant amplitude.

4.3.2 Complex Mass Scheme

We have seen that the inclusion of an imaginary part to the $WW\gamma$ vertex provides a gauge invariant amplitude. In this section we will observe that the CMS also provides a gauge independent result, but since the CMS is a renormalization scheme the procedure is more general and consistent than the previous one. We will try to find a correspondence between the previous method and the CMS by writing the full expression for the amplitude $\mathcal{M}_\mu$ in both procedures and seing how the cancellations occur when we contract with the photon momentum.

$WW\gamma$ vertex correction

First we want to compute the diagrams we mentioned in the last section explicitely, still using Baur and Zeppenfelds method. This will serve as a comparision when we perform the calculation in the CMS. We make the momenta assignment seen in figure 15.

For the amplitude of the first diagram we get

$$\begin{aligned}\mathcal{M}_1^\mu = i\frac{2}{3}\frac{g^3}{8}s_w\overline{v}(p_2)\gamma^\alpha(1-\gamma_5)\frac{\not{p}_1-\not{k}}{(p_1-k)^2}\gamma^\mu u(p_1)\frac{1}{(p_3+p_4)^2(1+i\gamma_W)-m_W^2}\\ \left(\eta_{\alpha\beta}-\frac{(p_3+p_4)_\alpha(p_3+p_4)_\beta}{m_W^2}(1+i\gamma_W)\right)\overline{u}(p_3)\gamma^\beta(1-\gamma_5)v(p_4).\end{aligned} \tag{4.24}$$

Since we are taking the limit of massless fermions from the Dirac equation we get that

$$\not{p}u(p)=\overline{u}(p)\not{p}=\not{p}v(p)=\overline{v}(p)\not{p}=0. \tag{4.25}$$

Equation (4.24) then becomes

$$\mathcal{M}_1^\mu = i\frac{2}{3}\frac{g^3}{8}s_wD^{-1}(p_3+p_4)\ \overline{v}(p_2)\gamma_\beta(1-\gamma_5)\frac{\not{p}_1-\not{k}}{(p_1-k)^2}\gamma^\mu u(p_1)\overline{u}(p_3)\gamma^\beta(1-\gamma_5)v(p_4). \tag{4.26}$$

Now we repeat this calculation for the remaining amplitudes, again using (4.25). This gives

$$\begin{aligned}\mathcal{M}_2^\mu =& i\frac{1}{3}\frac{g^3}{8}s_wD^{-1}(p_3+p_4)\ \overline{v}(p_2)\gamma^\mu\frac{\not{p}_2-\not{k}}{(k-p_2)^2}\gamma_\beta(1-\gamma_5)u(p_1)\overline{u}(p_3)\gamma^\beta(1-\gamma_5)v(p_4)\\
\mathcal{M}_3^\mu =& -i\frac{g^3}{8}\sin(\theta_w)\overline{v}(p_2)\gamma^\alpha(1-\gamma_5)u(p_1)D^{-1}(p_1+p_2)\left(\eta_{\alpha\rho}-\frac{(p_1+p_2)_\alpha(p_1+p_2)_\rho}{m_W^2}(1+i\gamma_W)\right)\\
&[(p_1+p_2+p_3+p_4)^\mu\eta^{\rho\sigma}-(p_1+p_2+k)^\sigma\eta^{\mu\rho}+(k-p_3-p_4)^\rho\eta^{\mu\sigma}](1+i\gamma_W)D^{-1}(p_3+p_4)\\
&\left(\eta_{\sigma\beta}-\frac{(p_3+p_4)_\sigma(p_3+p_4)_\beta}{m_W^2}(1+i\gamma_W)\right)\overline{u}(p_3)\gamma^\beta(1-\gamma_5)v(p_4)\\
=& -i\frac{g^3}{8}s_w\overline{v}(p_2)\gamma^\alpha(1-\gamma_5)u(p_1)D^{-1}(p_1+p_2)[(p_1+p_2+p_3+p_4)^\mu\eta_{\alpha\beta}-(p_1+p_2+k)_\beta\delta^\mu_\alpha\\
&+(k-p_3-p_4)_\alpha\delta^\mu_\beta](1+i\gamma_W)D^{-1}(p_3+p_4)\overline{u}(p_3)\gamma^\beta(1-\gamma_5)v(p_4)\\
\mathcal{M}_4^\mu =& -i\frac{g^3}{8}\sin(\theta_w)\overline{v}(p_2)\gamma^\alpha(1-\gamma_5)u(p_2)D^{-1}(p1+p2)\overline{u}(p_3)\gamma^\mu\frac{\not{p}_3+\not{k}}{(p_3+k)^2}\gamma_\alpha(1-\gamma_5)v(p_3),\end{aligned} \tag{4.27}$$

where we defined $D(p)=p^2(1+i\gamma_W)-m_W^2$.

Complex Mass Scheme

Now we will proceed with the computation of the same diagrams in the complex mass scheme. In this calculation we drop the triangle graph contributions to the $WW\gamma$ vertex and replace the W propagator expression by the CMS propagator. To obtain the CMS propagator, we just take the tree-level W propagator and substitute on-shell mass by the CMS mass $\hat{\mu}^2=m_W^2-im_W\Gamma_W$, which yields

$$\begin{aligned}D_W^{\mu\nu}(p) &= \frac{-i}{p^2-\hat{\mu}^2}\left(\eta^{\mu\nu}-\frac{p^\mu p^\nu}{\hat{\mu}^2}\right)\\ &= \frac{-i}{p^2-m_W^2+im_W\Gamma_W}\left(\eta^{\mu\nu}-\frac{p^\mu p^\nu}{m_W^2-im_W\Gamma_W}\right).\end{aligned} \tag{4.28}$$

In this calculation we must not forget that $\hat{\mu}$ dependent quantities now acquire a imaginary part, such as the Weinberg angle $s_W \to s'_W = 1 - \frac{m_W^2}{m_Z^2}(1 - i\gamma_W)$. The amplitude for the first diagram is

$$\begin{aligned}
\mathcal{M}^{\mu}_{1CMS} &= i\frac{2}{3}\frac{g^3}{8}s'_w\overline{v}(p_2)\gamma^{\alpha}(1-\gamma_5)\frac{\not{p}_1 - \not{k}}{(p_1-k)^2}\gamma^{\mu}u(p_1)\frac{1}{(p_3+p_4)^2 - m_W^2(1-\gamma_W)} \\
&\left(\eta_{\alpha\beta} - \frac{(p_3+p_4)_{\alpha}(p_3+p_4)_{\beta}}{m_W^2(1-i\gamma_W)}\right)\overline{u}(p_3)\gamma^{\beta}(1-\gamma_5)v(p_4) \\
&= i\frac{2}{3}\frac{g^3}{8}s'_w\overline{v}(p_2)\gamma^{\alpha}(1-\gamma_5)\frac{\not{p}_1 - \not{k}}{(p_1-k)^2}\gamma^{\mu}u(p_1)D'^{-1}(p_3+p_4)\overline{u}(p_3)\gamma_{\alpha}(1-\gamma_5)v(p_4)
\end{aligned} \tag{4.29}$$

where we again used the Dirac equation for massless fermions (4.25). The results for the remaining amplitudes are

$$\begin{aligned}
\mathcal{M}^{\mu}_{2CMS} =& i\frac{1}{3}\frac{g^3}{8}s'_w D'^{-1}(p_3+p_4)\ \overline{v}(p_2)\gamma^{\mu}\frac{\not{p}_2 - \not{k}}{(k-p_2)^2}\gamma_{\beta}(1-\gamma_5)u(p_1)\overline{u}(p_3)\gamma^{\beta}(1-\gamma_5)v(p_4) \\
\mathcal{M}^{\mu}_{3CMS} =& -i\frac{g^3}{8}s'_w\overline{v}(p_2)\gamma^{\alpha}(1-\gamma_5)u(p_1)D'^{-1}(p_1+p_2)\left(\eta_{\alpha\rho} - \frac{(p_1+p_2)_{\alpha}(p_1+p_2)_{\rho}}{m_W^2(1-i\gamma_W)}\right) \\
&[(p_1+p_2+p_3+p_4)^{\mu}\eta^{\rho\sigma} - (p_1+p_2+k)^{\sigma}\eta^{\mu\rho} + (k-p_3-p_4)^{\rho}\eta^{\mu\sigma}]D'^{-1}(p_3+p_4) \\
&\left(\eta_{\sigma\beta} - \frac{(p_3+p_4)_{\sigma}(p_3+p_4)_{\beta}}{m_W^2(1-i\gamma_W)}\right)\overline{u}(p_3)\gamma^{\beta}(1-\gamma_5)v(p_4) \\
&= -i\frac{g^3}{8}s_w\overline{v}(p_2)\gamma^{\alpha}(1-\gamma_5)u(p_1)D'^{-1}(p_1+p_2)[(p_1+p_2+p_3+p_4)^{\mu}\eta_{\alpha\beta} - (p_1+p_2+k)_{\beta}\delta^{\mu}_{\alpha} \\
&+ (k-p_3-p_4)_{\alpha}\delta^{\mu}_{\beta}]D'^{-1}(p_3+p_4)\overline{u}(p_3)\gamma^{\beta}(1-\gamma_5)v(p_4) \\
\mathcal{M}^{\mu}_{4CMS} =& -i\frac{g^3}{8}s'_w\overline{v}(p_2)\gamma^{\alpha}(1-\gamma_5)u(p_2)D'^{-1}(p1+p2)\overline{u}(p_3)\gamma^{\mu}\frac{\not{p}_3 + \not{k}}{(p_3+k)^2}\gamma_{\alpha}(1-\gamma_5)v(p_3),
\end{aligned} \tag{4.30}$$

where we defined $D'(p) = p^2 - m_W^2(1 - i\gamma_W)$. As we can see these amplitudes have the same structure as before, with the factor s_W appearing here appears as s'_W and the denominators $D(p)$ being replaced by $D'(p)$. The factor $(1 + i\gamma_W)$ has also disappeared from the third amplitude due to our not having included the triangle graphs in the $WW\gamma$ vertex. As we will show in the next section, upon contraction with k_μ both methods will yield the same results apart from a factor. Hence if one method satisfies gauge invariance so does the other, since the difference in factors is irrelevant when assessing whether $k_\mu\mathcal{M}^{\mu}$ is equal to zero.

Ward Identity

We have already showed that the Baur and Zeppenfeld method produces a gauge invariant expression by checking that it satisfies the electromagnetic Ward identity (4.19). Since we are now in posession of the explicit expressions for the amplitudes we can also confirm gauge invariance by making sure that $k_\mu\mathcal{M}^{\mu} = 0$.

For $k_\mu \mathcal{M}^\mu_{1,..,4}$ we get

$$
\begin{aligned}
k_\mu \mathcal{M}^\mu_1 =& i\frac{2}{3}\frac{g^3}{8} s_w D^{-1}(p_3+p_4)\ \overline{v}(p_2)\gamma_\beta(1-\gamma_5)\frac{\not{p}_1-\not{k}}{(p_1-k)^2}\not{k}u(p_1)\overline{u}(p_3)\gamma^\beta(1-\gamma_5)v(p_4)\\
k_\mu \mathcal{M}^\mu_2 =& i\frac{1}{3}\frac{g^3}{8} s_w D^{-1}(p_3+p_4)\ \overline{v}(p_2)\not{k}\frac{\not{p}_2-\not{k}}{(k-p_2)^2}\gamma_\beta(1-\gamma_5)u(p_1)\overline{u}(p_3)\gamma^\beta(1-\gamma_5)v(p_4)\\
k_\mu \mathcal{M}^\mu_3 =& -i\frac{g^3}{8} s'_w \overline{v}(p_2)\gamma^\alpha(1-\gamma_5)u(p_1)D^{-1}(p_1+p_2)[(p_1+p_2+p_3+p_4)\cdot k\,\eta_{\alpha\beta}-(p_1+p_2+k)_\beta k_\alpha\\
&+(k-p_3-p_4)_\alpha k_\beta](1+i\gamma_W)D^{-1}(p_3+p_4)\overline{u}(p_3)\gamma^\beta(1-\gamma_5)v(p_4)\\
k_\mu \mathcal{M}^\mu_4 =& -i\frac{g^3}{8} s'_w \overline{v}(p_2)\gamma^\alpha(1-\gamma_5)u(p_2)D^{-1}(p1+p2)\overline{u}(p_3)\not{k}\frac{\not{p}_3+\not{k}}{(p_3+k)^2}\gamma_\alpha(1-\gamma_5)v(p_3).
\end{aligned}
\tag{4.31}
$$

Again by making use of the Dirac equation (4.25) we get to the following identities

$$
\begin{aligned}
\frac{\not{p}_1-\not{k}}{(p_1-k)^2}\not{k}u(p_1) &= -\frac{(\not{p}_1-\not{k})^2}{(p_1-k)^2}u(p_1) = -u(p_1)\\
\overline{v}(p_2)\not{k}\frac{\not{p}_2-\not{k}}{(p_2-k)^2}\not{k} &= -\overline{v}(p_2)\frac{(\not{p}_2-\not{k})^2}{(p_1-k)^2} = -\overline{v}(p_2).
\end{aligned}
\tag{4.32}
$$

By virtue of momentum conservation we can write $p_3+p_4 = p_1+p_2-k$ in the expression for $k_\mu \mathcal{M}^\mu_3$. For the total amplitude we thus have

$$
\begin{aligned}
k_\mu \mathcal{M}^\mu_{BZ} =& i\frac{g^3}{8} s_w[D^{-1}(p_3+p_4)-D^{-1}(p_1+p_2)-(p_1+p_2+p_3+p_4)\cdot k\\
&D^{-1}(p_3+p_4)D^{-1}(p_1+p_2)(1+i\gamma_W)]\overline{v}(p_2)\gamma_\beta(1-\gamma_5)u(p_1)\overline{u}(p_3)\gamma^\beta(1-\gamma_5)v(p_4).
\end{aligned}
\tag{4.33}
$$

Now we note that

$$
\begin{aligned}
D^{-1}(p_3+p_4)-D^{-1}(p_1+p_2) &= \frac{1}{(p_3+p_4)^2(1+i\gamma_W)-m_W^2}-\frac{1}{(p_1+p_2)^2(1+i\gamma_W)-m_W^2}\\
&= [(p_1+p_2)^2-(p_3+p_4)^2]\frac{(1+i\gamma_W)}{D(p_3+p_4)D(p_1+p_2)}
\end{aligned}
\tag{4.34}
$$

On the other hand we can write $k=(p_1+p_2)-(p_3+p_4)$ such that

$$
\begin{aligned}
(p_1+p_2+p_3+p_4)\cdot k &= [(p_1+p_2)+(p_3+p_4)]\cdot[(p_1+p_2)-(p_3+p_4)]\\
&= (p_1+p_2)^2-(p_3+p_4)^2
\end{aligned}
\tag{4.35}
$$

This way expression (4.33) becomes

$$\begin{aligned} k_\mu \mathcal{M}^\mu_{BZ} =& i\frac{g^3}{8} s_w \frac{(1+i\gamma_W)}{D(p_3+p_4)D(p_1+p_2)}[\big((p_1+p_2)^2-(p_3+p_4)^2\big)-\big((p_1+p_2)^2-(p_3+p_4)^2\big)] \\ & \overline{v}(p_2)\gamma_\beta(1-\gamma_5)u(p_1)\overline{u}(p_3)\gamma^\beta(1-\gamma_5)v(p_4) \\ =& 0 \end{aligned} \tag{4.36}$$

This once again shows that the method is indeed gauge invariant. The calculation in the CMS is exactly the same up until (4.33) as long as we make the modifications $s_W \to s'_W$, $D(p) \to D'(p)$ and drop the $(1+i\gamma_W)$ factor in the second term. This gives

$$\begin{aligned} k_\mu \mathcal{M}^\mu_{CMS} =& i\frac{g^3}{8} s_w [D'^{-1}(p_3+p_4) - D'^{-1}(p_1+p_2) - (p_1+p_2+p_3+p_4)\cdot k\, D'^{-1}(p_3+p_4)D'^{-1}(p_1+p_2)] \\ & \overline{v}(p_2)\gamma_\beta(1-\gamma_5)u(p_1)\overline{u}(p_3)\gamma^\beta(1-\gamma_5)v(p_4) \end{aligned} \tag{4.37}$$

Finally we note that

$$\begin{aligned} D'^{-1}(p_3+p_4) - D'^{-1}(p_1+p_2) &= \frac{1}{(p_3+p_4)^2 - m_W^2(1-i\gamma_W)} - \frac{1}{(p_1+p_2)^2 - m_W^2(1-i\gamma_W)} \\ &= \frac{(p_1+p_2)^2-(p_3+p_4)^2}{D'(p_1+p_2)D'(p_3+p_4)} \end{aligned} \tag{4.38}$$

By using (4.35) we get that

$$\begin{aligned} k_\mu \mathcal{M}^\mu_{CMS} =& i\frac{g^3}{8} s'_w \frac{1}{D'(p_3+p_4)D'(p_1+p_2)}[\big((p_1+p_2)^2-(p_3+p_4)^2\big)-\big((p_1+p_2)^2-(p_3+p_4)^2\big)] \\ & \overline{v}(p_2)\gamma_\beta(1-\gamma_5)u(p_1)\overline{u}(p_3)\gamma^\beta(1-\gamma_5)v(p_4) \\ =& 0 \end{aligned} \tag{4.39}$$

Thus, we have reached our goal of proving that the implementation of the complex mass scheme provides a gauge invariant amplitude. In this section we have done this for a bosonic resonance so in the following section we will illustrate this is also the case for a fermionic resonance.

4.4. Fermionic resonance

Our next application of the complex mass scheme is to a fermionic resonance, namely top quark resonance. We will compute the tree-level amplitude $Wb \to t \to Wb\gamma$, which although it has unstable particles as external states it can be used as an example of how in principle the treatment of a fermionic resonance in the complex mass scheme would play out. For a fermion

we saw that the resummed propagator was given by

$$\Delta(\not{p}) = \frac{i}{\not{p} - m_t + i\Im\Sigma(\not{p})}, \tag{4.40}$$

so by defining $\hat{\mu}_t$ to be the complexed value pole of the $\Delta(\not{p})$ we have that the CMS propagator is

$$\Delta_{CMS}(\not{p}) = \frac{i}{\not{p} - \hat{\mu}_t} = \frac{i}{\not{p} - (m_t - i\Gamma_t)} = i\frac{\not{p} + (m_t - i\Gamma_t)}{p^2 - (m_t - i\Gamma_t)^2}. \tag{4.41}$$

We now proceed with the computation of the relevant amplitudes by making use of the CMS propagator. There are five diagrams contributing to this process, as we will see. The first diagram we need to compute is seen in figure 16.

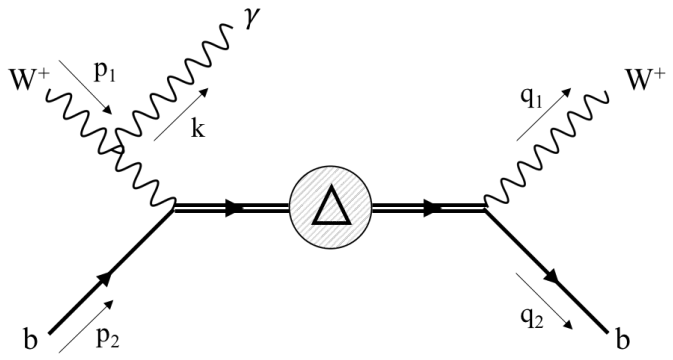

Figure 16: Diagram 1

The corresponding amplitude is given by

$$\begin{aligned}\mathcal{M}_1^{\mu} = &- i\frac{g^2 e}{8} D_t^{-1}(q_1+q_2) D_W^{-1}(p_1-k)\left[\eta_{\alpha\beta} - \frac{(p_1-k)_\alpha (p_1-k)_\beta}{m_W^2}\right][(2p_1-k)^\mu \eta^{\rho\alpha} - (p_1+k)^\alpha \eta^{\mu\rho} + \\ &+ (2k-p_1)^\rho \eta^{\mu\alpha}]\,\overline{u}(q_2)\gamma^\sigma(1-\gamma_5)[(\not{q}_1 + \not{q}_2) + (m_t - i\Gamma_t)]\gamma^\beta(1-\gamma_5)u(p_2).\end{aligned} \tag{4.42}$$

Now we contract this expression with k_μ and use that $\{\gamma^\mu, \gamma_5\} = 0$, $\left(\frac{1\pm\gamma_5}{2}\right)^2 = \frac{1\pm\gamma_5}{2}$ and $\frac{1+\gamma_5}{2}\cdot\frac{1-\gamma_5}{2} = \frac{1-\gamma_5}{2}\cdot\frac{1+\gamma_5}{2} = 0$. This gives

$$\begin{aligned}k_\mu \mathcal{M}_1^{\mu} = &- i\frac{g^2 e}{4} D_t^{-1}(q_1+q_2) D_W^{-1}(p_1-k)\left[\eta_{\alpha\beta} - \frac{(p_1-k)_\alpha (p_1-k)_\beta}{m_W^2}\right][(2p_1-k)\cdot k \eta^{\rho\alpha} - (p_1+k)^\alpha k^\rho + \\ &+ (2k-p_1)^\rho k^\alpha]\,\overline{u}(q_2)\gamma^\sigma(1-\gamma_5)(\not{q}_1 + \not{q}_2)\gamma^\beta u(p_2).\end{aligned} \tag{4.43}$$

After a little algebra we see that

$$\left[\eta_{\alpha\beta} - \frac{(p_1-k)_\alpha (p_1-k)_\beta}{m_W^2}\right][(2p_1-k)\cdot k\eta^{\rho\alpha} - (p_1+k)^\alpha k^\rho + (2k-p_1)^\rho k^\alpha] = 2(p_1\cdot k)\eta^{\beta\rho}, \tag{4.44}$$

so finally we get

$$k_\mu \mathcal{M}_1^\mu = -\,i\frac{g^2 e}{4} 2(p_1\cdot k) D_t^{-1}(q_1+q_2) D_W^{-1}(p_1-k)\ \overline{u}(q_2)\gamma^\sigma(1-\gamma_5)(\not{q}_1+\not{q}_2)\gamma^\rho u(p_2). \tag{4.45}$$

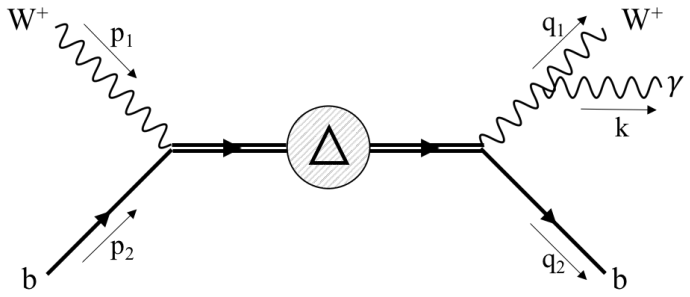

Figure 17: Diagram 2

For all the remaining diagrams we follow a very similar procedure. For the diagram in figure 17 the amplitude is

$$\begin{aligned}\mathcal{M}_2^\mu = &-\,i\frac{g^2 e}{8} D_t^{-1}(p_1+p_2) D_W^{-1}(q_1+k)\left[\eta_{\alpha\beta} - \frac{(q_1+k)_\alpha (q_1+k)_\beta}{m_W^2}\right][(2q_1+k)^\mu \eta^{\beta\sigma} - (2k+q_1)^\sigma \eta^{\mu\beta} + \\ &+ (k-q_1)^\beta \eta^{\mu\sigma}]\,\overline{u}(q_2)\gamma^\alpha(1-\gamma_5)[(\not{p}_1+\not{p}_2) + (m_t - i\Gamma_t)]\gamma^\rho(1-\gamma_5)u(q_1).\end{aligned} \tag{4.46}$$

Now we again use the properties of the chiral projection operators and contract with k_μ to obtain

$$\begin{aligned}k_\mu \mathcal{M}_2^\mu = &-\,i\frac{g^2 e}{4} D_t^{-1}(p_1+p_2) D_W^{-1}(q_1+k)\left[\eta_{\alpha\beta} - \frac{(q_1+k)_\alpha (q_1+k)_\beta}{m_W^2}\right][(2q_1+k)\cdot k\eta^{\beta\sigma} - (2k+q_1)^\sigma k^\beta + \\ &+ (k-q_1)^\beta k^\sigma]\,\overline{u}(q_2)\gamma^\alpha(1-\gamma_5)(\not{p}_1+\not{p}_2)\gamma^\rho u(p_2).\end{aligned} \tag{4.47}$$

After some algebra we see that

$$\left[\eta_{\alpha\beta} - \frac{(q_1+k)_\alpha (q_1+k)_\beta}{m_W^2}\right][(2q_1+k)\cdot k\eta^{\beta\sigma} - (2k+q_1)^\sigma k^\beta + (k-q_1)^\beta k^\sigma] = 2(q1\cdot k)\eta^{\alpha\sigma}, \tag{4.48}$$

which yields

$$k_\mu \mathcal{M}_2^\mu = -\,i\frac{g^2 e}{4} 2(q1\cdot k) D_t^{-1}(p_1+p_2) D_W^{-1}(q_1+k)\overline{u}(q_2)\gamma^\sigma(1-\gamma_5)(\not{p}_1+\not{p}_2)\gamma^\rho u(p_2). \tag{4.49}$$

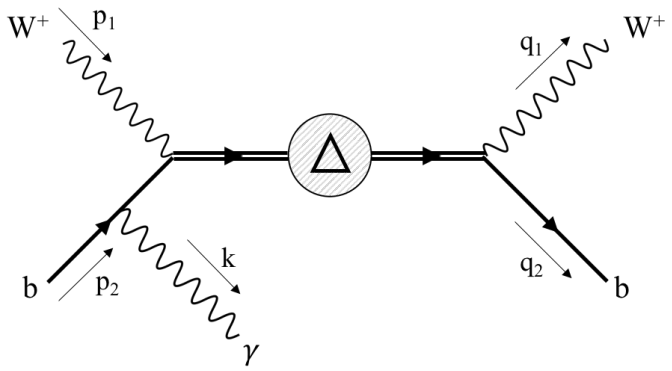

Figure 18: Diagram 3

The amplitude for the third diagram, which can be seen in figure 18, is

$$\mathcal{M}_3^\mu = \frac{1}{3} i \frac{g^2 e}{8} D_t^{-1}(q_1+q_2) D_b^{-1}(p_2-k)\overline{u}\gamma^\sigma(1-\gamma_5)[(\not{q}_1+\not{q}_2)+(m_t-i\Gamma_t)]\gamma^\rho(1-\gamma_5)(\not{p}_2-\not{k})\gamma^\mu u(p_2). \tag{4.50}$$

We contract with k_μ and use the usual set of techniques

$$\begin{aligned} k_\mu \mathcal{M}_3^\mu &= \frac{1}{3} i \frac{g^2 e}{4} \overline{u}(q_2)\gamma^\sigma(1-\gamma_5)(\not{q}_1+\not{q}_2)\gamma^\rho(\not{p}_2-\not{k})\not{k}u(p_2) \\ &= -\frac{1}{3} i \frac{g^2 e}{4} \overline{u}(q_2)\gamma^\sigma(1-\gamma_5)(\not{q}_1+\not{q}_2)\gamma^\rho u(p_2) \end{aligned}$$

where we used that $\frac{(\not{p}_2-\not{k})\not{k}}{(p_2-k)^2}u(p_2) = -\frac{(\not{p}_2-\not{k})^2}{(p_2-k)^2} = -u(p_2)$.

The fourth diagram we need to consider is displayed in figure 19.

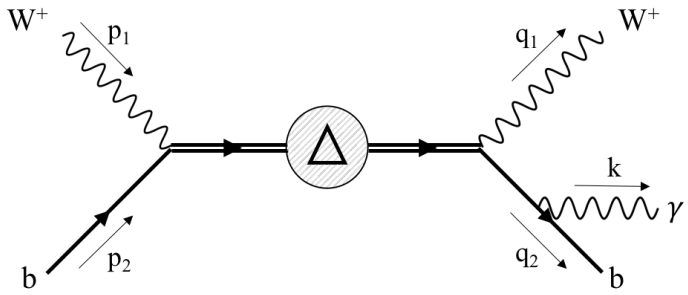

Figure 19: Diagram 4

The corresponding amplitude is

$$\mathcal{M}_4^\mu = \frac{1}{3} i \frac{g^2 e}{8} D_t^{-1}(p_1+p_2) D_b^{-1}(q_2+k)\overline{u}\gamma^\mu(\not{q}_2+\not{k})\gamma^\sigma(1-\gamma_5)[(\not{p}_1+\not{p}_2)+(m_t-i\Gamma_t)]\gamma^\rho(1-\gamma_5)u(p_2), \tag{4.51}$$

which gives

$$\begin{aligned} k_\mu \mathcal{M}_4^\mu =& \frac{1}{3} i \frac{g^2 e}{4} D_t^{-1}(p_1+p_2) D_b^{-1}(q_2+k) \overline{u} \not{k}(\not{q}_2+\not{k}) \gamma^\sigma (1-\gamma_5)(\not{p}_1+\not{p}_2)\gamma^\rho u(p_2) \\ =& \frac{1}{3} i \frac{g^2 e}{4} D_t^{-1}(p_1+p_2) \overline{u}(q_2) \gamma^\sigma (1-\gamma_5)[\not{p}_1+\not{p}_2]\gamma^\rho u(p_2), \end{aligned}$$

where we used $\overline{u}(q_2)\frac{\not{k}(\not{q}_2+\not{k})}{(q_2+k)^2} = \overline{u}(q_2)\frac{\not{k}(\not{q}_2)^2}{(q_2+k)^2} = \overline{u}(q_2)$

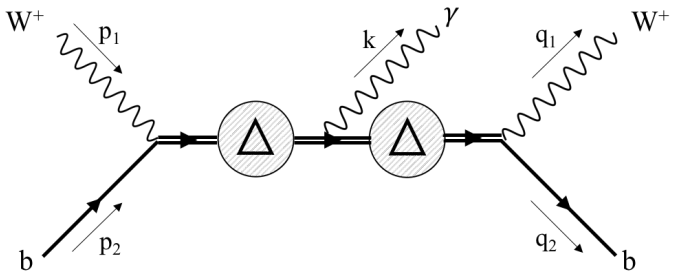

Figure 20: Diagram 5

Finally for the fifth diagram, displayed in figure 20 we get

$$\begin{aligned} \mathcal{M}_5^\mu =& \frac{2}{3}\left(-i\frac{g^2 e}{8}\right) D_t^{-1}(p_1+p_2) D_t^{-1}(q_1+q_2)\overline{u}(q_2)\gamma^\sigma(1-\gamma_5)[(\not{q}_1+\not{q}_2)+(m_t-i\Gamma_t)]\gamma^\mu \\ & [(\not{p}_1+\not{p}_2)+(m_t-i\Gamma_t)]\gamma^\rho(1-\gamma_5)u(p_2), \end{aligned} \tag{4.52}$$

which yields,

$$\begin{aligned} k_\mu \mathcal{M}_5^\mu =& \frac{2}{3}\left(-i\frac{g^2 e}{4}\right) D_t^{-1}(p_1+p_2) D_t^{-1}(q_1+q_2)\overline{u}(q_2)\gamma^\sigma(1-\gamma_5)[(\not{q}_1+\not{q}_2)\not{k}(\not{p}_1+\not{p}_2)+ \\ & + (m_t-i\Gamma_t)^2\not{k}]\gamma^\rho u(p_2) \end{aligned} \tag{4.53}$$

Since we have the expressions for $k_\mu \mathcal{M}_i^\mu$ we can now assess whether the Ward identity is satisfied by manipulating these expressions and see if they add up to zero.

Ward Identity

To verify the Ward identity $k_\mu \mathcal{M}^\mu = 0$, we start by adding (4.45) and (4.51).

$$\begin{aligned} k_\mu(\mathcal{M}_1^\mu + \mathcal{M}_3^\mu) =& i\frac{g^2 e}{4} D_t^{-1}(q_1+q_2)\left[\frac{-2(p_1\cdot k)}{(p_1-k)^2-m_W^2}-\frac{1}{3}\right]\overline{u}(q_2)\gamma^\sigma(1-\gamma_5)(\not{q}_1+\not{q}_2)\gamma^\rho u(p_2) \\ =& i\frac{g^2 e}{4} D_t^{-1}(q_1+q_2)\left(\frac{2}{3}\right)\overline{u}(q_2)\gamma^\sigma(1-\gamma_5)(\not{q}_1+\not{q}_2)\gamma^\rho u(p_2) \end{aligned} \tag{4.54}$$

Subsequently we add diagrams (4.49) and (4.52)

$$\begin{aligned}
k_\mu(\mathcal{M}_2^\mu+\mathcal{M}_4^\mu) =& i\frac{g^2e}{4}D_t^{-1}(p_1+p_2)\left[-\frac{2(p_1\cdot k)}{(q_1+k)^2-m_W^2}+\frac{1}{3}\right]\overline{u}(q_2)\gamma^\sigma(1-\gamma_5)(\not{p}_1+\not{p}_2)\gamma^\rho u(p_2)\\
=& i\frac{g^2e}{4}D_t^{-1}(p_1+p_2)\left(-\frac{2}{3}\right)\overline{u}(q_2)\gamma^\sigma(1-\gamma_5)(\not{p}_1+\not{p}_2)\gamma^\rho u(p_2)\\
=& i\frac{g^2e}{4}D_t^{-1}(p_1+p_2)\left(-\frac{2}{3}\right)\overline{u}(q_2)\gamma^\sigma(1-\gamma_5)(\not{q}_1+\not{q}_2)\gamma^\rho u(p_2)\\
&+ i\frac{g^2e}{4}D_t^{-1}(p_1+p_2)\left(-\frac{2}{3}\right)\overline{u}(q_2)\gamma^\sigma(1-\gamma_5)\not{k}\gamma^\rho u(p_2),
\end{aligned} \tag{4.55}$$

where we used that $p_1^2=q_1^2=m_W^2$ and in the last step we made use of $p_1+p_2=q_1+q_2+k$. Now we add expressions (4.54) and (4.55) to get

$$\begin{aligned}
k_\mu(\mathcal{M}_1^\mu+...+\mathcal{M}_4^\mu) =& \frac{2}{3}[2(q_1+q_2)\cdot k]i\frac{g^2e}{4}D_t^{-1}(q1+q2)D_t^{-1}(p1+p2)\overline{u}(q_2)\gamma^\sigma(1-\gamma_5)(\not{q}_1+\not{q}_2)\gamma^\rho u(p_2)\\
&-\frac{2}{3}i\frac{g^2e}{4}D_t^{-1}(p_1+p_2)\overline{u}(q_2)\gamma^\sigma(1-\gamma_5)\not{k}\gamma^\rho u(p_2)
\end{aligned} \tag{4.56}$$

Now we take (4.53) and rewrite it noting the photon is on-shell $k^2=0$ and using

$$\begin{aligned}
(\not{q}_1+\not{q}_2)\not{k}(\not{p}_1+\not{p}_2) =& (\not{q}_1+\not{q}_2)\not{k}(\not{q}_1+\not{q}_2)\\
=& [\not{q}_1+\not{q}_2](2k\cdot(q_1+q_2)-[\not{q}_1+\not{q}_2]\not{k}\\
=& 2k\cdot(q_1+q_2)[\not{q}_1+\not{q}_2]-(q_1+q_2)^2\not{k}
\end{aligned} \tag{4.57}$$

such that it becomes

$$\begin{aligned}
k_\mu\mathcal{M}_5^\mu =& -\frac{2}{3}[2k\cdot(q_1+q_2)]i\frac{g^2e}{4}D_t^{-1}(p_1+p_2)D_t^{-1}(q_1+q_2)\overline{u}(q_2)\gamma^\sigma(1-\gamma_5)(\not{q}_1+\not{q}_2)\gamma^\rho u(p_2)+\\
&+\frac{2}{3}i\frac{g^2e}{4}[(q_1+q_2)^2-(m_t-i\Gamma_t)^2]D_t^{-1}(p_1+p_2)D_t^{-1}(q_1+q_2)\overline{u}(q_2)\gamma^\sigma(1-\gamma_5)\not{k}]\gamma^\rho u(p_2)\\
=& -\frac{2}{3}[2k\cdot(q_1+q_2)]i\frac{g^2e}{4}D_t^{-1}(p_1+p_2)D_t^{-1}(q_1+q_2)\overline{u}(q_2)\gamma^\sigma(1-\gamma_5)(\not{q}_1+\not{q}_2)\gamma^\rho u(p_2)+\\
&+\frac{2}{3}i\frac{g^2e}{4}D_t^{-1}(p_1+p_2)\overline{u}(q_2)\gamma^\sigma(1-\gamma_5)\not{k}\gamma^\rho u(p_2)
\end{aligned} \tag{4.58}$$

So finally we see that the terms in (4.58) cancel the terms in (4.56). This means that we have verified

$$k_\mu\mathcal{M}^\mu=k_\mu(\mathcal{M}_1^\mu+...+\mathcal{M}_5^\mu)=0 \tag{4.59}$$

We have then confirmed that the Complex Mass Scheme provides a gauge invariant amplitude in the case of a fermionic resonance also.

4.5. CMS in $t\bar{t}H$ Higgs production

In this section we will test the implementation of the complex mass scheme in one of the main Higgs production mechanisms used at hadron colliders, namely Higgs production associated with a top quark pair. We will present a more detailed discussion of Higgs phenomenology in our next chapter, here we just make use of $pp \to t\bar{t}H$ to check some properties of the complex mass scheme. We will do this by resorting to a widely used tool in collider simulations, *Madgraph* [14]. Madgraph is a Monte Carlo event generator which is very useful for providing all the necessary elements of SM and BSM (Beyond Standard Model) calculations, including cross sections and decay rates. We explain how Monte Carlo event generators work in detail in chapter 6, where we also implement our own MC program for one of the processes contributing to Higgs production associated with top quark pair, namely $qq \to t\bar{t}$ and compare our results with Madgraph. A full calculation of the amplitude $pp \to t\bar{t}H$, and its square, can also be found in appendix B, where we also explain some aspects of computing cross sections in perturbative QCD.

Fortunately the implementation of the complex mass scheme in Madgraph is quite straightforward. All one needs to do is set the *Complex Mass Scheme* setting to true and Madgraph automatically implements the CMS feynman rules in its computation of cross sections.

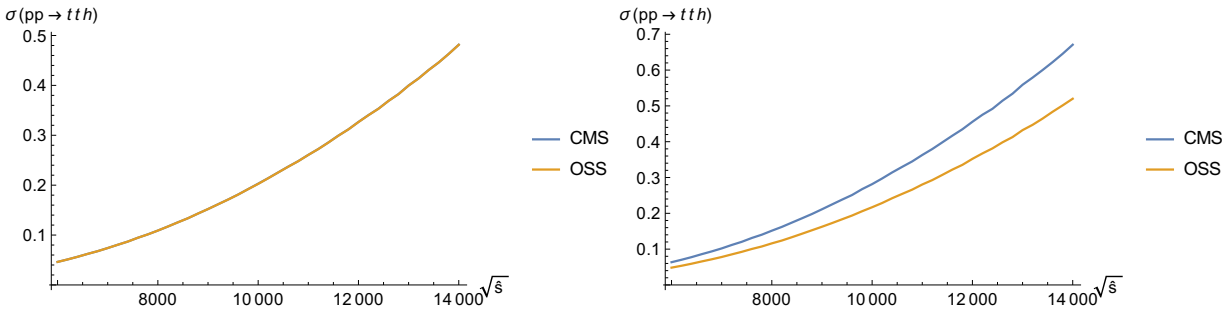

(a) Cross section for $\Gamma_t = 1.49$ GeV

(b) Cross sections for $\Gamma_t = 150$ GeV

Figure 21: $\sigma(pp \to t\bar{t}H)$ both in the complex mass scheme and on-shell scheme for two different values of Γ_t

We generate the cross section $\sigma(pp \to t\bar{t}H)$ in Madgraph as a function of the center of mass energy $\sqrt{s}$ both with CMS implementation and with on-shell scheme implementation. The plot can be seen in figure 21a. As we can see the two curves are very similar to each other, as was expected. To see why we note that the difference between the two approaches lies on the top-propagators used

$$\begin{aligned} \Delta_{BW} =& \frac{i(\not{p} + m_t)}{p^2 - m_t^2 + i m_t \Gamma_t} \\ \Delta_{CMS} =& i\frac{\not{p} + (m_t - i\Gamma_t)}{p^2 - (m_t - i\Gamma_t)^2}, \end{aligned} \tag{4.60}$$

as well as on the fact that the whole amplitude $|\mathcal{M}| \sim m_t^2$ in the on-shell scheme implementation and $\sim |m_t - i\Gamma_t|^2$ when using the complex mass scheme. Thus, we expect the CMS amplitude $|\mathcal{M}|^2$ to be larger but not noticeably so, since $\Gamma_t \sim 1.5$ GeV for a value of the top quark mass of

$m_t \sim 173$ GeV. To see this is the case we can use an unphysical and unreallistic value for the top quark width in our computation of the cross section. In figure 21b we plot the same cross section having set the top width to a value closer to its mass, $\Gamma_t \sim 150GeV$. In this plot the differences between the two approaches become evident and behave as we predicted.

Lastly we plot the value of the cross section as a function of the top width (in the fixed width scheme) Γ_t at $\sqrt{s} = 13TeV$ in both implementations. The plot is displayed in figure 22. This once again corroborates our prediction for the differences between the two approaches as the top width assumes large unphysical values.

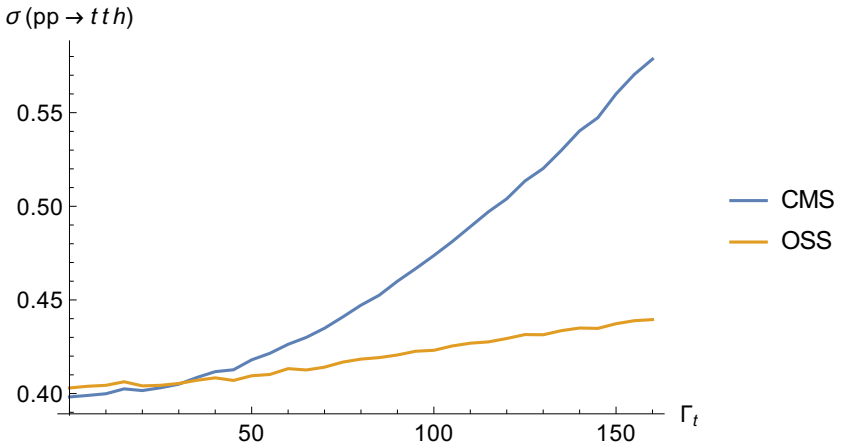

Figure 22: $\sigma(pp \to t\bar{t}H)$ at $\sqrt{s} = 13$ TeV as a function of the top width Γ_t

5 Higgs Phenomenology

5.1. Higgs Production

In this section we will address some of the main Higgs production modes that led to its discovery in 2012. As we saw, the Higgs couples very weakly to light-flavor quarks (the coupling is proportional to the fermion mass) and has no tree level coupling to gluons, which are massless since the QCD $SU(3)$ symmetry is not broken. At hadron colliders like the LHC (pp collider) and the retired Tevatron ($p\overline{p}$ collider) there are four dominant production mechanisms, namely by decreasing order of their cross sections, gluon fusion (ggF), weak boson fusion (WBF), Higgs-strahlung i.e. production associated with a gauge boson, and production associated with top quark pair ($t\bar{t}H$). The general diagrams for these processes can be seen in figure 23, and their respective cross sections can be seen in figure 24.

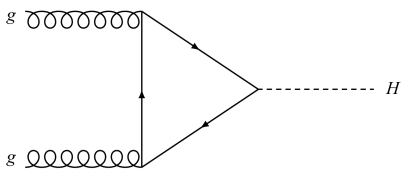

(a) Gluon fusion

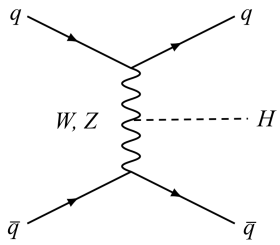

(b) Weak boson fusion

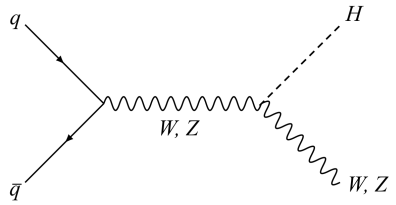

(c) Higgsstrahlung

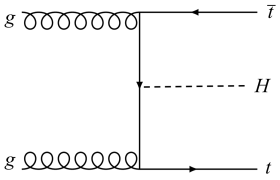

(d) Associated production with top quark pair

Figure 23: Main Higgs production processes at hadron colliders

We see that Higgs production through gluon fusion is the dominant process so we will calculate its cross section to leading order in the next section. QCD radiative corrections to this process turn out to be very significant and have been studied in detail. NLO corrections increase the leading order result for the cross section by 80%, while NNLO correction increase the NLO result by another 30%. Electroweak radiative corrections have also been computed at NLO an increase the cross section by 5% at $m_H = 125$ GeV.

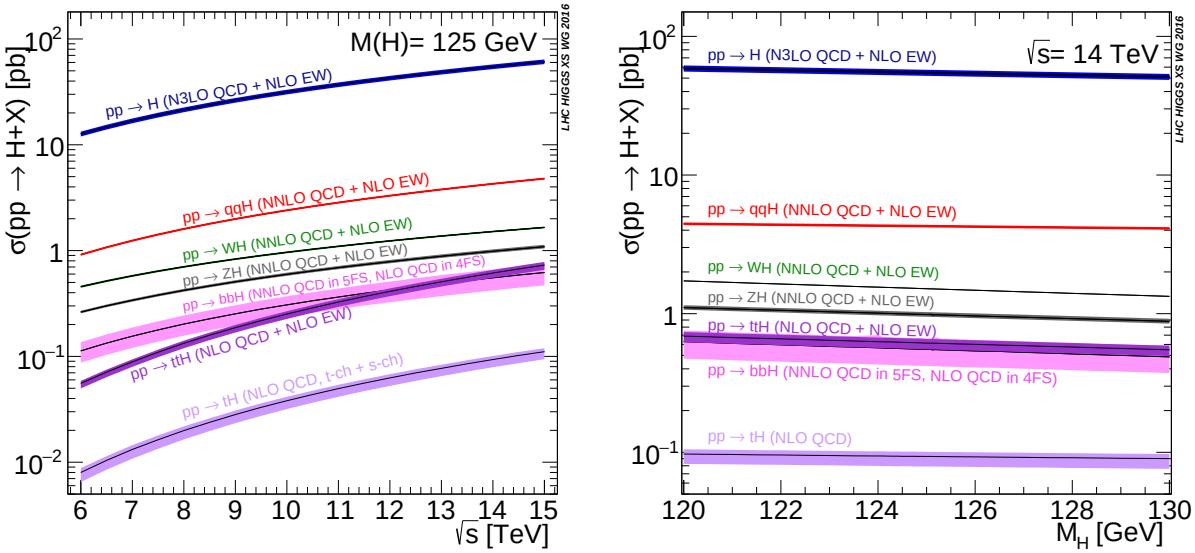

(a) The cross section for the Standard Model Higgs production as a function of $\sqrt{s}$ for proton-proton collisions

(b) The cross section for the Standard Model Higgs production as a function of the Higgs mass at $\sqrt{s} = 14$ TeV

Figure 24: Higgs production cross sections. The bands represent theoretical uncertainties [16]

While gluon fusion has the largest Higgs production cross section the other channels play an important role as well. The second most dominant production process is weak boson fusion, as seen in figure 24. In this process two light quarks scatter by interchange of a W or Z boson via either the t-channel or the u-channel, and a Higgs boson is emitted from the internal weak boson propagator. This is an important mode for Higgs searches as well as for the determination of the Higgs coupling to weak bosons.

Next we have Higgs associated production with Z or W bosons, the third most dominant mechanism, where two quarks annihilate to form a weak boson that radiates off a Higgs boson. Lastly we have Higgs production associated with top quark pair, which is the process we used to study some of the characteristics of the complex mass scheme. Even though its cross section is smaller than the other processes' it can provide important information about the top-Higgs Yukawa coupling as well as give access to the Higgs decay into two bottom quarks. In the next chapter we will use $q\bar{q} \to t\bar{t}H$ to showcase how one uses Monte Carlo integration in the computation of cross sections whose processes have three or more final state particles. As such we have computed the corresponding amplitude in section 6.2. We have also computed the amplitude for the process $gg \to t\bar{t}H$ in appendix B as well as its square. This allows for the implementation of a Monte Carlo program, analougous to what we will do for $q\bar{q} \to t\bar{t}H$. This way we have computed all the ten diagrams contributing to Higgs production associated with top quark pair.

5.1.1 Gluon Fusion: $gg \to H$

In this section we tackle the main production process for the Higgs boson used in the first run of the LHC, which led to its discovery. We will closely follow Bentvelsen, Laenen and Motylinsky [20] and take the oportunity to introduce some important techniques used in loop calculations,

such as Passarino-Veltmann reduction.

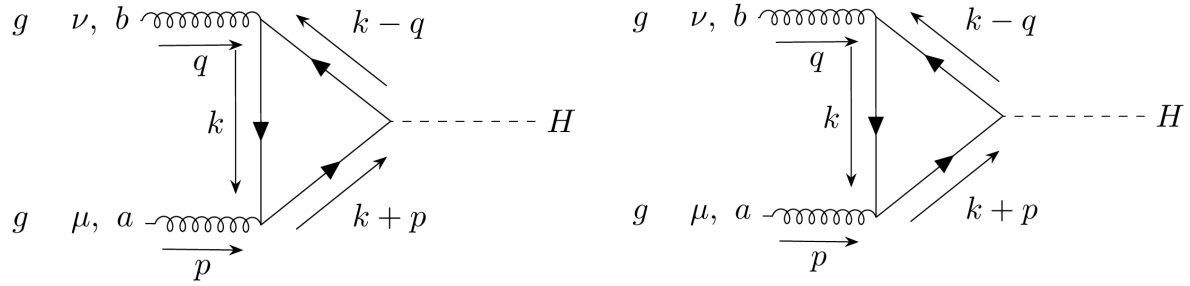

Figure 25: Diagrams contributing to Higgs production through gluon fusion

The diagrams to be considered are shown in figure 25. Since the coupling of the Higgs to fermions is proportional to the fermion mass we only need to consider contributions from the diagrams with a top quark loop. If we also take into account a bottom quark loop for example (since it is the next heaviest quark), we have that $m_b \sim 4$ GeV and $m_t \sim 173$ GeV so there would be a relative supression of $\left(\frac{m_t}{m_b}\right)^2 \sim 43^2$ of the contribution to $|\mathcal{M}|^2$, which for our intents and purposes is negligible.

As is costumary we use the Feynman rules from appendix A, which yield the following expression for the amplitude

$$\mathcal{M} = -g_s^2 \frac{y_t}{\sqrt{2}} Tr[t_a t_b] \epsilon_\mu(p) \epsilon_\nu(q) \int \frac{d^n k}{(2\pi)^n} \frac{1}{D_1 D_2 D_3} Tr[(\not{k} + \not{p} + m_t)\gamma^\mu(\not{k} + m_t)\gamma^\nu(\not{k} - \not{q} + m_t) + \\ + (-\not{k} + \not{q} + m_t)\gamma^\nu(-\not{k} + m_t)\gamma^\mu(-\not{k} - \not{p} + m_t)], \tag{5.1}$$

where we defined,

$$\begin{aligned} D_1 &= k^2 - m_t^2 \\ D_2 &= (k+p)^2 - m_t^2 \\ D_3 &= (k-q)^2 - m_t^2 \end{aligned} \tag{5.2}$$

There are a couple of things to point out. First, even though there is a loop integral over k in (5.1) we know *a priori* that the expression will be finite. This is due to the fact that there is no ggH coupling in the standard model (only in Higgs effective field theories -HEFT's - once you integrate out the top quark loop). Thus it would not be possible to perform the renormalization procedure to absorb the infinities, since there is no coupling constant to renormalize. The diagram must then be finite. Finally, we have to compute the trace in expression (5.1). This can be done making use of the algebraic manipulation program FORM [15], which we will use many times throughout this thesis. Here we just cite the result from the code, which ouputs

$$Tr[...] = 8m[q^\mu p^\nu + 4k^\mu k^\nu - \eta^{\mu\nu} p \cdot q - \eta^{\mu\nu} k^2 + \eta^{\mu\nu} m_t^2], \tag{5.3}$$

where we dropped the terms proportional to p^μ and q^ν since these vanish when contracted with their respective polarizations $\epsilon_\mu(p)$ and $\epsilon_\nu(q)$ in the expression for the amplitude.

Passarino-Veltmann reduction

The main difficulty arising in this calculation is the existence of tensor and vector integrals. Our aim is to write these integrals as a function of scalar integrals, which are much more tractable and allow us to proceed with our calculation. In our notation we will use the letter C to denote integrals with three denominators (D_1, D_2 and D_3), the letter B for integrals with two (different) denominators. We thus define

$$\begin{aligned} C_{\mu\nu} &= \int \frac{d^n k}{(2\pi)^n} \frac{k_\mu k_\nu}{D_1 D_2 D_3}, \\ C_\mu &= \int \frac{d^n k}{(2\pi)^n} \frac{k_\mu}{D_1 D_2 D_3}, \\ C_0 &= \int \frac{d^n k}{(2\pi)^n} \frac{1}{D_1 D_2 D_3} \end{aligned} \tag{5.4}$$

and

$$\begin{aligned} B_\mu(i,j) &= \int \frac{d^n k}{(2\pi)^n} \frac{k_\mu}{D_i D_j}, \\ B_0(i,j) &= \int \frac{d^n k}{(2\pi)^n} \frac{1}{D_i D_j}, \end{aligned} \qquad \text{for } i \neq j \tag{5.5}$$

To start breaking down these tensor and vector integrals we write the most general expression consistent with their Lorentz structure, noting that $C_{\mu\nu}$ is symmetric under the interchange of μ and ν. We obtain

$$\begin{aligned} C_{\mu\nu} &= p_\mu p_\nu C_{21} + q_\mu q_\nu C_{22} + (p_\mu q_\nu + q_\mu p_\nu) C_{23} + \eta_{\mu\nu} C_{24} \\ C_\mu &= C_{11} p_\mu + C_{12} q_\mu \end{aligned} \quad , \tag{5.6}$$

and,

$$\begin{aligned} B_\mu(1,2) &= B_1(1,2) p_\mu \\ B_\mu(1,3) &= B_1(1,3) q_\mu \\ B_\mu(2,3) &= B_1(2,3) p_\mu + B_2(2,3) q_\mu. \end{aligned} \tag{5.7}$$

It all comes down to knowing the coefficients present in these expressions as functions of scalar integrals. We can determine these constants by making contractions with p_μ and q_μ and the metric, and making use of the on-shell conditions $p^2 = q^2 = 0$ and $(p+q)^2 = m_H^2$. Let's start by obtaining the coefficients for the B integrals. If we contract the first equation in (5.7) with p_μ then the LHS is

$$\begin{aligned} p^\mu B_\mu(1,2) &= \int \frac{d^n k}{(2\pi)^n} \frac{p \cdot k}{D_1 D_2} = \frac{1}{2} \int \frac{d^n k}{(2\pi)^n} \frac{(p+k)^2 - k^2 - p^2}{D_1 D_2} \\ &= \frac{1}{2} \int \frac{d^n k}{(2\pi)^n} \left(\frac{1}{D_1} - \frac{1}{D_2} - \frac{p^2}{D_1 D_2} \right) \\ &= -\frac{1}{2} \int \frac{d^n k}{(2\pi)^n} \frac{p^2}{D_1 D_2}, \end{aligned} \tag{5.8}$$

where in the last step shifted the integration variable in the second integral $k \to k - p$, cancelling the first two integrals. In the RHS we have $p^2 B_1(1,2)$, so equating these two expressions we get

$$B_1(1,2) = -\frac{1}{2} B_0(1,2). \tag{5.9}$$

Following the same procedure for the second equation in (5.7) we get

$$B_1(1,3) = \frac{1}{2} B_0(1,3). \tag{5.10}$$

Finally for $B_\mu(2,3)$ we have

$$\begin{aligned} B_\mu(2,3) &= \int \frac{d^n k}{(2\pi)^n} \frac{k_\mu}{D_2 D_3} = \int \frac{d^n k}{(2\pi)^n} \frac{k_\mu + q_\mu}{[k^2 - m_t^2][(k+p+q)^2 - m_t^2]} \\ &= \int \frac{d^n k}{(2\pi)^n} \frac{k_\mu}{[k^2 - m_t^2][(k+p+q)^2 - m_t^2]} + q_\mu B_0(2,3). \end{aligned} \tag{5.11}$$

If we make $Q = p + q$ then the first term takes the form of $B_\mu(1,2)$ with p replaced by Q. As such we know this is equal to $-Q_\mu \frac{1}{2} B_0^{(p=Q)}(1,2)$, which after shifting the integration momenta $k \to k - q$ becomes $-\frac{1}{2}(p+q)_\mu B_0(2,3)$ in the usual definition. We have arrived at the expressions for $B_\mu(i,j)$ as a function of the scalar integrals only, which are

$$\begin{aligned} B_\mu(1,2) &= -\frac{1}{2} B_0(1,2) p_\mu \\ B_\mu(1,3) &= \frac{1}{2} B_0(1,3) q_\mu \\ B_\mu(2,3) &= \frac{1}{2}(q_\mu - p_\mu) B_0(2,3) \end{aligned} \tag{5.12}$$

Now we have to determine the constants in the C integrals. We start by defining R_i as

$$\begin{aligned} R_3 &= P_p^\mu C_{\mu\nu} p^\nu \\ R_4 &= P_q^\mu C_{\mu\nu} p^\nu \\ R_5 &= P_p^\mu C_{\mu\nu} q^\nu \\ R_6 &= P_q^\mu C_{\mu\nu} q^\nu, \end{aligned} \tag{5.13}$$

where $P_{k_i}^\mu k_j = \delta_{ij}$ is a momentum projection operator, for example $P_p^\mu = \frac{2}{s} q^\mu$ and $P_q^\mu = \frac{2}{s} p^\mu$. To obtain these R_i we start by writing $k \cdot p = \frac{1}{2}(D_2 - D_1)$ and $k \cdot q = -\frac{1}{2}(D_3 - D_1)$ and use this to compute

$$\begin{aligned} C_{\mu\nu} p^\nu &= \frac{1}{2}(B_\mu(1,3) - B_\mu(2,3)) \\ C_{\mu\nu} q^\nu &= -\frac{1}{2}(B_\mu(1,2) - B_\mu(2,3)). \end{aligned} \tag{5.14}$$

We can now plug in our results for $B_\mu(i,j)$ from equation (5.12) and obtain

$$\begin{aligned} C_{\mu\nu}p^\nu &= \frac{1}{4}(B_0(1,3) - B_0(2,3))q_\mu + \frac{1}{4}B_0(2,3)p_\mu \\ C_{\mu\nu}q^\nu &= \frac{1}{4}(B_0(1,2) - B_0(2,3))p_\mu + \frac{1}{4}B_0(2,3)q_\mu. \end{aligned} \tag{5.15}$$

Finally, by applying the projection operators to these equations we get the expressions for the R_i

$$\begin{aligned} R_3 =& \frac{1}{4}B_0(2,3) \\ R_4 =& \frac{1}{4}(B_0(1,3) - B_0(2,3)) \\ R_5 =& \frac{1}{4}(B_0(1,2) - B_0(2,3)) \\ R_6 =& \frac{1}{4}B_0(2,3). \end{aligned} \tag{5.16}$$

We have obtained these results for the R_i by taking the integral definition of $C_{\mu\nu}$ and going from there. However we can also obtain other expressions for the R_i by taking $C_{\mu\nu}$ given by (5.6). We then get

$$\begin{aligned} R_3 =& \frac{m_H^2}{2}C_{23} + C_{24} \\ R_4 =& \frac{m_H^2}{2}C_{22} \\ R_5 =& \frac{m_H^2}{2}C_{21} \\ R_6 =& \frac{m_H^2}{2}C_{23} + C_{24} \end{aligned} \tag{5.17}$$

All that is left is to invert equation (5.17) and write the C coefficients as a function of the R_i, which in turn are given by (5.16). Let us first state the result and then show the procedure for this inversion. The coefficients are

$$\begin{aligned} C_{21} =& \frac{2}{m_H^2}R_5 \\ C_{22} =& \frac{2}{m_H^2}R_4 \\ C_{23} =& \frac{2}{m_H^2}(R_6 - C_{24}) \\ C_{24} =& \frac{1}{n-2}(B_0(2,3) + m^2C_0 - R_3 - R_6). \end{aligned} \tag{5.18}$$

Only the expressions for C_{23} and C_{24} require special care. We define the projection operator

$$P^{\mu\nu} = \frac{1}{n-2}(\eta^{\mu\nu} - P_p^\mu p^\nu - P_q q^\nu). \tag{5.19}$$

When we apply this on (5.6) we see that it isolates the C_{24} coefficient

$$P^{\mu\nu}C_{\mu\nu} = \frac{1}{n-2}\left[m_H^2 C_{23} + (n-2)C_{24} - m_H^2 C_{23}\right] = C_{24}. \tag{5.20}$$

Then we apply $P^{\mu\nu}$ in the integral definition of $C_{\mu\nu}$(5.4). The last two terms of $P^{\mu\nu}$ applied on $C_{\mu\nu}$ are the definition of R_3 and R_6. The remaining term is

$$\eta^{\mu\nu}C_{\mu\nu} = \int \frac{d^n k}{(2\pi)^n}\frac{k^2}{D_1 D_2 D_3} = B_0(2,3) + m_t^2 C_0. \tag{5.21}$$

We have managed to write all the tensor and vector integrals in terms of scalar integrals, so all the terms coming out of the trace (5.3) can now be written as a function of these scalars. The next step is to evaluate this integrals using dimensional regularization.

Evaluation of the scalar integrals

Our next step is to evaluate the scalar integrals $B_0(i,j)$ and C_0. The computation of the latter is a little more involved than of the former, as we will see.

First, let us write the amplitude in terms of the scalar integrals, by plugging in our recently found expressions for the tensor and vector integrals (5.6) and (5.12) in the full amplitude $\mathcal{M} = \epsilon_\mu(p)\epsilon_\nu(q)\mathcal{M}^{\mu\nu}$. Since we are about to apply dimensional regularization on the scalar integrals we make $n = 4 - 2\epsilon$, which appears in this expression through the dependence of C_{23} and C_{24} on n. For small epsilon we expand $\frac{1}{4-2\epsilon} = \frac{1}{2}(1+\epsilon) + \mathcal{O}(\epsilon^2)$ and the amplitude becomes

$$\mathcal{M} = -g_s^2\frac{y_t}{\sqrt{2}}Tr[t_a t_b]\left[(\epsilon(p)\cdot\epsilon(q))\,A + (p\cdot\epsilon(q))\,(q\cdot\epsilon(p))\,B\right], \tag{5.22}$$

with

$$\begin{aligned} A =& 8m_t\epsilon B_0(2,3) - 4m_t M_H^2 C_0 + 16m_t^3(1+\epsilon)C_0 \\ B =& -\frac{2}{M_H^2}A \end{aligned} \tag{5.23}$$

This expression can readily be further simplified by taking into account two points. First, we expect C_0 to be finite just by looking at the UV behaviour of the integrand. The numerator goes as k^3 and the denominator as k^6, so the integrand scales with k^{-3}, hence the integral converges. Since we are going to set ϵ to zero, we can then drop any $\mathcal{O}(\epsilon)$ term multiplying C_0 since these terms will vanish. We also note that we do not expect $B_0(i,j)$ to have second order poles in ϵ since this would mean that that the amplitude would be infinite and not renormalizable. We will prove this is the case in the next section so we can just go ahead and drop the $\mathcal{O}(\epsilon^2)B_0(i,j)$ terms now.

Dimensional Regularization

To compute $B_0(2,3)$ we start by introducing a scale μ which will be ensure the correct dimensions when using dimensional regularization. So

$$B_0(2,3) = \mu^{2\epsilon} \int \frac{d^n k}{(2\pi)^n} \frac{1}{[k^2 - m_t^2][(k+p+q)^2 - m_t^2]}. \tag{5.24}$$

Next we use the Feynman Trick, as usual

$$\frac{1}{AB} = \int_0^1 dx \frac{1}{[xA + (1-x)B]^2}, \tag{5.25}$$

in our case we pick $A = (k+p+q)^2 - m_t^2$ and $B = k^2 - m_t^2$. We get

$$B_0(2,3) = \mu^{2\epsilon} \int \frac{d^n k}{(2\pi)^n} \int_0^1 dx \frac{1}{\big((1-x)[k^2 - m_t^2] + x[(k+p+q)^2 - m_t^2]\big)^2}. \tag{5.26}$$

We call $Q = p + q$, and write the denominator as $k^2 + 2xl \cdot k + x m_H^2 - m_t^2$ and subsequently make the shift $k \to k + xQ$ to obtain

$$B_0(2,3) = \mu^{2\epsilon} \int_0^1 dx \int \frac{d^n k}{(2\pi)^n} \frac{1}{[k^2 - M^2]}, \tag{5.27}$$

where we defined $M = x(1-x)m_H^2 - m_t^2$. Now we use the formula for this type of integral in n dimensions (inserir referencia)

$$\int \frac{d^n k}{(2\pi)^n} \frac{1}{[k^2 - M^2]^\alpha} = i(-1)^\alpha \frac{\pi^{n/2}}{(2\pi)^n} \frac{\Gamma(\alpha - \frac{n}{2})}{\Gamma(\alpha)} (M^2)^{\frac{n}{2} - \alpha}. \tag{5.28}$$

In our case $\alpha = 2$ and $n = 4 - 2\epsilon$, which yields

$$B_0(2,3) = i \frac{\mu^{2\epsilon}}{16\pi^2} \Gamma(\epsilon)(4\pi)^\epsilon \int_0^1 dx [M(x)]^{-\epsilon}. \tag{5.29}$$

The integral in x can be approximated to 1, since $[M(x)]^{-\epsilon} = e^{-\log(M(x)\epsilon} = 1 - \epsilon \log(M(x)) + \mathcal{O}(\epsilon^2)$, so only the constant term survives when $\epsilon \to 0$. Now we use that the Γ function has the property $\Gamma(z) = \frac{1}{z} - \gamma_E + \mathcal{O}(z)$ and that $(4\pi)^\epsilon = 1 + \log(4\pi)\epsilon + \mathcal{O}(\epsilon^2)$ to finally obtain

$$B_0(2,3) = \frac{i}{16\pi^2} \left(\frac{1}{\epsilon} - \gamma_E + \log(4\pi) \right). \tag{5.30}$$

As we expected $B_0(2,3)$ only has a single pole in ϵ. Plugging this in (5.23) we get

$$\begin{aligned} A =& \frac{8 m_t}{16\pi^2} \left[i - \frac{1}{2} M_H^2 (1-\tau) 16\pi^2 C_0 \right] \\ B =& -\frac{2}{m_H^2} A, \end{aligned} \tag{5.31}$$

where we defined $\tau = \frac{4m_t^2}{M_H^2}$.

Now we proceed by evaluating the cross-section for this process. For the scattering of two incoming massless particles, the master formula for cross-sections is given by

$$\hat{\sigma} = \frac{1}{2\hat{s}} \int d\text{LIPS} \overline{\sum} |\mathcal{M}|^2, \tag{5.32}$$

where $\overline{\sum}$ denotes the average over the initial particles' spin and color, and the sum over the final particles' spin and color. Since the Higgs is a scalar and has no color this last sum does not exist, so all we have to do is the averaging of the initial particle's color and spin. For this $2 \to 1$ process the integral over the Lorentz inavriant phase-space (LIPS) is just given by

$$\int d\text{LIPS} = \int \frac{d^4k}{(2\pi)^4} (2\pi)\delta(\hat{s} - M_H^2)(2\pi)^4 \delta^{(4)}(k - p - q) = (2\pi)\delta(\hat{s} - M_H^2). \tag{5.33}$$

From averaging over color we have a factor of $\frac{1}{8^2}$ (gluons transform under the adjoint representation of $SU(3)$), and averaging over spin gives us a factor of $\frac{1}{2^2}$. We also use that $g_s^4 = 16\pi^2\alpha_s^2$ and $y_t^2/2 = \sqrt{2}G_F m_t^2$. The trace over color is $Tr[t_a t_b] = \frac{1}{2}\delta_{ab}$, so the factor $Tr[t_a t_b]Tr[t^a t^b]$ coming from $|\mathcal{M}|^2$ is just $\frac{1}{4}\delta_{ab}\delta^{ab} = 2$. So the cross-section is

$$\hat{\sigma} = \frac{\alpha_s^2 \pi^3 m_t^2 \sqrt{2} G_F}{16 M_H^2} \sum_{spin} |\left[(\epsilon(p) \cdot \epsilon(q))\, A + (p \cdot \epsilon(q))\,(q \cdot \epsilon(p))\, B \right]|^2 \delta(\hat{s} - m_H^2) \tag{5.34}$$

To compute the module squared appearing in the cross section we use the completeness relation for gluons when summing over spin states. Since the gluons are massless particles we only sum over two polarizations states, so to write the completeness relations we introduce a light-like vector n_μ such that $n^2 = 0$ and write

$$P_{\mu\nu}(p) := \sum_\lambda \epsilon_\mu(\lambda, p)\bar{\epsilon}_\nu(\lambda, p) = -\eta_{\mu\nu} + \frac{n_\mu p_\nu + n_\nu p_\mu}{n \cdot p} \quad . \tag{5.35}$$

After a little algebra we see that this operator $P_{\mu\nu}(p)$ we defined satisfies the following properties

$$\begin{aligned} P^{\mu\nu}(p) P_{\mu\nu}(q) &= 2 \\ P^{\mu\nu}(p) q_\mu q_\nu &= M_H^2 \\ P^{\mu\nu}(q) p_\mu p_\nu &= M_H^2 \\ P^{\rho\alpha} p_\rho P_{\sigma\alpha} q^\sigma &= M_H^2 \end{aligned} \tag{5.36}$$

Now we use that for the sum of two complex numbers $|a+b|^2 = (a+b)^*(a+b) = |a|^2 + |b|^2 + a^*b + (a^*b)^* = |a|^2 + |b|^2 + 2\Re(a^*b)$, so we have

$$
\begin{aligned}
&\sum_{\lambda_1,\lambda_2} |\epsilon_\alpha(\lambda_1,p)\epsilon^\alpha(\lambda_2,q)A + p_\alpha q_\beta \epsilon^\alpha(\lambda_2,q)\epsilon^\beta(\lambda_1,p)B|^2 \\
=&\sum_{\lambda_1,\lambda_2} \epsilon_\alpha(\lambda_1,p)\bar{\epsilon}_\beta(\lambda_1,p)\epsilon^\alpha(\lambda_2,q)\bar{\epsilon}^\beta(\lambda_2,q)|A|^2 + p_\alpha q_\beta p_\rho q_\sigma \epsilon^\alpha(\lambda_2,q)\bar{\epsilon}^\rho(\lambda_2,q)\epsilon^\beta(\lambda_1,p)\bar{\epsilon}^\sigma(\lambda_1,p)|B|^2 \\
&+ 2\Re[\epsilon^\rho(\lambda_2,q)\epsilon^\sigma(\lambda_1,p)\bar{\epsilon}_\alpha(\lambda_1,p)\bar{\epsilon}^\alpha(\lambda_2,q)p_\rho q_\sigma A^* B] \\
=&P_{\mu\nu}(p)P^{\mu\nu}(q)|A|^2 + p_\alpha q_\beta p_\rho q_\sigma P^{\alpha\rho}(q)P^{\beta\sigma}(p)|B|^2 + 2\Re[P^{\rho\alpha}(q)P_{\sigma\alpha}p_\rho q^\sigma A^* B] \\
=&2|A|^2
\end{aligned} \tag{5.37}
$$

where in the last step we made use of the identities (5.36).

Finally, after some simplification of the pre-factors we can write the cross section

$$
\hat{\sigma} = \frac{\alpha_s^2\sqrt{2}G_F}{16\pi}\left(\frac{m_t^2}{M_H^2}\right)^2 \left| i - \frac{1}{2}M_H^2(1-\tau)16\pi^2 C_0 \right| M_H^2\delta(\hat{s}-m_H^2). \tag{5.38}
$$

We see that to obtain the explicit expression for the cross section the last thing we need to do is evaluate the scalar integral C_0.

Computation of C_0

We recall C_0 can be written as

$$
\begin{aligned}
C_0 &= \int \frac{d^n k}{(2\pi)^n} \frac{1}{[k^2-m_t^2][(k-q)^2-m_t^2][(k+p)^2-m_t^2]} \\
&= \int \frac{d^n k}{(2\pi)^n} \frac{1}{[k^2-m_t^2][k^2-2k\cdot q-m_t^2][k^2+2k\cdot q-m_t^2]}
\end{aligned} \tag{5.39}
$$

Just as before we apply the Feynman trick (5.25), in this case to the first two denominators with $A = (k-q)^2 - m_t^2$ and $B = k^2 - m_t^2$. This gives

$$
C_0 = \int \frac{\mathrm{d}^n k}{(2\pi)^n} \int_0^1 \mathrm{d}x \, \frac{1}{[k^2 - 2xk\cdot q - m_t^2]^2} \frac{1}{[k^2+2k\cdot p - m_t^2]} \tag{5.40}
$$

Now we will make use of the generalization of the Feynman trick to higher powers of the fraction, which reads

$$
\frac{1}{A_1^{\alpha_1}...A_n^{\alpha_n}} = \frac{\Gamma(\alpha_1+...+\alpha_n)}{\Gamma(\alpha_1)...\Gamma(\alpha_n)} \int_0^1 \mathrm{d}x_1...\mathrm{d}x_n \delta(1-x_1-...-x_n) \frac{x_1^{\alpha_1-1}...\, x_n^{\alpha_n-1}}{[x_1A_1+...+x_nA_n]^{(\alpha_1+...+\alpha_n)}}. \tag{5.41}
$$

Applying this to (5.40) by evaluating the fraction $\frac{1}{A^2B}$ with $A = k^2 - 2xk\cdot q - m_t^2$ and $B = k^2 + 2k\cdot p - m_t^2$ gives

$$
C_0 = \frac{\Gamma(3)}{\Gamma(1)\Gamma(2)} \int \frac{\mathrm{d}^n k}{(2\pi)^n} \int_0^1 \mathrm{d}x \int_0^1 \mathrm{d}y \frac{y}{[k^2 - 2xyk\cdot q + 2(1-y)k\cdot p - m_t^2]^3} \tag{5.42}
$$

We note that by defining $\Delta = [yp - x(1-y)q]$ we can write the denominator as $(k+\Delta)^2 - \Delta^2 - m_t^2$. Hence, by making the shift $k \to k - \Delta$ we write C_0 as

$$C_0 = 2 \int \frac{\mathrm{d}^n k}{(2\pi)^n} \int_0^1 \mathrm{d}x \int_0^1 \mathrm{d}y \frac{y}{[k^2 - (m_t^2 + \Delta^2)]^3}. \tag{5.43}$$

We see that we have rewritten the integral in such a way that we can resort to formula (5.28) in order to evaluate it. We get

$$\int \frac{\mathrm{d}^n k}{(2\pi)^n} \frac{1}{k^2 - (m_t^2 + \Delta^2)} = -\frac{(4\pi)^\epsilon}{16\pi^2} \frac{\Gamma(1+\epsilon)}{2} [m_t^2 + \Delta^2]^{\epsilon - 1}. \tag{5.44}$$

In the calculation of the B_0 integrals we saw that $\Gamma(1+\epsilon) \sim e^{-\epsilon \gamma_E}$, which does not have a pole at $\epsilon = 0$. This means expression (5.44) is finite, and we can therefore take the limit $\epsilon \to 0$ without any problem. The expression we get for C_0 is then

$$C_0 = -\frac{i}{16\pi^2} \int_0^1 \mathrm{d}x \int_0^1 \mathrm{d}y \frac{y}{m_t^2 - xy(1-y)M_H^2}, \tag{5.45}$$

where we used that $\Delta^2 = [x(1-y)q - yp]^2 = -xy(1-y)M_H^2$. We proceed by first evaluating the integral over x, which gives

$$\begin{aligned} C_0 =& \frac{i}{16\pi^2} \int_0^1 \mathrm{d}y \frac{y}{y(1-y)M_H^2} \ln\left(m_t^2 - xy(1-y)M_H^2\right) \Big|_{x=0}^{x=1} \\ =& \frac{i}{16\pi^2} \int_0^1 \mathrm{d}y \frac{1}{(1-y)M_H^2} \ln\left(\frac{m_t^2 - y(1-y)M_H^2}{m_t^2}\right) \\ =& \frac{i}{16\pi^2} \int_0^1 \mathrm{d}y \frac{1}{(1-y)M_H^2} \ln\left(1 - \frac{4y(1-y)}{\tau}\right), \end{aligned} \tag{5.46}$$

where we recall $\tau = \frac{4m_t^2}{M_H^2}$. Now we make the change of variables $y \to 1 - y$, which yields

$$C_0 = -\frac{i}{16\pi^2 M_H^2} \int_0^1 \mathrm{d}y \frac{1}{y} \ln\left(1 - \frac{4y(1-y)}{\tau}\right). \tag{5.47}$$

We see that the function $f(y) = 4y(1-y)$ has a maximum at $y_{max} = \frac{1}{2}$ whose value is $f(y_{max}) = 1$. So we notice that for values of $\tau < 1$, the argument of the logarithm goes negative and thus it acquires an imaginary part. Integrating (5.47) by parts we get

$$C_0 = -\frac{i}{16\pi^2 M_H^2} \frac{4}{\tau} \int_0^1 \mathrm{d}y \frac{(1-2y)\ln(y)}{1 - 4y(1-y)/\tau}. \tag{5.48}$$

Now we determine the poles of the zeroes $y_\pm$ of the denominator resorting to the quadratic formula, which gives

$$y_\pm = \frac{1 \pm \sqrt{1-\tau}}{2}, \tag{5.49}$$

so we can write C_0 as

$$C_0 = -\frac{i}{16\pi^2 M_H^2}\frac{4}{\tau}\int_0^1 \mathrm{d}y \frac{(1-2y)\ln(y)}{(y-y_+)(y-y_-)} \quad . \tag{5.50}$$

We split the fraction in the integrand to obtain

$$C_0 = -\frac{i}{16\pi^2 M_H^2}\frac{1}{\beta}\int_0^1 \mathrm{d}y (1-2y)\ln(y)\left[\frac{1}{y-y_+} - \frac{1}{y-y_-}\right], \tag{5.51}$$

where we define $\beta = y_+ - y_- = \sqrt{1-\tau}$. Now we can split the integral into the contributions coming from the poles and from the rest of the integration domain. To achieve this we use the standard identity

$$\int \frac{dx'}{x - x' \mp \epsilon} = P\int \frac{dx'}{x'-x} \pm i\pi\delta(x'-x), \tag{5.52}$$

where P denotes the principal value integral. For a function $f(x)$ with a pole at b, the principal value integral is defined as

$$P\int_a^c \mathrm{d}x f(x) = \lim_{\delta\to 0^+}\left[\int_a^{b-\delta}\mathrm{d}x f(x) + \int_{b+\delta}^c \mathrm{d}x f(x)\right], \tag{5.53}$$

such that we are integrating over the original domain except for a tiny region around the pole. As we claimed before, for $\tau < 1$ the integral becomes complex, so it is suitable to divide the evaluation of the integral into the regions $\tau < 1$ and $\tau > 1$.

For $\tau < 1$ we start by computing the imaginary part of the integral

$$I \equiv \frac{1}{\beta}\int_0^1 \mathrm{d}y (1-2y)\ln(y)\left[\frac{1}{y-y_+} - \frac{1}{y-y_-}\right]. \tag{5.54}$$

Using (5.52) we obtain

$$\begin{aligned} i\Im I =& \frac{i\pi}{\beta}\left(\int_0^1 \mathrm{d}y\delta(y-y_+)(1-2y)\ln(y) + \int_0^1 \mathrm{d}y\delta(y-y_-)(1-2y)\ln(y)\right) \\ =& \frac{i\pi}{\beta}[(1-2y_+)\ln y_+ p + (1-2y_-)\ln y_-]. \end{aligned} \tag{5.55}$$

From (5.49) we see that $(1-2y_+) = -\beta$ and $(1-2y_-) = \beta$ such that

$$\begin{aligned} i\Im I =& i\pi[\ln y_- \ln y_+] \\ =& -i\pi \ln\frac{y_+}{y_-} \\ =& -i\pi\ln\frac{1+\sqrt{1-\tau}}{1-\sqrt{1-\tau}}. \end{aligned} \tag{5.56}$$

To obtain the real part for $\tau < 1$ first we define $\xi = 4/\tau$ and evaluate the derivative with respect

to ξ such that

$$\begin{aligned}\frac{\mathrm{d}I}{\mathrm{d}\xi} &= \int_0^1 \frac{\mathrm{d}}{\mathrm{d}\xi}\left[1-\xi y(1-y)\right] \\ &= -\int_0^1 \mathrm{d}y \frac{1-y}{1-y(1-y)\xi}.\end{aligned} \tag{5.57}$$

We now change the variable of integration to u such that $y = \frac{1}{2}(1+u)$ and hence $1-y = \frac{1}{2}(1-u)$. The expression then becomes

$$\begin{aligned}\frac{\mathrm{d}I}{\mathrm{d}\xi} &= -\int_{-1}^1 \mathrm{d}u \frac{1-u}{4-\xi+\xi u^2} \\ &= -\int_{-1}^1 \frac{\mathrm{d}u}{4-\xi+\xi u^2}, \\ &= -\frac{1}{\xi}\int_{-1}^1 \frac{\mathrm{d}u}{u^2-\beta^2},\end{aligned} \tag{5.58}$$

where we dropped the anti symmetric part of the integral and used $\beta = \sqrt{1-4/\xi}$. Now we note that

$$\frac{1}{2\beta\xi}\left(\frac{1}{u+\beta}-\frac{1}{u-\beta}\right) = -\frac{1}{\xi}\frac{1}{u^2-\beta^2}, \tag{5.59}$$

so

$$\frac{\mathrm{d}I}{\mathrm{d}\xi} = \frac{1}{2\beta\xi}\int_{-1}^1 \mathrm{d}u\left(\frac{1}{u+\beta}-\frac{1}{u-\beta}\right). \tag{5.60}$$

Now for $\tau = 4/\xi < 1$, β is real so this intergal is easy to perform, as we will show. Also, since now we are only interested in the real part of this integral, we can replace the regular integral by the principal value integral. This yields

$$\frac{\mathrm{d}I}{\mathrm{d}\xi} = \frac{1}{2\beta\xi}P\int_{-1}^1 \mathrm{d}u\left(\frac{1}{u+\beta}-\frac{1}{u-\beta}\right). \tag{5.61}$$

We can compute the principal value integral from its definition (5.53), so

$$\begin{aligned}P\int_{-1}^1 \frac{\mathrm{d}u}{u-\beta} &= \lim_{\delta\to 0^+}\left[\int_{-1}^{\beta-\delta}\frac{\mathrm{d}u}{u-\beta}+\int_{\beta+\delta}^1\frac{\mathrm{d}u}{u-\beta}\right] \\ &= \lim_{\delta\to 0^+}\left[\ln\left(\frac{\delta}{1+\beta}\right)+\ln\left(\frac{1-\beta}{\delta}\right)\right] \\ &= \ln\left(\frac{1-\beta}{1+\beta}\right).\end{aligned} \tag{5.62}$$

Likewise we get

$$P\int_{-1}^1 \frac{\mathrm{d}u}{u+\beta} = \ln\left(\frac{1+\beta}{1-\beta}\right), \tag{5.63}$$

and as such

$$\frac{\mathrm{d}I}{\mathrm{d}\xi} = \frac{1}{\beta\xi}\ln\left(\frac{1+\beta}{1-\beta}\right). \tag{5.64}$$

Having done this we change the integration variable to β by writing

$$I = \int \mathrm{d}\xi \frac{\mathrm{d}I}{\mathrm{d}\xi} = \int \mathrm{d}\beta \frac{\mathrm{d}\xi}{\mathrm{d}\beta}\frac{\mathrm{d}I}{\mathrm{d}\xi}, \tag{5.65}$$

and since $\beta = \sqrt{1-4/\xi}$ we compute

$$\frac{\mathrm{d}\xi}{\mathrm{d}\beta} = \left[\frac{\mathrm{d}\beta}{\mathrm{d}\xi}\right]^{-1} = \left[-\frac{1}{2\beta}\frac{4}{\xi^2}\right]^{-1} = \frac{\beta\xi^2}{2}, \tag{5.66}$$

which leads us to the following expression for the integral

$$I = \int \mathrm{d}\beta \frac{\xi}{2}\ln\left(\frac{1+\beta}{1-\beta}\right). \tag{5.67}$$

We can rewrite this by noting that

$$\frac{\mathrm{d}}{\mathrm{d}\beta}\ln\left(\frac{1+\beta}{1-\beta}\right) = \frac{1}{1+\beta} + \frac{1}{-\beta} = \frac{2}{1-\beta^2} = \frac{\xi}{2}, \tag{5.68}$$

meaning we can write the integrand as a total derivative

$$\begin{aligned} I =& \frac{1}{2}\int \mathrm{d}\beta \frac{\mathrm{d}}{\mathrm{d}\beta}\left[\ln^2\left(\frac{1+\beta}{1-\beta}\right)\right] \\ =& \frac{1}{2}\ln^2\left(\frac{1+\beta}{1-\beta}\right) + \text{constant}. \end{aligned} \tag{5.69}$$

With this we were able to compute both the real and imaginary part of the integral for $\tau < 1$.

For $\tau > 1$, β will be imaginary so we write $|\beta| = \frac{4}{\xi} - 1$. We take expression (5.58) and make the change of variable $v = \frac{u}{|\beta|}$, which yields

$$\begin{aligned} \frac{\mathrm{d}I}{\mathrm{d}\xi} =& -\frac{1}{\xi|\beta|}\int_{-1/|\beta|}^{\beta}\frac{\mathrm{d}v}{1+v^2} \\ =& -\frac{2}{\xi|\beta|}\arctan\left(\frac{1}{|\beta|}\right). \end{aligned} \tag{5.70}$$

Now we use the identity $\sin(\arctan(x)) = \frac{x}{\sqrt{1+x^2}}$, such that

$$\begin{aligned} \arctan\left(\frac{1}{|\beta|}\right) =& \arcsin\left(\sin\left[\arctan\left(\frac{1}{|\beta|}\right)\right]\right) \\ =& \arcsin\left(\frac{1}{\sqrt{1+|\beta|^2}}\right) \\ =& \arcsin\left(\sqrt{\frac{\xi}{4}}\right). \end{aligned} \tag{5.71}$$

Finally we integrate over ξ to obtain the expression for I. We make the change of variables $x = \sqrt{\frac{\xi}{4}}$ to get

$$\begin{aligned} I &= -\int \mathrm{d}\xi \frac{2}{\sqrt{\xi(4-\xi)}} \arcsin\left(\sqrt{\frac{\xi}{4}}\right) \\ &= -4\int \mathrm{d}x \frac{1}{\sqrt{1-x^2}} \arcsin(x) \\ &= -2\int \mathrm{d}x \frac{\mathrm{d}}{\mathrm{d}x}\left[\arcsin^2(x)\right] \\ &= -2\arcsin^2\left(\sqrt{\frac{\xi}{4}}\right). \end{aligned} \tag{5.72}$$

So far we have seen that

$$I = \begin{cases} \frac{1}{2}\ln^2\left(\frac{1+\beta}{1-\beta}\right) - i\pi \ln\left(\frac{1+\beta}{1-\beta}\right) + \text{constant} & ,\tau < 1 \\ -2\arcsin^2\left(\frac{1}{\sqrt{\tau}}\right) & ,\tau > 1. \end{cases} \tag{5.73}$$

We can choose the integration constant such that I is continuous at $\tau = 1$, which implies constant $= -\frac{\pi}{2}$. With this we are finally able to write the expression for the original integral $C_0 = \frac{i}{16\pi^2 M_H^2} I$ as

$$C_0 = \frac{i}{16\pi^2 M_H^2} \begin{cases} \frac{1}{2}\left[\ln\left(\frac{1+\beta}{1-\beta}\right) - i\pi\right]^2 & \tau < 1 \\ -2\arcsin^2\left(\frac{1}{\sqrt{\tau}}\right) & \tau > 1, \end{cases} \tag{5.74}$$

with $\beta = \sqrt{1-\tau}$. We can plug this in expression (5.38) and after some rearrangement of the factors we obtain our desired result

$$\sigma_{L0} = \frac{G_F \alpha_s^2}{288\sqrt{2}\pi} M_H^2 |A(\tau)|^2 \delta(\hat{s} - M_H^2), \tag{5.75}$$

with

$$A(\tau) = \frac{3}{2}\tau[1 + (1-\tau)f(\tau)] \quad \text{and} \quad f(\tau) = \begin{cases} \arcsin^2\left(\frac{1}{\sqrt{\tau}}\right) & ,\tau \geq 1 \\ -\frac{1}{4}\left[\ln\frac{1+\sqrt{1-\tau}}{1-\sqrt{1-\tau}} - i\pi\right]^2 & ,\tau < 1. \end{cases} \tag{5.76}$$

This is the standard result for the leading order cross section for gluon fusion, which can be found for example in [20].

5.2. Higgs Decay

In the previous section we discussed the main Higgs production mechanisms at hadron colliders and explicitely computed the cross section for the most dominant process, gluon fusion. In this section we will talke about Higgs decay processes, and in particular the main one used at the LHC: $H \to \gamma\gamma$.

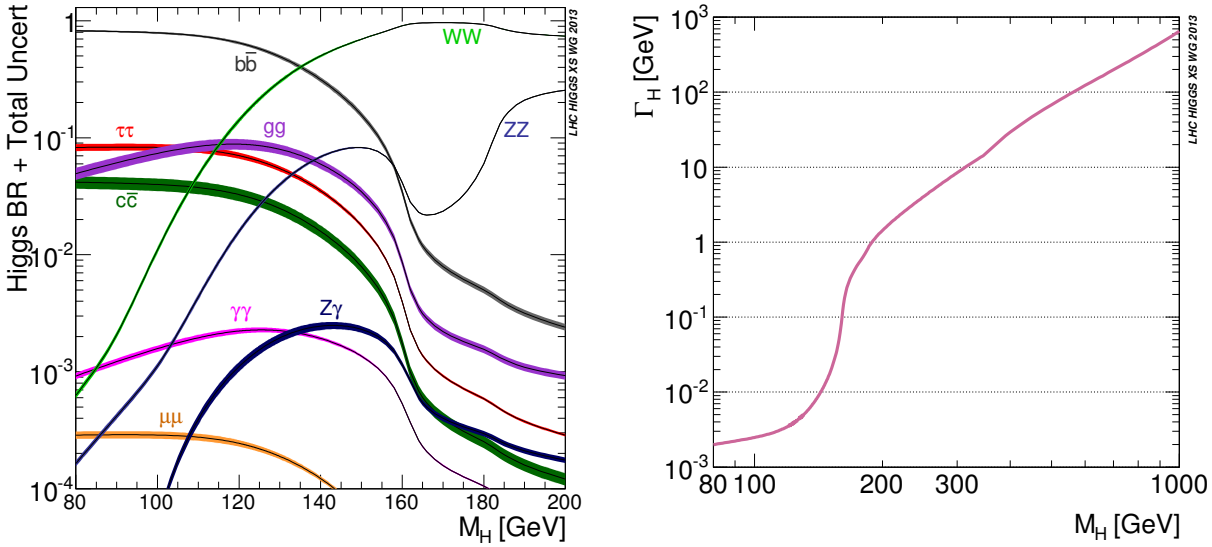

(a) Higgs branching ratios as a function of m_H

(b) Higgs total width Γ_H as function of m_H

Figure 26: Higgs BR and Γ_H as function of mass

The Higgs boson can in principle decay (off-shell) to all Standard Model particles, which at tree-level are given by its SM couplings to other particles. Since these couplings are proportional to the particle's mass this means the prefered modes of decay occur for the heaviest particles. This can be seen in figure 26a, where the branching ratios of the Higgs are plotted as a function of its mass. We see that for small m_H the decay to $b\bar{b}$ dominates, since the b quark is the heaviest particle the Higgs can decay into at that mass value. Once off-shell decays to W^+W^- are allowed they quickly dominate (we emphasize this is an off-shell decay since at $m_H^2 < 2m_W$ the on-shell decay is not kinematically allowed). We also note that even though the mass of the Z is greater than that of the W, the reason the decay to ZZ is not as dominant as to WW is because the latter has two degrees of freedom in the final state (W^+W^- and W^-W^+) as opposed to one. When the on-shell decay to WW becomes kinematically allowed, i.e. $m_H > 2m_W$, we see a drop in the ZZ branching ration until its own on-shell decay also becomes allowed.

When $m_H > 2m_t$ the $t\bar{t}$ decay becomes significant but it never really dominates since the coupling to fermions is proportional to m_f whereas the coupling to the weak bosons is proportional to m_W^2 and m_Z^2, as we saw in chapter 2. At $m_H = 125$ GeV the Higgs branching ratios are summarized in table 2.

By summing over all the branching ratios one obtains the total decay width Γ_H, which can be seen as a function of the Higgs mass in figure (26b). At $m_H = 125$GeV the Higgs width is $\Gamma_H = 4$ MeV, which is relatively small compared to other EW particles like the W, the Z and the top which have widths on the order of $1 - 2$ GeV.

Up until now we spoke only of the tree-level decays, but loop-induced decays, and as we said before $H \to \gamma\gamma$ in particular, play a very important role in LHC phenomenology. We will explicitely calculate this decay, which occurs both through top quark loop and W boson loop, in the following sections.

Decay mode	Branching Ratio	Relative Uncertainty
$H \to \gamma\gamma$	2.27×10^{-3}	$+5.0\%$ -4.9%
$H \to ZZ$	2.62×10^{-2}	$+4.3\%$ -4.1%
$H \to W^+W^-$	2.14×10^{-1}	$+4.3\%$ -4.2%
$H \to \tau^+\tau^-$	6.27×10^{-2}	$+5.7\%$ -5.7%
$H \to b\bar{b}$	5.84×10^{-1}	$+3.2\%$ -3.3%
$H \to Z\gamma$	1.53×10^{-3}	$+9.0\%$ -8.9%
$H \to \mu^+\mu^-$	2.18×10^{-4}	$+6.0\%$ -5.9%

Table 2: Higgs branching ratios and respective uncertainties at $m_H = 125$ GeV

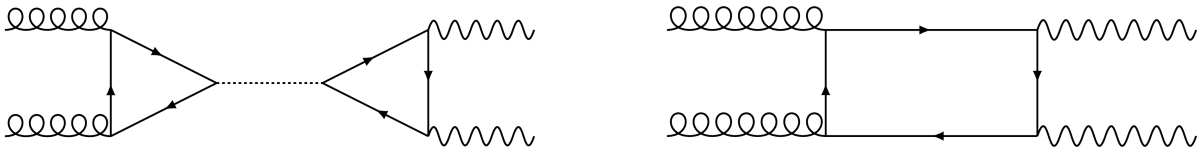

(a) Signal **(b)** Background

Figure 27: Example of signal and background processes for $gg \to \gamma\gamma$

The reason why $H \to \gamma\gamma$ is important has to do with LHC detectors. We have to deal with the fact that there is no signal without background. When we talk about background we mean processes that produce the same final state particles as the process we intend to study but are not in fact that process, as we illustrate in figure 27. To extract the signal for a process we measure the four momenta of the detected particles and compute the invariant mass. The signal has a resonance at m_H and therefore should peak at that energy, while the background is expected to stay relatively flat. The LHC detectors are particularly good at measuring the photon energy and momentum, in fact the resolution in this channel is ten times better than any other decay channel with the notable exception of muons. Another important point is that photons do not decay so all events can be used. This is in constrast with the W and the Z, whose decay to two jets turns out not to be very useful given the overwhelming QCD background. So despite having a small branching ratio $H \to \gamma\gamma$ was one of the main discovery channels of the Higgs boson at the LHC.

In the following two sections we will compute the main processes contributing to $H \to \gamma\gamma$ at one-loop, namely through top-quark loop and W-boson loop.

5.2.1 $H \to \gamma\gamma$ through top-quark loop

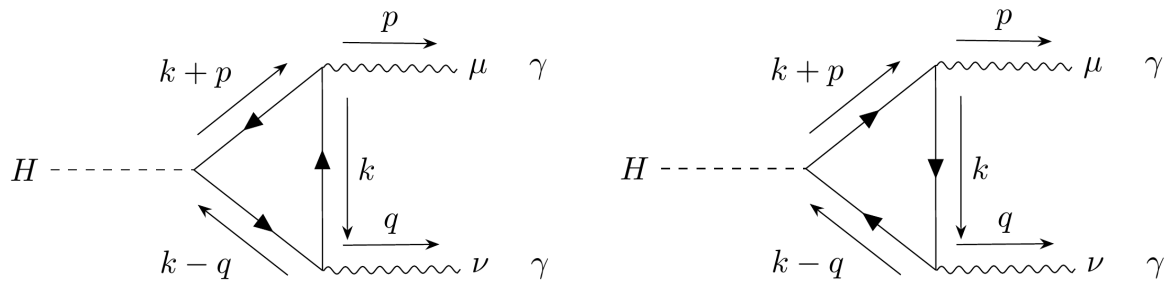

Figure 28: Diagrams contributing to Higgs decay to two γ through top quark loop

The diagrams for this process, which can be seen in figure 28, are quite similar to gluon fusion. Since we have already computed $gg \to H$ explicitly much of that calculation can be reused to compute $H \to \gamma\gamma$ through top-quark loop. The only modifications that are in order are substituting the QCD gluon-fermion coupling by the QED photon-fermion coupling. In practice this means we take the result from the invariant amplitude (5.22) and replace g_s^2 by $(Q_t e)^2$ as well as substitute the color factor $Tr[t_a t_b]$ by $\delta_i^{\ i} = N_C$, where N_C designates the number of colors. This means we are able to shortcut the computation and by using that $\frac{y_t}{\sqrt{2}} = \frac{g}{2}\frac{m_t}{m_W}$ we can write

$$i\mathcal{M} = -N_C(Q_t e)^2 \frac{g}{2}\frac{m_t}{m_W}\left[(\epsilon(p)\cdot\epsilon(q)) - \frac{2}{M_H^2}(p\cdot\epsilon(q))(q\cdot\epsilon(p))\right]A, \tag{5.77}$$

with

$$A = \frac{8m_t}{16\pi^2}\left(i - \frac{1}{2}M_H^2(1-\tau)16\pi^2 C_0\right). \tag{5.78}$$

When we computed the gluon fusion cross section we also saw that the integral C_0 was given by (5.74), so we can write this amplitude as

$$\mathcal{M} = N_c Q_t^2 \frac{e^2 g}{16\pi^2 m_W} F(\tau)\left(\frac{M_H^2}{2}\eta_{\mu\nu} - q^\mu p^\nu\right)\epsilon_\mu(p)\epsilon_\nu(q), \tag{5.79}$$

with $F(\tau) = -2\tau[1 + (1-\tau)f(\tau)]$, where $f(\tau)$ is again given by

$$f(\tau) = \begin{cases} \arcsin^2\left(\frac{1}{\sqrt{\tau}}\right) & ,\tau \geq 1 \\ -\frac{1}{4}\left[\ln\frac{1+\sqrt{1-\tau}}{1-\sqrt{1-\tau}} - i\pi\right]^2 & ,\tau < 1. \end{cases} \tag{5.80}$$

5.2.2 $H \to \gamma\gamma$ through W-boson loop

For the decay through W-boson loop the diagrams pertaing to the $H \to \gamma\gamma$ process can be seen in figure 29.

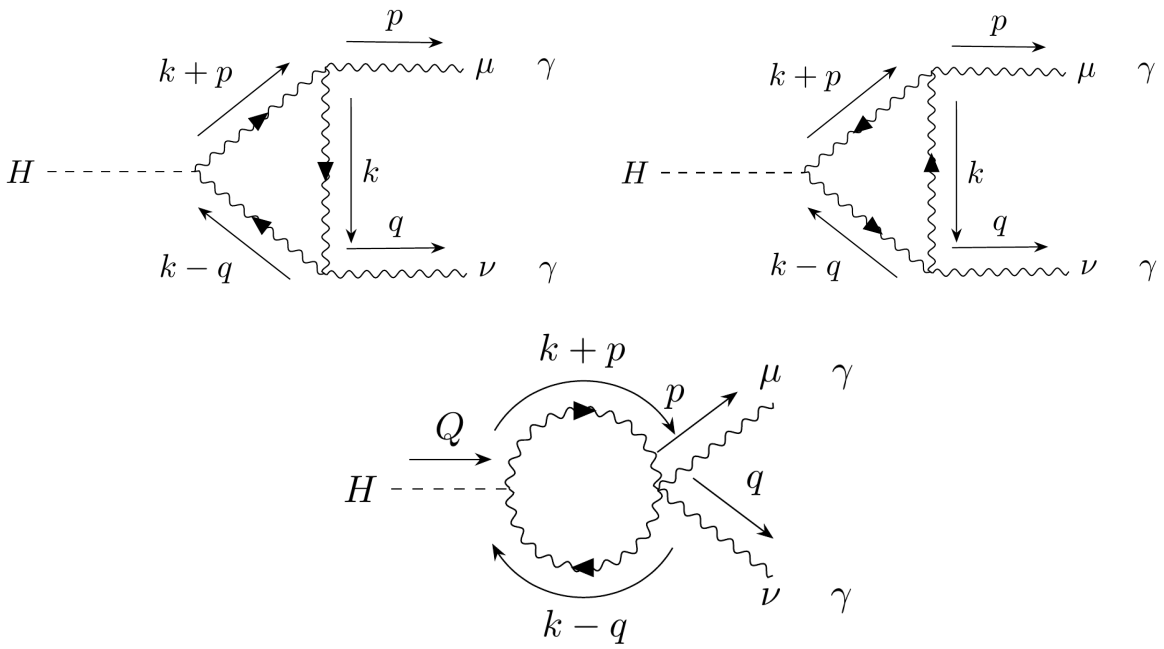

Figure 29: Diagrams contributing to Higgs decay to two γ through W boson quark loop

First thing we note is that the first two diagrams have the same expression since the two overall minus sign coming from the $WW\gamma$ vertices (relative to the first diagram) cancel. As is costumary we use the feynman rules in appendix A to compute the amplitude of this process, which give the following expression

$$\mathcal{M}_{\mu\nu} = gM_W e^2 (A_{\mu\nu} - B_{\mu\nu}), \tag{5.81}$$

with

$$\begin{aligned} A_{\mu\nu} = \int \frac{d^n k}{(2\pi)^n} 2 \cdot \frac{1}{D_1 D_2 D_3} & \left[\eta^{\alpha_1\beta_1} - \frac{(k+p)^{\alpha_1}(k+p)^{\beta_1}}{m_W^2}\right] \\ & [\eta_{\beta_1\alpha_2}(2k+p)_\mu + \eta_{\alpha_2\mu}(-k+p)_{\beta_1} - \eta_{\mu\beta_1}(k+2p)_{\alpha_2}] \left[\eta^{\alpha_2\beta_2} - \frac{k^{\alpha_2}k^{\beta_2}}{m_W^2}\right] \\ & [\eta_{\beta_2\alpha_3}(2k-q)_\nu + \eta_{\alpha_3\nu}(2q-k)_{\beta_2} - \eta_{\nu\beta_2}(k+q)_{\alpha_3}] \cdot \\ & \cdot \left[\eta^{\alpha_3\beta_3} - \frac{(k-q)^{\alpha_3}(k-q)^{\beta_3}}{m_W^2}\right] \eta_{\beta_3\alpha_1} \end{aligned} \tag{5.82}$$

$$\begin{aligned} B_{\mu\nu} = \int \frac{d^n k}{(2\pi)^n} \frac{1}{D_2 D_3} & \left[\eta^{\alpha_1\beta_1} - \frac{(k+p)^{\alpha_1}(k+p)^{\beta_1}}{m_W^2}\right] \cdot \\ & \cdot [2\eta_{\beta_1\alpha_2}\eta_{\mu\nu} - \eta_{\beta_1\mu}\eta_{\alpha_2\nu} - \eta_{\beta_1\nu}\eta_{\alpha_2\mu}] \left[\eta^{\alpha_2\beta_2} - \frac{(k-q)^{\alpha_2}(k-q)^{\beta_2}}{m_W^2}\right] \eta_{\alpha_1\beta_2}, \end{aligned} \tag{5.83}$$

where we used the same definition for D_1, D_2, D_3 as before, given by equation (5.2). To compute this amplitude we could proceed as before and use Passarino-Veltmann reduction to write the tensor and vector integrals as functions of scalar integrals. However this would be a quite cumbersome endeavor, so it would be pleasant to find a way to get the result without recurring

to PV-reduction. This can be achieved and it goes as follows. First, we note that the amplitude is symmetric under the simultaneous interchange of p with q and μ with ν. We also know that it satisfies the Ward identities

$$\begin{aligned} p^\mu \mathcal{M}_{\mu\nu} =& 0 \\ q^\nu \mathcal{M}_{\mu\nu} =& 0. \end{aligned} \tag{5.84}$$

Thus, we are free to make the following decomposition

$$\begin{aligned} \mathcal{M}_{\mu\nu} =& (p\cdot q\,\eta_{\mu\nu} - q_\mu p_\nu)\mathcal{M}^{(1)}(p,q) \\ &+ (p^2q^2\eta_{\mu\nu} - q^2 p_\mu p_\nu - p^2 q_\mu q_\nu + p\cdot q\, p_\mu q_\nu)\mathcal{M}^{(2)}(p,q). \end{aligned} \tag{5.85}$$

We contract with the metric $\eta^{\mu\nu}$ and with $q^\mu p^\nu$ and then invert the 2x2 matrix, such that we have $\mathcal{M}^{(1)}(p,q)$ and $\mathcal{M}^{(2)}(p,q)$ as a function of $q^\lambda \mathcal{M}_{\lambda\tau} p^\tau$ and $\mathcal{M}^\rho_\rho$. This yields

$$\begin{aligned} \mathcal{M}^{(1)}(p,q) =& \frac{p\cdot q}{(n-2)[(p\cdot q)^2 - p^2q^2]}\mathcal{M}^\rho_\rho - \frac{(p\cdot q)^2 + (n-2)p^2q^2}{(n-2)[(p\cdot q)^2 - p^2q^2]^2} q^\lambda \mathcal{M}_{\lambda\tau} p^\tau \\ \mathcal{M}^{(2)}(p,q) =& -\frac{1}{(n-2)[(p\cdot q)^2 - p^2q^2]}\mathcal{M}^\rho_\rho - \frac{(n-1)(p\cdot q)}{(n-2)[(p\cdot q)^2 - p^2q^2]^2} q^\lambda \mathcal{M}_{\lambda\tau} p^\tau. \end{aligned} \tag{5.86}$$

Now we make use of the on-shell relations $p^2 = q^2 = 0$ and $(p+q)^2 = m_H^2$ so (5.86) becomes

$$\begin{aligned} \mathcal{M}^{(1)}(p,q) =& \frac{2}{(n-2)m_H^2}\left(\mathcal{M}^\rho_\rho - \frac{2}{m_H^2} q^\lambda \mathcal{M}_{\lambda\tau} p^\tau\right) \\ \mathcal{M}^{(2)}(p,q) =& -\frac{4}{(n-2)m_H^4}\left(\mathcal{M}^\rho_\rho - \frac{2(n-1)}{m_H^2} q^\lambda \mathcal{M}_{\lambda\tau} p^\tau\right). \end{aligned} \tag{5.87}$$

Of these two coefficients we only need to compute $\mathcal{M}^{(1)}(p,q)$, since upon taking the momenta on-shell in (5.85) and contracting with the polarizations only the first term remains. To compute $\mathcal{M}^\rho_\rho$ and $q^\lambda \mathcal{M}_{\lambda\tau} p^\tau$ we will require some assistance from FORM. We will instruct FORM that there are a number of simplifications one can make in this calculation, by shifting the integration variable and making use of $p^2 = 0$ and $q^2 = 0$. These are

$$\begin{aligned} \int \frac{d^nk}{(2\pi)^n}\frac{1}{D_1} &= \int \frac{d^nk}{(2\pi)^n}\frac{1}{D_2} = \int \frac{d^nk}{(2\pi)^n}\frac{1}{D_3} = A_0 \\ \int \frac{d^nk}{(2\pi)^n}\frac{D_2}{D_1} &= \int \frac{d^nk}{(2\pi)^n}\frac{D_1}{D_2} = 0 \\ \int \frac{d^nk}{(2\pi)^n}\frac{D_3}{D_1} &= \int \frac{d^nk}{(2\pi)^n}\frac{D_1}{D_3} = 0 \\ \int \frac{d^nk}{(2\pi)^n}\frac{D_3}{D_2} &= \int \frac{d^nk}{(2\pi)^n}\frac{D_2}{D_3} = m_H^2 A_0 \\ \int \frac{d^nk}{(2\pi)^n}\frac{D_1}{D_2D_3} &= A_0 - \frac{m_H^2}{2}\int \frac{d^nk}{(2\pi)^n}\frac{1}{D_2D_3} \\ \int \frac{d^nk}{(2\pi)^n}\frac{D_2}{D_1D_3} &= A_0 + \frac{m_H^2}{2}\int \frac{d^nk}{(2\pi)^n}\frac{1}{D_1D_3} \\ \int \frac{d^nk}{(2\pi)^n}\frac{D_3}{D_1D_2} &= A_0 + \frac{m_H^2}{2}\int \frac{d^nk}{(2\pi)^n}\frac{1}{D_1D_2}. \end{aligned} \tag{5.88}$$

The expression for $\mathcal{M}^{\rho}_{\rho}$ after we make simplifications (5.88) is provided by the FORM code in appendix C.1.1. We note that we drop the constant term appearing in the output since this corresponds to a scaleless integral, which is zero by dimensional regularization. The result is

$$\begin{aligned}\mathcal{M}^{\rho}_{\rho} = gM_W e^2 \int \frac{d^n k}{(2\pi)^n} \frac{1}{D_1 D_2 D_3} \Bigg[& -\frac{1}{4}\frac{m_H^6}{m_W^2} - 9m_H^2\left(n - \frac{13}{9}\right) + 8m^2(n-1)\Bigg] \\ & + \frac{1}{D_1 D_2}\left[2(n-1) + \frac{5}{8}\frac{m_H^4}{m_W^4} + \frac{m_H^2}{m_W^2}\right] \\ & + \frac{D_3^2}{D_1 D_2}\left[-\frac{1}{2m_W^4}\right] \\ & + \frac{1}{D_1 D_3}\left[2(n-1) + \frac{5}{8}\frac{m_H^4}{m_W^4} + \frac{m_H^2}{m_W^2}\right] \\ & + \frac{D_2^2}{D_1 D_3}\left[-\frac{1}{2m_W^4}\right] \\ & + \frac{1}{D_2 D_3}\left[6\left(n - \frac{2}{3}\right) + \frac{1}{16}\frac{m_H^6}{m_W^6} - \frac{3}{8}\frac{m_H^4}{2m_W^4} - \frac{m_H^2}{m_W^2}(n-2) - 2n^2\right] \\ & + \frac{1}{D_1}\left[-\frac{1}{4}\frac{m_H^4}{m_W^6} + 2\frac{m_H^2}{m_W^4}\right].\end{aligned} \tag{5.89}$$

Similarly, the expression for $q^{\lambda}\mathcal{M}_{\lambda\tau}p^{\tau}$ after we make the simplifications (5.88) is provided by the FORM code in appendix C.1.2. We drop the constant term for the same reasons as before. The result is

$$\begin{aligned}q^{\lambda}\mathcal{M}_{\lambda\tau}p^{\tau} = gM_W e^2 \int \frac{d^n k}{(2\pi)^n} \frac{1}{D_1 D_2 D_3} \Bigg[& -\frac{1}{8}\frac{m_H^8}{m_W^4} + \frac{1}{4}\frac{m_H^6}{m_W^2} - \frac{m_H^2}{2}(n+7)\Bigg] \\ & + \frac{1}{D_1 D_2}\left[(n-1)m_H^2 + \frac{5}{16}\frac{m_H^6}{m_W^4} + \frac{1}{2}\frac{m_H^4}{m_W^2}\right] \\ & + \frac{D_3^2}{D_1 D_2}\left[-\frac{m_H^2}{4m_W^4}\right] \\ & + \frac{1}{D_1 D_3}\left[(n-1)m_H^2 + \frac{5}{16}\frac{m_H^6}{m_W^4} + \frac{1}{2}\frac{m_H^4}{m_W^2}\right] \\ & + \frac{D_2^2}{D_1 D_3}\left[-\frac{m_H^2}{4m_W^4}\right] \\ & + \frac{1}{D_2 D_3}\left[\frac{1}{32}\frac{m_H^8}{m_W^6} - \frac{3}{16}\frac{m_H^6}{m_W^4} - \frac{m_H^4}{m_W^2} - 2m_H^2(n-1)\right] \\ & + \frac{1}{D_1}\left[-\frac{1}{8}\frac{m_H^6}{m_W^6} + \frac{m_H^4}{m_W^4}\right].\end{aligned} \tag{5.90}$$

Again we make use of FORM, this time the code in apendix C.1.3 to get the expression for $\mathcal{M}^{(1)}$.

$$\mathcal{M}^{(1)} = gM_W e^2 \frac{2}{(n-2)m_H^2}\left(\left[10\left(n - \frac{8}{10}\right) - (n-4)\frac{m_H^2}{m_W^2}\right]B_0(2,3) - \left[8m_H^2\left(n - \frac{5}{2}\right) + (n-1)m_W^2\right]C_0\right) \tag{5.91}$$

Dimensional Regularization

Again we have to perform dimensional regularization to compute this amplitude. Luckily, most of the work is already cut out for us since we have the expression for $B_0(2,3)$ from (5.30) and C_0 from (5.74). We recall that C_0 is finite, so we can intruct FORM to use the following identities in the limit $\epsilon \to 0$

$$\begin{aligned} \epsilon\, C_0 =& 0 \\ \epsilon\, B_0 =& \frac{i}{16\pi^2} \\ \frac{1}{(n-2)} =& -\frac{1}{2}(1+\epsilon+O(\epsilon^2)) \end{aligned} \tag{5.92}$$

Once more we use the code in appendix C.1.3, this time to perform the dimensional regularization. This yields the result

$$\mathcal{M}^{(1)} = \frac{ge^2}{m_W m_H^2}\frac{2i}{16\pi^2}\left[m_H^2 + 6m_W^2 - 6m_W^2(m_H^2 - 2m_W^2)(-i16\pi^2)C_0\right]. \tag{5.93}$$

Finally we contract the amplitude $\mathcal{M}_{\mu\nu}$ with the polarizations to obtain

$$i\mathcal{M} = \frac{ige^2}{16\pi^2 m_W m_H^2}[m_H^2 + 6m_W^2 - 6m_W^2(m_H^2 - 2m_W^2)(-i16\pi^2)C_0](m_H^2\eta^{\mu\nu} - 2q^\mu p^\nu)\bar{\epsilon}_\mu(p)\bar{\epsilon}_\nu(q) \tag{5.94}$$

with C_0 given by (5.74). Similarly to what we did for the Higgs decay through top quark loop, we can define $\tau = \frac{4m_W^2}{m_W^2}$ in order to rewrite the expression for the invariant amplitude

$$\mathcal{M} = \frac{e^2 g}{16\pi^2 m_W} F(\tau)\left(\frac{M_H^2}{2}\eta_{\mu\nu} - q^\mu p^\nu\right)\epsilon_\mu(p)\epsilon_\nu(q), \tag{5.95}$$

where $F(\tau) = 2 + 3\tau + 3\tau(2-\tau)f(\tau)$ with $f(\tau)$ again given by (5.80). This is indeed the result found in the literature, for example by Marciano, et al [21] however our calculation happens to be less involved since we avoided the computation of five amplitudes and did not have to resort to Passarino-Veltmann reduction.

5.2.3 Partial decay width $\Gamma(H \to \gamma\gamma)$

Now that we have computed the individual amplitudes of the Higgs decay to two photons through top-loop and through W-boson loop we can write the total decay amplitude. For the Higgs decay through fermion loop we claimed that only the top-loop contribution was dominant and other contributions would be supressed. However, for the sake of completeness in this section we will include all fermion loop contributions. This means we can take amplitude (5.79) and sum over all quarks and leptons. Naturally $N_C = 3$ for the quarks, and $N_C = 1$ for the leptons. In addition, by taking into account our results for the decay through W-loop (5.95)

we can write the total $H \to \gamma\gamma$ amplitude as

$$\mathcal{M} = \frac{e^2 g}{16\pi^2 m_W} F(\tau_f, \tau_W) \left(\frac{M_H^2}{2} \eta_{\mu\nu} - q^\mu p^\nu \right) \epsilon_\mu(p) \epsilon_\nu(q), \tag{5.96}$$

with

$$F(\tau_f, \tau_W) = F_W(\tau_W) + \sum_f N_C Q_f^2 F_f(\tau_f), \tag{5.97}$$

where $F_f(\tau_f)$ and $F_W(\tau_W)$ are given by the $F(\tau)$ function we computed for the top-loop and W-loop cases respectively

$$\begin{aligned} F_f(\tau_f) =& -2\tau_f[1 + (1-\tau_f) f(\tau_f)] \\ F_W(\tau_W) =& 2 + 3\tau_W + 3\tau(2-\tau_W) f(\tau_W). \end{aligned} \tag{5.98}$$

Here $f(\tau)$ is given by the usual expression (5.80), and also $\tau_f = \frac{4m_f^2}{M_H^2}$ and $\tau_W = \frac{4m_W^2}{M_H^2}$.

The goal of this section is to compute the partial width $\Gamma(H \to \gamma\gamma)$, which we can achieve by using the definition (2.100). To facilitate obtaining the standard result, first we note that we can rewrite $\mathcal{M}$ as

$$\mathcal{M} = 2\frac{\alpha}{4\pi} \left(\frac{g}{2m_W} \right) \frac{M_H^2}{2} F(\tau_f, \tau_W) \left(\eta_{\mu\nu} - \frac{2}{M_H^2} q^\mu p^\nu \right) \epsilon_\mu(p) \epsilon_\nu(q), \tag{5.99}$$

such that

$$|\mathcal{M}|^2 = \sqrt{2} G_F \left(\frac{\alpha}{4\pi} \right)^2 M_H^4 |F(\tau_f, \tau_W)|^2 \left| \left(\eta_{\mu\nu} - \frac{2}{M_H^2} q^\mu p^\nu \right) \epsilon_\mu(p) \epsilon_\nu(q) \right|^2, \tag{5.100}$$

where we used that $(\frac{g}{2m_W^2})^2 = \sqrt{2} G_F$. We still have to sum over the final states' polarizations. This we have already done in (5.37) where we saw that

$$\sum_{\lambda_1, \lambda_2} \left| \left(\eta_{\mu\nu} - \frac{2}{M_H^2} q^\mu p^\nu \right) \epsilon_\mu(\lambda_1, p) \epsilon_\nu(\lambda_2, q) \right|^2 = 2, \tag{5.101}$$

and as such

$$\sum |\mathcal{M}|^2 = 2\sqrt{2} G_F \left(\frac{\alpha}{4\pi} \right)^2 M_H^4 |F(\tau_f, \tau_W)|^2. \tag{5.102}$$

Since $|\mathcal{M}|$ has no dependence on the momenta we can write

$$\Gamma(H \to \gamma\gamma) = \frac{1}{2M_H} \sum |\mathcal{M}|^2 \int \frac{d^3p}{(2\pi)^3 2|\mathbf{p}|} \frac{d^q p}{(2\pi)^3 2|\mathbf{q}|} (2\pi)^4 \delta^{(4)}(Q - p - q). \tag{5.103}$$

All that is left is to compute the two particle phase space integral. To do this, we refer to the formula in chapter 3 of the book [1] for the phase space integral of two particles with masses m_1

and m_2

$$\begin{aligned} I(s, m_1^2, m_2^2) \equiv & \frac{1}{(2\pi)^2} \int \frac{d^3p_1 d^3p_2}{4\omega_1\omega_2} \delta^{(4)}(Q - p_1 - p_2) \\ = & \frac{1}{32\pi^2} \frac{\lambda^{1/2}(s, m_1^2, m_2^2)}{s} \int \mathrm{d}\Omega_{CM}. \end{aligned} \tag{5.104}$$

In our case the final particles are massless and identical, which means we only integrate over half of the total solid angle. This yields $I(s, 0, 0) = \frac{1}{16\pi}$.

Pluging the phase-space integral in (5.103) we obtain the known result

$$\Gamma(H \to \gamma\gamma) = \frac{G_F M_H^2}{8\sqrt{2}\pi} \left(\frac{\alpha}{4\pi}\right)^2 |F(\tau_f, \tau_W)|^2, \tag{5.105}$$

which is in agreement with the one presented in [21].

6 Monte Carlo Methods

6.1. Monte Carlo Integration

We are often interested in the theoretical prediction of cross-sections and decay rates which we can subsequently compare with experimental results. Up until now in our calculations, be it for cross sections or for decay rates, we had at most two final state particles which made the integration over phase space simple enough to be handled analytically. However obtaining such analytical predictions is often not possible. To see why let us consider a general scattering process with two incoming particles of mass m_1 and m_2 and momenta p_1 and p_2, and n outgoing particles with momenta $k_i, i = 1, ..., n$. We recall the general expression of the cross-section for this process is given by

$$\sigma = \frac{1}{2\lambda^{1/2}(s, m_1^2, m_2^2)} \int \prod_{j=1}^{n} d\Pi_j (2\pi)^4 \delta^{(4)} \left(p_1 + p_2 - \sum_i k_i \right) |\mathcal{M}|^2, \tag{6.1}$$

where $d\Pi_j = \frac{d^3 k_j}{2\omega(k_j)}$, $\mathcal{M}$ is the invariant amplitude of the process, $s = (p_1 + p_2)^2$ is the square of the center of mass energy $s = (p_1 + p_2)^2$the λ function is defined as

$$\lambda(x, y, z) = x^2 + y^2 + z^2 - 2xy - 2xz - 2yz. \tag{6.2}$$

Similarly, the expression for the decay rate in a general reference where the decaying particle has spatial momentum $\mathbf{p}$ and the outgoing particles momenta $k_i, i = 1, ..., n$ is

$$\Gamma(\mathbf{p}) = \frac{1}{2\omega(p)} \int \prod_{j=1}^{n} d\Pi_j (2\pi)^4 \delta^{(4)} \left(p - \sum_i k_i \right), \tag{6.3}$$

with $\mathcal{M}$ being the invariant amplitude of the decay.

As we stated before, both of these expressions require an integral over the phase space of final state particles. As the number of outgoing particles increases so does the complexity of these integrals, so we are only able to provide the analytical solutions to the simplest of cases. Moreover, the difficulty in performing the analytical calculation increases substantially if we impose restrictions on the integration domain, for example in case we wanted it to match the accessible phase-space of a given detector. In a typical LHC event we have $\sim 10^3$ particles, leading to $\sim 3 \times 10^3$ phase space integrals [23], hence analytical computations are out of the question.

One has then to resort to numerical methods in order to perform these integrals, in particular

to Monte Carlo integration. In this method one can compute multi-dimensional integrals by approximating the original integral to

$$\int_{a_1}^{b_1} dx_1 ... \int_{a_d}^{b_d} dx_n f(x_1, ..., x_d) \simeq (b_1 - a_1)...(b_d - a_d) \frac{1}{N} \sum_i^N f\left(x_1(i), ..., x_d(i)\right), \tag{6.4}$$

where $x_k(i) = a_k + \rho_i(b_k - a_k)$, with ρ_i being a random number between zero and one and N representing the number of integration points. Put in words what we are doing is approximating the function in the integrand $f(x_1, ..., x_d)$ by its average over the random collection of points $x_1(i), ..., x_n(i)$, with $i = 1, ..., N$ determined by the random numbers ρ_i and subsequently multiplying by the range of the integration domain. To estimate the error of this calculation we can employ the central limit theorem which states that the distribution $\langle f \rangle$ will tend to a Gaussian curve with $\sigma_{int} = \frac{\sigma_i}{\sqrt{N}}$, where σ_i is the standard deviation of $f(x_1(i), ..., x_d(i))$. This means the error decreases with the number of MC points as $\frac{1}{\sqrt{N}}$. Explicitly the error of the Monte Carlo computation is given by

$$E = \sqrt{\frac{V_N}{N}}, \quad \text{with} \quad V_N = \frac{1}{N} \sum_i W_i^2 - \left[\frac{1}{N} W_i\right]^2, \tag{6.5}$$

where we defined the weight W_i as

$$W_i = (a_1 - b_1)...(a_d - b_d) f(x_1(i), ..., x_d(i)). \tag{6.6}$$

In the computation of cross sections we see that the role of the integrand is played by $|\mathcal{M}|^2$. Also, we see that for n final state particles we have a $3n - 4$ dimensional integral, since there are $3n$ integrals over the components of the spatial momenta restricted by energy and momenta conservation. The next step in our MC integration of phase-space is to generate a set of four-momenta that obey energy-momentum conservation using random numbers, which implies $k_l = k_l(x_i)$. These momenta will serve as the argument of the function we intend to integrate. Since we want to perform the integration over x_i this means we will have to perform the change of variables and compute the appropriate Jacobian. To generate the momenta we will use a s-type branching algorithm, which for n particles with masses $m_1, ..., m_n$ allows us to compute their on-shell momenta making use of $3n - 4$ random numbers. In this example we do not restrict the integration domain.

The algorithm goes as follows. We start in the center of mass (COM) frame of the collision, with momentum Q_1 satisfying $Q_1^2 = s$. Then we split this momentum into the on-shell momentum k_1 (which will correspond to the external momentum of particle 1) and the off-shell momentum Q_2. Next, we go now to the rest frame of Q_2 (no longer the COM frame) and split it into a on-shell momentum k_2 and a off-shell momentum Q_3. Although k_2 is on-shell, since it was generated in the Q_2 rest frame we need to boost it into the COM frame before we can use it as an argument. We repeat this procedure until we get to Q_{n-1}, which splits into the two final on-shell momenta k_{n-1} and k_n.

To show explicitely how this happens let us define the following auxilliary quantities

$$s_i = \sum_{j=i}^{n} m_j \quad m_i^Q = \left(\sum_{j=i}^{n} k_j\right)^2 \quad \text{and} \quad E_i^Q = \sum_{j=i}^{n} E_j. \tag{6.7}$$

We will work iteratively and assume that at iteration i, $k_{i-1}, ..., k_1$ have already been determined in the COM frame. At an intermediate iteration i, to determine k_i and Q_{i+1} from Q_i we proceed as follows. First we write

$$k_i^\mu = (E_i, |\mathbf{k}_i| \sin\theta_i \cos\phi_i, |\mathbf{k}_i| \sin\theta_i \sin\phi_i, |\mathbf{k}_i| \cos(\theta_i)), \tag{6.8}$$

with $E_i = \sqrt{|\mathbf{k}_i^2| + m_i^2}$. We can now set Q_{i+1} by momentum conservation

$$Q_{i+1} = (E_{i+1}^Q, -\mathbf{k}_i). \tag{6.9}$$

In turn, $|\mathbf{k}_i|$ can be obtained by

$$|\mathbf{k_i}| = \frac{\sqrt{\lambda(m_i^{Q\,2}, m_i^2, m_{i+1}^{Q\,2})}}{2m_i^Q}. \tag{6.10}$$

Thus, there are only three unknown variables we need to parametrize with random numbers, these being ϕ_i, θ_i and m_{i+1}^Q. We note that $s_{i+1} \leq m_{i+1}^Q \leq m_i^Q - m_i$ so we can parametrize these parameters as

$$\phi_i = 2\pi x_1^i, \quad \cos\theta_i = 1 - x_2^i, \quad \text{and} \quad m_{i+1}^Q = s_{i+1} + x_3^i(m_i^Q - s_i), \tag{6.11}$$

with x_1^i, x_2^i and x_3^i being random numbers between zero and one. Having done this we are finally able to use expressions (6.8) and (6.9) to obtain k_i and Q_{i+1} in the rest frame of Q_i. Naturally, in the end we want to obtain the k_i all in the same frame, namely the COM frame. This means we still need to apply Lorentz boosts to the values of k_i we have obtained through this algorithm, in order to have them in the desired frame of reference. The Lorentz tranformation for energy and momenta from a frame S with velocity v measured in a frame S' is

$$\begin{aligned} E' &= \gamma\left(E + v\mathbf{k}_{i\|}\right) \\ \mathbf{k'}_{i\|} &= \gamma\left(\mathbf{k}_{i\|} + vE\right) \\ \mathbf{k'}_{i\perp} &= \mathbf{k}_{i\perp}, \end{aligned} \tag{6.12}$$

where $v = \beta = \frac{|\mathbf{Q}_i|}{Q_i^0}$, and $\gamma = \frac{1}{\sqrt{1-\beta^2}} = \frac{Q_i^0}{m_i^Q}$. To define $\mathbf{k}_{i\perp}$ and $\mathbf{k}_{i\|}$ we resort to a unit vector parallel to the direction of the boost $\hat{n}_i = \frac{\mathbf{Q}_i}{Q_i^0}$, such that

$$\mathbf{k}_{i\|} = \hat{n}_i \cdot \mathbf{k}_i \ \text{, and} \quad \mathbf{k}_{i\perp} = \mathbf{k}_i - \mathbf{k}_{i\|}\hat{n}_i. \tag{6.13}$$

The last thing we need to do is find the the Jacobian of the coordinate transformation that allows us to perform the integral over the random numbers x_1^i, x_2^i and x_3^i. We can start by

writing $d^3k_i = |\mathbf{k}_i|^2 d|\mathbf{k}_i| d(\cos\theta) d\phi$, noting that we have

$$d(\cos\theta_i) = 2dx_2^i \quad \text{and} \qquad d\phi_i = 2\pi dx_1^i. \tag{6.14}$$

For all but the last iteration, we can use the chain rule to write $|\mathbf{k}|^2 d|\mathbf{k}|$ as

$$|\mathbf{k}|^2 d|\mathbf{k}| = |\mathbf{k}|^2 \frac{d|\mathbf{k}|}{d|\mathbf{k}|^2} \frac{d|\mathbf{k}|^2}{dm_i^2} \frac{dm_i^2}{dm_{i+1}^Q} \frac{dm_{i+1}^Q}{dx_3^i} dx_3^i. \tag{6.15}$$

After having computed these derivatives we see that we can rewrite

$$\frac{\mathrm{d}^3 k_i}{(2\pi)^3 2E_i} = \frac{|\mathbf{k}_i|}{4\pi^2}(m_i^Q - s_i)\frac{m_{i+1}^Q}{m_i^Q} dx_1^i dx_2^i dx_3^i \tag{6.16}$$

For the last iteration the procedure is similar but we only need two random numbers for ϕ_{n-1} and $\cos\theta_{n-1}$. The random number for m_n^Q is not required since $m_n^Q = m_n$. So in this last step we need to consider

$$\frac{\mathrm{d}^3 k_{n-1}}{(2\pi)^3 2E_{n-1}} \frac{\mathrm{d}^3 k_n}{(2\pi)^3 2E_n} (2\pi)^4 \delta^{(4)}\left(Q^\mu - \sum k_i^\mu\right). \tag{6.17}$$

Once again we can write

$$d^3 k_{n-1} = 4\pi |\mathbf{k}_{n-1}|^2 d|k_{n-1}| dx_1^{n-1} dx_2^{n-1}. \tag{6.18}$$

Now we can integrate over $|\mathbf{k}_{n-1}|$ by writing

$$d|\mathbf{k}_{n-1}| \delta(Q_1^0 - m_1^Q) = \sum_{zeroes} \left(\frac{\partial m_1^Q}{\partial |\mathbf{k}_{n-1}|}\right)^{-1}. \tag{6.19}$$

Since this is the final iteration we note that $|\mathbf{k}_n| = |\mathbf{k}_{n-1}|$ and hence

$$E_{n-1}^2 = |\mathbf{k}_{n-1}|^2 + m_{n-1}^2 \quad \text{and} \quad E_n^2 = |\mathbf{k}_{n-1}|^2 + m_n^2. \tag{6.20}$$

Now since $m_1^Q = \sum_{j=1}^n$ only the two last terms of the sum depend on $|\mathbf{k}|_{n-1}$ so we have

$$\frac{\partial m_1^Q}{\partial |\mathbf{k}_{n-1}|} = \frac{\partial E_{n-1}}{\partial |\mathbf{k}_{n-1}|} + \frac{\partial E_n}{\partial |\mathbf{k}_{n-1}|} = |\mathbf{k}_1| \frac{E_n + E_{n+1}}{E_n E_{n-1}} = |\mathbf{k}_1| \frac{m_{n-1}^Q}{E_n E_{n-1}}. \tag{6.21}$$

This means we finally have

$$\frac{\mathrm{d}^3 k_{n-1}}{(2\pi)^3 2E_{n-1}} \frac{\mathrm{d}^3 k_n}{(2\pi)^3 2E_n} (2\pi)^4 \delta^{(4)}\left(Q^\mu - \sum k_i^\mu\right) = \frac{|k_{n-1}|}{4\pi m_{n-1}^Q} dx_1^{n-1} dx_2^{n-2}. \tag{6.22}$$

Thus, we were able to parametrize the original phase-space integral as the integral over $3n-4$ random numbers going from zero to one. All the conditions are met so that we can finally perform a Monte Carlo integration of phase space, which is what we will do in the next section.

6.2. Cross section for $q\overline{q} \to t\bar{t}$

In this section we will exemplify the procedure we just introduced for $q\overline{q} \to t\bar{t}$. Although this process only has two final state particles and therefore is simple enough to be handled analytically, we take this opportunity to test our Monte Carlo implementation by obtaining the analytical expression and comparing our numerical results to it. We will also compare them to the results coming out of Madgraph, which as we explained in chapter 4 is a Monte Carlo event generator one can use to obtain numerical values for the cross sections and decay widths of various processes. We start by computing the amplitude of the following diagram 30,

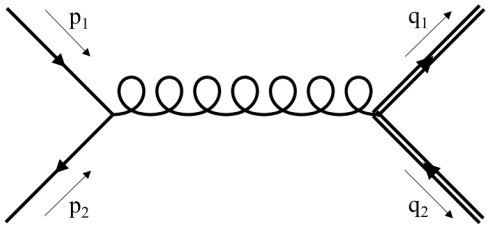

Figure 30: $q\overline{q} \to g \to t\bar{t}$

which is

$$\mathcal{M} = \frac{(-i)(ig_s)^2}{\hat{s}} \overline{u}(q_1)\gamma^\mu v(q_2)\overline{v}(p_2)\gamma_\mu u(p_1)[t_a]^{j_1,j_2}[t^a]^{i_1 i_2}, \tag{6.23}$$

where $\hat{s} = (p_1 + p_2)^2$ is equal to the center of mass energy squared. To compute the squared amplitude we start by writing the complex conjugate of (6.23) by noting identity

$$\left[\overline{u}^s(p1)\Gamma u^t(p2)\right]^* = \overline{u}^t(p2)\gamma_0\Gamma^\dagger\gamma^0 u^s(p1), \tag{6.24}$$

with Γ being a general Dirac structure. We also use the identities $\gamma_0\gamma^0 = 1$ and $(\gamma^\dagger)^\mu = \gamma_0\gamma^\mu\gamma^0$. This yields

$$\mathcal{M}^* = -i\frac{g_s^2}{\hat{s}} \overline{v}(q_2)\gamma^\mu u(q_1)\overline{u}(p_1)\gamma_\mu v(p_2)[t_a]^{j_2,j_1}[t^a]^{i_2 i_1}, \tag{6.25}$$

where we also used that the SU(3) generators t^a are anti-hermitian. We assume the incoming quarks are massless, while the top and anti-top have a mass m_t. Finally, to obtain the squared amplitude we use that the sum over particle and anti particle spinors is

$$\begin{aligned} \sum_{s=1}^{2} u^s(p)\overline{u}^s(p) &= \not{p} + m \\ \sum_{s=1}^{2} v^s(p)\overline{v}^s(p) &= \not{p} - m, \end{aligned} \tag{6.26}$$

so we obtain

$$\frac{1}{9\cdot 4}\sum_{spins,color}|\mathcal{M}|^2=\frac{g_s^2}{4\hat{s}^2}Tr\left[(\not{q}_2-m_t)\gamma^\mu(\not{q}_1+m_t)\gamma^\nu\right]Tr\left[\not{p}_2\gamma_\mu\not{p}_1\gamma_\nu\right]Tr[t_at_b]Tr[t^at^b], \quad (6.27)$$

where we sum over final states' spin and color and average over the initial states' spin and color. Using $Tr[t_at_b]=\frac{1}{2}\delta_{ab}$, we get $\frac{1}{9}Tr[t_at_b]Tr[t^at^b]=\frac{1}{9}\frac{\delta_{ab}\delta^{ab}}{4}=2/9$. We compute the traces in FORM to obtain

$$\frac{1}{9\cdot 4}\sum_{spins,color}|\mathcal{M}|^2=\frac{2}{9}\frac{g_s^4}{4}[16m_t^2\hat{s}+32(p_1\cdot q_1)(p_2\cdot q_2)+32(p_1\cdot q_2)(p_2\cdot q_1)]. \quad (6.28)$$

To obtain a more pragmatic formula we go to the rest frame and express the invariant products between momenta as a function of the angle relative to the center of mass and the energy of the incoming beams. Let us call E to the energy of the incoming quark, as well as of the incoming anti-quark, such that $\sqrt{\hat{s}}=2E\Rightarrow\hat{s}=4E^2$. We see that in the rest frame of the collision q_1 and q_2 must have opposite spatial momenta with the same norm $|\mathbf{q}|=\sqrt{E^2-m_t^2}$. This means that they also have the same energy, which must be E by energy conservation. Bearing in mind that $m_1=0, m_2=0$ this means $|\mathbf{p_1}|=E$ and $|\mathbf{p_2}|=E$. Finally we can write

$$\begin{aligned}p_1\cdot q_1&=E^2-|\mathbf{p}||\mathbf{q}|\cos\theta=E^2-E|\mathbf{q}|\cos\theta=p_2\cdot q_2\\ p_1\cdot q_2&=E^2+|\mathbf{p}||\mathbf{q}|\cos\theta=E^2+E|\mathbf{q}|\cos\theta=p_2\cdot q_1,\end{aligned} \quad (6.29)$$

with $\cos\theta$ defined in figure 31.

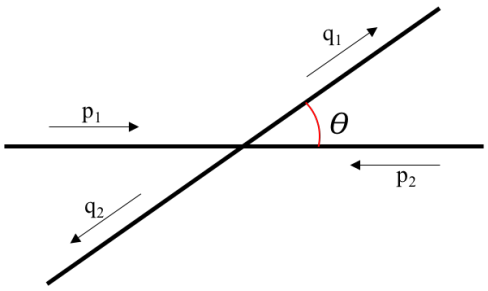

Figure 31: Angle θ is defined as the angle between incoming and outgoing particles' spatial momenta

We can now compute

$$(p_1\cdot q_1)(p_2\cdot q_2)+(p_1\cdot q_2)(p_2\cdot q_1)=2E^2\left[1+\left(1-\frac{m_t^2}{E^2}\right)\cos^2\theta\right]. \quad (6.30)$$

Making $E^2=\hat{s}/4$ we obtain

$$\frac{1}{9\cdot 4}\sum_{spins,color}|\mathcal{M}|^2=\frac{2}{9}g_s^4\left[\frac{4m_t^2}{\hat{s}}+1+\left(1-\frac{4m_t^2}{\hat{s}}\right)\cos^2\theta\right]. \quad (6.31)$$

Since it is now convenient for us to integrate over angles we use that $\frac{\mathrm{d}\sigma}{\mathrm{d}\Omega}$ for a collision with two

final state particles in the center of mass frame is

$$\left(\frac{\mathrm{d}\hat{\sigma}}{\mathrm{d}\Omega}\right)_{CM} = \frac{1}{64\pi^2\hat{s}}\frac{|\mathbf{q}|}{|\mathbf{p}|}\overline{\sum}|\mathcal{M}|^2\Theta\left(\hat{s}-m_3-m_4\right). \tag{6.32}$$

In our case we have

$$\frac{|\mathbf{q}|}{|\mathbf{p}|} = \frac{\sqrt{E^2-m_t^2}}{E} = \sqrt{1-\frac{4m_t^2}{\hat{s}}}, \tag{6.33}$$

so by writing $g_s^2 = 4\pi\alpha_s$ we obtain

$$\left(\frac{\mathrm{d}\hat{\sigma}}{\mathrm{d}\Omega}\right)_{CM} = \frac{2}{9}\frac{\alpha_s^2}{4}\sqrt{1-\frac{4m_t^2}{\hat{s}}}\left[\frac{4m_t^2}{\hat{s}}+1+\left(1-\frac{4m_t^2}{\hat{s}}\right)\cos^2\theta\right]. \tag{6.34}$$

To get the total cross section we integrate over $\mathrm{d}\phi\mathrm{d}(\cos\theta)$ to obtain

$$\begin{aligned}\hat{\sigma} =& \frac{2}{9}\frac{2\pi\alpha_s^2}{4\hat{s}}\sqrt{1-\frac{4m_t^2}{\hat{s}}}\int_{-1}^{1}\mathrm{d}(\cos\theta)\left[\frac{4m_t^2}{\hat{s}}+1+\left(1-\frac{4m_t^2}{\hat{s}}\right)\cos^2\theta\right] \\ =& \frac{2}{9}\frac{\alpha_s^2\pi}{\hat{s}}\sqrt{1-\frac{4m_t^2}{\hat{s}}}\left[\frac{4m_t^2}{\hat{s}}+1+\frac{1}{3}\left(1-\frac{4m_t^2}{\hat{s}}\right)\right].\end{aligned} \tag{6.35}$$

We have just obtained the analytical result for the cross section $\sigma(q\overline{q}\to g\to t\bar{t})$ at leading order. We can perform a check on this expression by taking the high-energy (or massless particles) limit $m_t/\hat{s}\to 0$ and see that we obtain

$$\hat{\sigma} = \frac{2}{9}\alpha_s\cdot\frac{4\pi}{3\hat{s}}, \tag{6.36}$$

which if we drop the color factor $2/9$ and make $\alpha_s\to\alpha_e$ is the famous expression for the $e^+e^-\to\gamma\to\mu^-\mu^+$. This serves as a good indicator that our expression is indeed correct.

	σ(pb)		
$\sqrt{\hat{s}}$(TeV)	MC program	Madgraph	Analytical
0.5	18.063 ± 0.002	18.06 ± 0.05	18.063
1	5.018 ± 0.001	5.010 ± 0.008	5.019
5	$(2.020\pm0.001)\times10^{-1}$	$(2.016\pm0.002)\times10^{-1}$	2.018×10^{-1}
10	$(5.046\pm0.001)\times10^{-2}$	$(5.052\pm0.008)\times10^{-2}$	5.047×10^{-2}
13	$(2.986\pm0.001)\times10^{-2}$	$(2.986\pm0.005)\times10^{-2}$	2.986×10^{-2}
14	$(2.575\pm0.005)\times10^{-2}$	$(2.574\pm0.004)\times10^{-2}$	2.575×10^{-2}

Table 3: Values of the $q\overline{q}\to t\bar{t}$ cross section for our MC program, Madgraph and the analytical result

In table 3 we can compare both our results and Madgraph's to the analytical result and see that indeed MC integration provides a very good estimate for the value of the cross-section. We used $N = 1\times10^6$ events in our program, and set $\alpha_s = 0.118$ and $m_t = 172$ GeV in all three computations.

6.3. Higgs production associated with top quark pair

In the previous section we applied Monte Carlo integration to a simple case and compared it both with the analytical result and with Madgraph. Since there were only two final state particles performing Lorentz boosts turned out not to be necessary, since both q_1 and q_2 are automatically generated in the COM frame.

We would now like to apply MC integration to a more involved amplitude, one that we would not be able to obtain solely through analytical methods. The process we will focus on in this section will be one of the main Higgs production channels at hadron colliders we mentioned in chapter 5, namely Higgs production associated with top quark pair. Since we are smashing protons the incoming particles can be either quarks or gluons so we have to differentiate between $q\bar{q} \to t\bar{t}H$ and $gg \to t\bar{t}H$. Here we will only compute the cross-section $\sigma(q\bar{q} \to t\bar{t}H)$, and have relegated the calculation of the $gg \to t\bar{t}H$ amplitude and its square to appendix B.

$q\bar{q} \to t\bar{t}H$ Amplitude

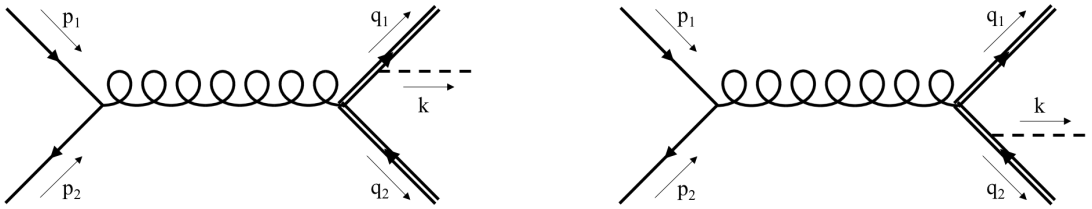

(a) $\mathcal{M}_1$ **(b)** $\mathcal{M}_2$

Figure 32: Diagrams contributing to $q\bar{q} \to t\bar{t}H$

The diagrams contributing to this amplitude can be seen in figure 32 and their respective expressions are

$$\begin{aligned}\mathcal{M}_1 =& ig_s^2 \frac{y_t}{\sqrt{2}} D_t^{-1}(q_1+k) D_g^{-1}(p_1+p_2)\overline{u}(q_1)[(\not{q}_1+\not{k})+m_t]\gamma^\alpha v(q_2)\ \overline{v}(p_2)\gamma_\alpha u(p_1)\ [t^a]^{i_1,i_2}[t_a]^{j_2 j_1} \\ \mathcal{M}_2 =& ig_s^2 \frac{y_t}{\sqrt{2}} D_t^{-1}(q_2+k) D_g^{-1}(p_1+p_2)\overline{u}(q_1)\gamma^\alpha[-(\not{q}_2+\not{k})+m_t]v(q_2)\ \overline{v}(p_2)\gamma_\alpha u(p_1)\ [t^a]^{i_1,i_2}[t_a]^{j_2 j_1}.\end{aligned} \tag{6.37}$$

Our goal is to obtain the cross section $\sigma(q\bar{q} \to t\bar{t}H)$, so we need to compute $|\mathcal{M}_1+\mathcal{M}_2|^2 = |\mathcal{M}_1|^2 + |\mathcal{M}_2|^2 + 2Re(\mathcal{M}_1^*\mathcal{M}_2)$. Again we start by writing the complex conjugates of (6.37) by using the identity

$$\left[\overline{u}^s(p1)\Gamma u^t(p2)\right]^* = \overline{u}^t(p2)\gamma_0\Gamma^\dagger\gamma^0 u^s(p1), \tag{6.38}$$

as well as $\gamma_0\gamma^0 = 1$ and $(\gamma^\dagger)^\mu = \gamma_0\gamma^\mu\gamma^0$. This yields

$$\begin{aligned}\mathcal{M}_1^* =& -ig_s^2\frac{y_t}{\sqrt{2}}D_t^{-1}(q_1+k)D_g^{-1}(p_1+p_2)\overline{v}(q_2)\gamma_\mu[\not{q}_1+\not{k}+m_t]u(q_1)\overline{u}(p_1)\gamma^\mu v(p2)\ [t^a]^{i_2,i_1}[t_a]^{j_1,j_2}\\ \mathcal{M}_2^* =& -ig_s^2\frac{y_t}{\sqrt{2}}D_t^{-1}(q_2+k)D_g^{-1}(p_1+p_2)\overline{v}(q_2)\gamma_\mu[\not{q}_1+\not{k}+m_t]u(q_1)\overline{u}(p_1)\gamma^\mu v(p2)\ [t^a]^{i_2,i_1}[t_a]^{j_1,j_2},\end{aligned} \tag{6.39}$$

where we also used that the SU(3) generators t^a are anti-hermitian. Finally to obtain the squared amplitude we again use the sum over particle and anti particle spinors given by (6.26). We get

$$\begin{aligned}|\mathcal{M}_1|^2 =& 2\left(g_s^2\frac{y_t}{\sqrt{2}}\right)^2 D_t^{-2}(q_1+k)D_g^{-2}(p_1+p_2)Tr\left[(\not{q}_2-m_t)\gamma_\mu[\not{q}_1+\not{k}+m_t](\not{q}_1+m_t)\right.\\ &\left.[(\not{q}_1+\not{k})+m_t]\gamma_\alpha\right]Tr\left[\not{p}_1\gamma^\mu\not{p}_2\gamma^\alpha\right]\end{aligned}$$

$$\begin{aligned}|\mathcal{M}_2|^2 =& 2\left(g_s^2\frac{y_t}{\sqrt{2}}\right)^2 D_t^{-2}(q_2+k)D_g^{-2}(p_1+p_2)Tr\left[(\not{q}_2-m_t)[-(\not{q}_2+\not{k})+m_t]\gamma_m u(\not{q}_1+m_t)\gamma_\alpha\right.\\ &\left.[-(\not{q}_2+\not{k})+m_t]\right]Tr\left[\not{p}_1\gamma^\alpha\not{p}_2\gamma^\mu\right]\end{aligned}$$

$$\begin{aligned}Re(\mathcal{M}_1^*\mathcal{M}_2) =& 2\left(g_s^2\frac{y_t}{\sqrt{2}}\right)^2 D_t^{-1}(q_2+k)D_t^{-1}(q_1+k)D_g^{-2}(p_1+p_2)Tr\left[(\not{q}_2-m_t)\gamma_\mu[\not{q}_1+\not{k}+m_t]\right.\\ &\left.(\not{q}_1+m_t)\gamma_\alpha[-(\not{q}_2+\not{k})+m_t]\right]Tr\left[\not{p}_1\gamma^\alpha\not{p}_2\gamma^\mu\right],\end{aligned} \tag{6.40}$$

where we used that $Tr[t_a t^b]Tr[t^a t_b] = \frac{1}{4}\delta_a^a = 2$. We delegate the computation of the traces to FORM and as such we have found the square of the amplitude $|\mathcal{M}|^2$. Now we are in the condition of building a MC program and comparing to Madgraph. The results can be found in table 4 table, where we can see there is a very good agreement between both. Our full MC code that provided these results can be found in appendix C.2 .

	$\hat{\sigma}$(pb)	
$\sqrt{\hat{s}}$(TeV)	MC program	Madgraph
0.5	$(9.70 \pm 0.001) \times 10^{-3}$	$(9.69 \pm 0.004) \times 10^{-3}$
1	$(6.38 \pm 0.001) \times 10^{-2}$	$(6.36 \pm 0.001) \times 10^{-2}$
5	$(4.42 \pm 0.003) \times 10^{-3}$	$(4.42 \pm 0.001) \times 10^{-3}$
10	$(1.29 \pm 0.001) \times 10^{-3}$	$(1.31 \pm 0.003) \times 10^{-3}$
13	$(8.21 \pm 0.001) \times 10^{-4}$	$(8.19 \pm 0.001) \times 10^{-4}$
14	$(7.16 \pm 0.001) \times 10^{-4}$	$(7.18 \pm 0.002) \times 10^{-4}$

Table 4: Values of the $q\overline{q} \to t\bar{t}H$ partonic cross section for our MC program and Madgraph

We can also adapt this code to produce histograms of the transverse momentum $p_T = \sqrt{p_x^2 + p_y^2}$ for any of the particles involved. In figure 33 we plot $\frac{\mathrm{d}\sigma}{\mathrm{d}p_T}$ as a function of p_T for the top, the anti-top, the Higgs, and lastly for the $t\bar{t}$ pair at $\sqrt{\hat{s}} = 13$ TeV.

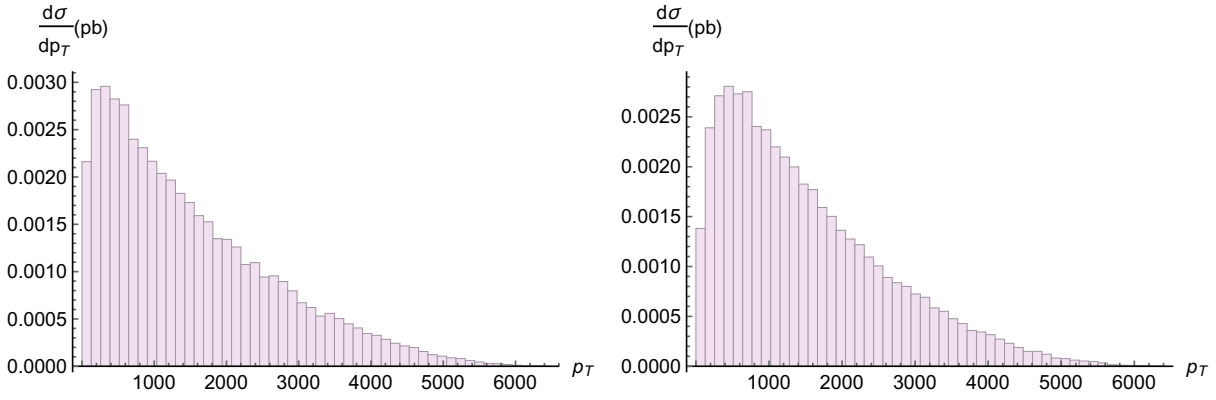

(a) Top quark

(b) Anti-top quark

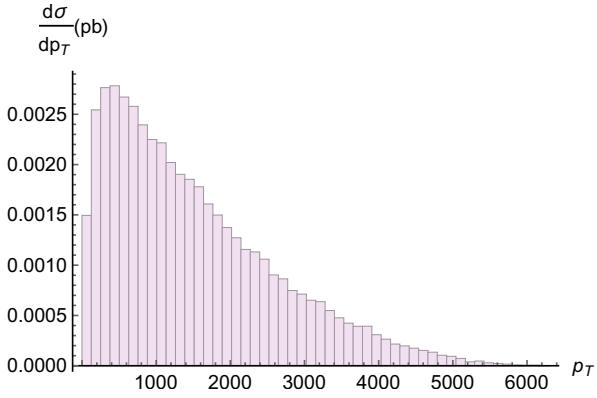

(c) Higgs

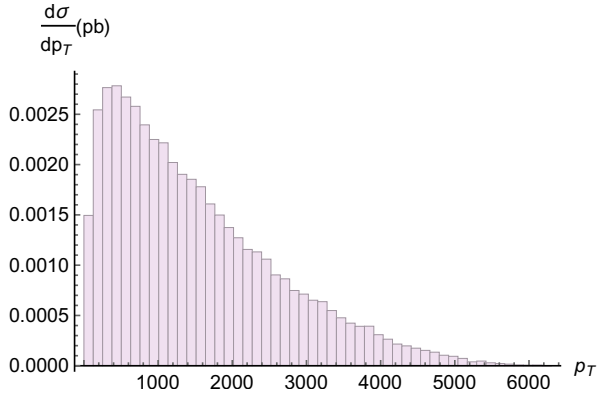

(d) $t\bar{t}$

Figure 33: $\frac{\mathrm{d}\sigma}{dp_T}$ after integrating over PDFs at $\sqrt{s} = 13$ TeV

By analyzing figure 33, we immediately notice that the differential cross section decreases as the transverse momentum increases. This is due to the fact that for large values of p_T the top propagator becomes increasingly off-shell, which decreases the value of the differential cross section. One may also notice that the plots for the Higgs and the $t\bar{t}$ appear to be exactly the same. This is indeed the case, since the sum of the p_T of the top and anti-top must be equal in magnitude but with opposite direction to the p_T of the Higgs, in order to satisfy momentum conservation.

We should note that to generate the plots in figure 33 we had to integrate over the parton distribution functions (PDFs) of the incoming quarks. This is a concept we introduce and briefly discuss in appendix B, but ultimately lies outside the scope of this thesis.

The code can also be adapted to provide any of the plots that are commonly used when analyzing scattering processes. A very useful quantity in hadron collider physics is the *rapidity*, which is commonly used for describing the angle between an outgoing particle and the beam axis. It is defined as

$$y \equiv \frac{1}{2} \ln \left(\frac{E + p_L}{E - p_L} \right). \tag{6.41}$$

This quantity is usually preferred over the polar angle θ since it is better behaved under Lorentz boosts. In fact, the difference of two rapidities is Lorentz invariant. This is easily seen

by noting that under a boost the energy and longitudinal momentum transform as

$$\begin{aligned} E' =& E\cosh\gamma - p_z \sinh\gamma \\ p'_L =& p_L \cosh\gamma - E\sinh\gamma, \end{aligned} \tag{6.42}$$

such that the rapidity transforms as

$$\begin{aligned} y \to y' =& \frac{1}{2}\ln\left(\frac{E'+p'_L}{E'-p'_L}\right) \\ =& \frac{1}{2}\ln\left(\frac{E\cosh\gamma - p_L\sinh\gamma + p_L\cosh\gamma - E\sinh\gamma}{E\cosh\gamma - p_L\sinh\gamma - p_L\cosh\gamma + E\sinh\gamma}\right) \\ =& \frac{1}{2}\ln\left(\frac{(E+p_L)(\cosh\gamma - \sinh\gamma)}{(E-p_L)(\cosh\gamma+\sinh\gamma)}\right) \\ =& y + \frac{1}{2}\ln\left(\frac{e^{-\gamma}}{e^{\gamma}}\right) \\ =& y - \gamma. \end{aligned} \tag{6.43}$$

Thus $\Delta y \equiv y_1 - y_2 \to \Delta y' = y'_1 - y'_2 = y_1 - y_2$ remains invariant under a Lorentz boost along the beam axis. The rapidity turns out not to be a very intuitive quantity however, so more commonly the *pseudorapidity* is used instead. This quantity is defined as

$$\eta \equiv \frac{1}{2}\ln\left(\frac{|\mathbf{p}|+p_L}{|\mathbf{p}|-p_L}\right). \tag{6.44}$$

We can manipulate this expression to make the relation with angle θ more apparent

$$\begin{aligned} \eta =& \frac{1}{2}\ln\left(\frac{1+\frac{p_L}{|\mathbf{p}|}}{1-\frac{p_L}{|\mathbf{p}|}}\right) = \frac{1}{2}\ln\left(\frac{1+\cos\theta}{1-\cos\theta}\right) \\ =& \frac{1}{2}\ln\left(\frac{(1+\cos\theta)^2}{\sin^2\theta}\right)^{\frac{1}{2}} = \ln\left(\frac{1+\cos\theta}{\sin\theta}\right) \\ =& -\ln\left(\tan\frac{\theta}{2}\right), \end{aligned} \tag{6.45}$$

where in the last step we used the trigonometric identity $\frac{\sin\theta}{1+\cos\theta} = \tan\frac{\theta}{2}$.

In figure 34 we plot $\frac{\mathrm{d}\sigma}{\mathrm{d}y}$ and $\frac{\mathrm{d}\sigma}{\mathrm{d}\eta}$, both for the Higgs and the top quark. We see that the differential cross section decreases as the direction of the outgoing particle becomes less collinear with the direction of the beam.

Finally, one would be remiss not to mention that all of these plots agree with the ones obtained through MadAnalysis (the plotting framework for MadGraph). The MC program we developed therefore appears to be perfectly adequate to perform a complete analysis of the scattering process.

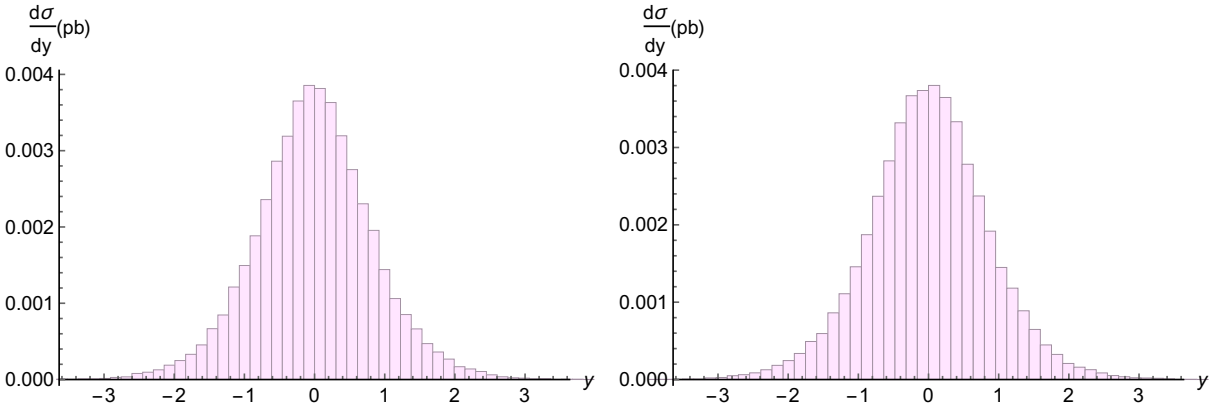

(a) Top quark rapidity

(b) Higgs rapidity

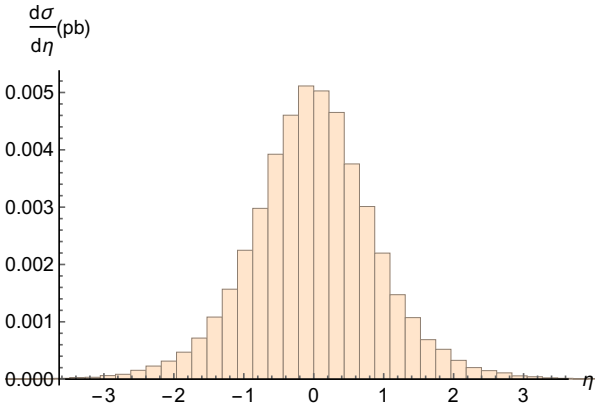

(c) Top quark pseudorapidity

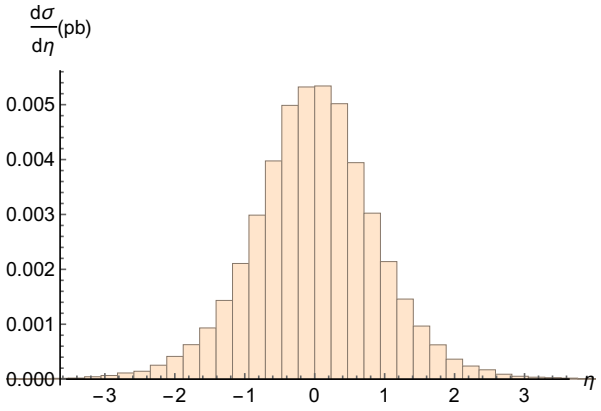

(d) Higgs pseudorapidity

Figure 34: Rapidity and pseudorapidity after integrating over PDFs at $\sqrt{s} = 13$ TeV

7 Conclusion

In this thesis we addressed some of the modern techniques used in the treatment of unstable particles. We motivated and introduced the Complex Mass Scheme and illustrated how it was able to produce gauge invariant results, thereby being a very useful approach when dealing with resonances of unstable particles while still being valid throughout phase-space. In section 4.5 we also described how the application of the CMS affected the cross section for one of the main Higgs production processes, namely Higgs production associated with a top quark pair, which became apparent when we set the width of the top quark to large, unphysical values. The CMS has been shown to maintain gauge invariance and unitarity at least to NLO, making it our go-to tool to include the finite width effects of unstable particles in our calculations.

We then presented the full calculation of Higgs production cross section as well as the decay width used at hadron colliders, namely $\sigma(gg \to H)$ through top quark-loop and $\Gamma(H \to \gamma\gamma)$, which includes the top-quark and W-boson loop. Our computation for the W-boson loop was done in a way that did not require Passarino-Veltmann reduction and is simpler than what is currently found in the literature. We again used Higgs associated production with a top quark pair, this time to implement our Monte Carlo event generator, whose result for the cross-section agreed with *Madgraph*'s to excellent precision.

A Feynman Rules

Unless explicitely stated otherwise, throughout this thesis we use the Feynman rules presented below.

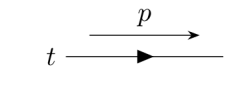

$$= i\frac{\not{p} + m}{p^2 - m^2}$$

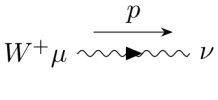

$$= \frac{-i}{p^2 - m_W^2}\left(\eta_{\mu\nu} - \frac{p_\mu p_\nu}{m_W^2}\right)$$

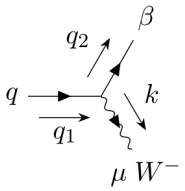

$$= i\frac{g}{\sqrt{2}}\gamma_\mu\frac{1 - \gamma_5}{2}$$

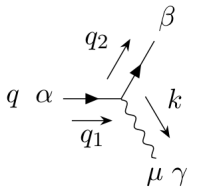

$$= -ieQ_{EM}\gamma^\mu$$

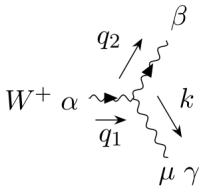

$$= +ie[(q_1 + q_2)_\mu\eta_{\alpha\beta} - (k + q_1)_\beta\eta_{\mu\alpha} + (k - q_2)_\alpha\eta_{\mu\beta}]$$

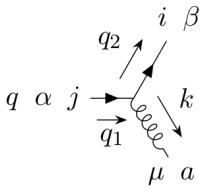

$$= -ig_s[\gamma^\mu]_{\beta\alpha}[t^a]_{ji}$$

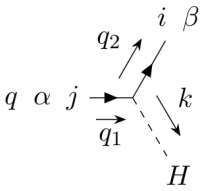

$$= -i\frac{y_q}{\sqrt{2}}\delta_{\beta\alpha}\delta_{ji}$$

B Higgs production associated with top quark pair

In chapter 6 we computed the cross section for $q\bar{q} \to t\bar{t}H$. However this is only one of the two processes that constitute $pp \to t\bar{t}H$, the other one being of course $gg \to t\bar{t}H$. Since the computation of the cross section of the latter is much more involved than the one for the incoming quark pair we refrained from doing it in the main text. However in this appendix we show how one would have to proceed to obtain the full cross section $\sigma(pp \to t\bar{t}H)$.

The hadronic cross section for $\sigma(pp \to t\bar{t}H)$ where the two incoming protons have momenta P is given by

$$\begin{aligned}\sigma\left((p(P)p(P) \to t\bar{t}H\right) = &\int_0^1 \mathrm{d}x_2\mathrm{d}x_1 f_g(x_1) f_g(x_2)\ \hat{\sigma}\left(g(x_1P)g(x_2P) \to t\bar{t}H\right) + \\ &+ \int_0^1 \mathrm{d}x_2\mathrm{d}x_1 \sum_f f_f(x_1) f_{\bar{f}}(x_2)\ \hat{\sigma}\left(q_f(x_1P)\bar{q}_f(x_2P) \to t\bar{t}H\right)\end{aligned} \tag{B.1}$$

In this formula x_1 and x_2 represent the momentum fractions the partons, i.e. the momentum of the incoming particles 1 and 2, be it quarks or gluons, is related to the momentum of the proton P by $p_1 = x_1P$ and $p_2 = x_2P$. Also, f_f and f_g designate the so called parton distribution functions for the quarks and gluons respectively. More precisely, a parton distribution function $f_g(x_1, \mu^2)$ is the probability density for finding a gluon with longitudinal momentum fraction x_1 at the factorization scale μ^2. In this example we have set $\mu^2 = M_Z^2$ and dropped the argument. The same definition goes for the parton distribution functions of quarks. Lastly, $\hat{\sigma}$ denotes the partonic cross section, in other words, the cross section computed by the usual formula (6.1) when the incoming particles are partons - the collective name for quarks and gluons.

To obtain this cross section we then have to compute $\hat{\sigma}\left(gg \to t\bar{t}H\right)$. This requires the calculation of $|\mathcal{M}(gg \to t\bar{t}H)|^2$ which is what we are going to do in the next section. Everything else, including the integration over PDF's, is just a straightforward generalization of the MC method we presented in chapter 6 and should be relatively easy to implement.

$gg \to t\bar{t}H$ Amplitude

The diagrams contributing to this amplitude can be seen in figure 36, with their corresponding expressions presented in equation (B.2). Once again we have used the Feynman rules in appendix A.

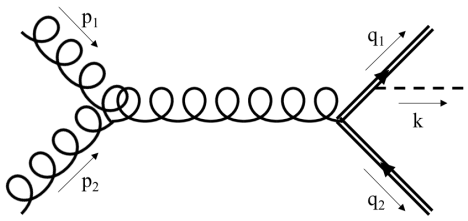

(a) $\mathcal{M}_3$

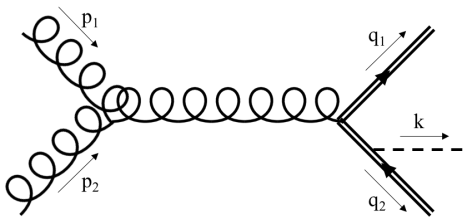

(b) $\mathcal{M}_4$

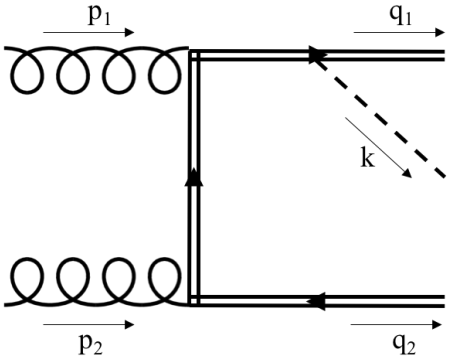

(c) $\mathcal{M}_5$

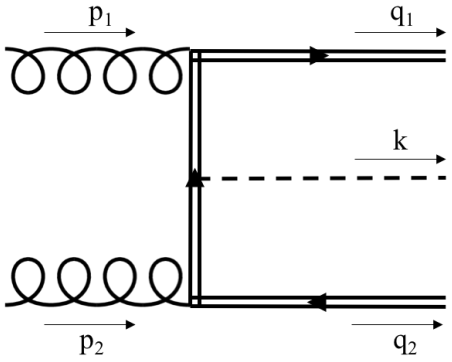

(d) $\mathcal{M}_6$

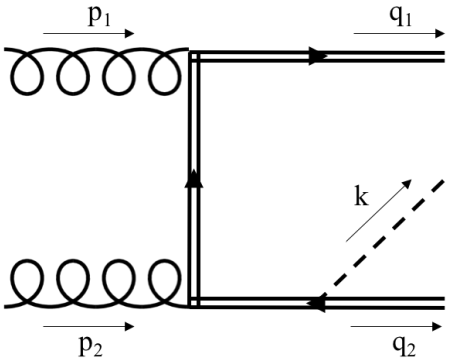

(e) $\mathcal{M}_7$

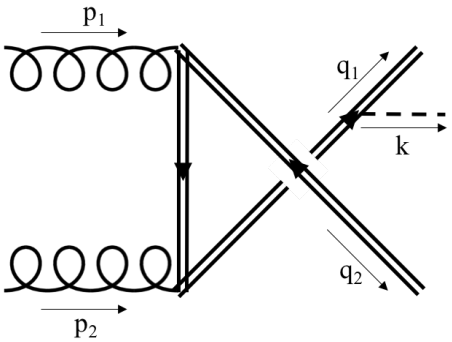

(f) $\mathcal{M}_8$

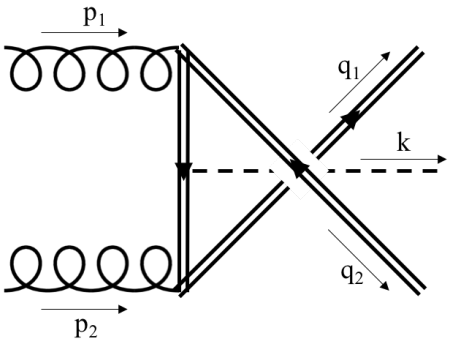

(g) $\mathcal{M}_9$

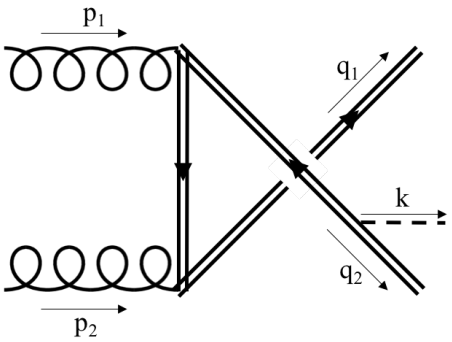

(h) $\mathcal{M}_10$

Figure 36: Amplitudes contributing to $gg \to t\bar{t}H$

$$
\begin{aligned}
\mathcal{M}_3^{\mu\nu} =& g_s^2 \frac{y_t}{\sqrt{2}} D_t^{-1}(q_1+k) D_g^{-1}(p_1+p_2)\overline{u}(q_1)[(\not{q}_1+\not{k})+m_t]\gamma_\alpha v(q_2)[t_c]^{i_1 i_2}\cdot \\
& f^{abc}[\eta^{\mu\nu}(p_1-p_2)^\alpha + \eta^{\nu\alpha}(2p_2+p_1)^\mu - \eta^{\alpha\mu}(2p_1+p_2)^\nu] \\
\mathcal{M}_4^{\mu\nu} =& g_s^2 \frac{y_t}{\sqrt{2}} D_t^{-1}(q_2+k) D_g^{-1}(p_1+p_2)\overline{u}(q_1)\gamma_\alpha[-(\not{q}_2+\not{k})+m_t]v(q_2)[t_c]^{i_1 i_2}\cdot \\
& f^{abc}[\eta^{\mu\nu}(p_1-p_2)^\alpha + \eta^{\nu\alpha}(2p_2+p_1)^\mu - \eta^{\alpha\mu}(2p_1+p_2)^\nu] \\
\mathcal{M}_5^{\mu\nu} =& -ig_s^2 \frac{y_t}{\sqrt{2}} D_t^{-1}(p_2-q_2) D_t^{-1}(q_1+k)\overline{u}(q_2)[\not{q}_1+\not{k}+m_t]\gamma^\mu[(\not{p}_2-\not{q}_2)+m_t]\gamma^\nu v(q_2)\cdot \\
& [t^a t^b]^{i_1 i_2} \\
\mathcal{M}_6^{\mu\nu} =& -ig_s^2 \frac{y_t}{\sqrt{2}} D_t^{-1}(q_1-p_1) D_t^{-1}(p_2-q_2)\overline{u}(q_1)\gamma^\mu[\not{q}_1-\not{p}_1+m_t][(\not{p}_2-\not{q}_2)+m_t]\gamma^\nu v(q_2)\cdot \\
& [t^a t^b]^{i_1 i_2} \\
\mathcal{M}_7^{\mu\nu} =& -ig_s^2 \frac{y_t}{\sqrt{2}} D_t^{-1}(p_1-q_1) D_t^{-1}(q_2+k)\overline{u}(q_1)\gamma^\mu[\not{q}_1-\not{p}_1+m_t]\gamma^\nu[-(\not{q}_2+\not{k})+m_t]v(q_2)\cdot \\
& [t^a t^b]^{i_1 i_2} \\
\mathcal{M}_8^{\mu\nu} =& -ig_s^2 \frac{y_t}{\sqrt{2}} D_t^{-1}(q_1+k) D_t^{-1}(p_1-q_2)\overline{u}(q_1)[\not{q}_1+\not{k}+m_t]\gamma^\nu[(\not{p}_1-\not{q}_2)+m_t]\gamma^\mu v(q_2)\cdot \\
& [t^a t^b]^{i_1 i_2} \\
\mathcal{M}_9^{\mu\nu} =& -ig_s^2 \frac{y_t}{\sqrt{2}} D_t^{-1}(p_2-q_1) D_t^{-1}(p_1-q_2)\overline{u}(q_1)\gamma^\nu[\not{q}_1-\not{p}_2+m_t][(\not{p}_1-\not{q}_2)+m_t]\gamma^\mu v(q_2)\cdot \\
& [t^a t^b]^{i_1 i_2} \\
\mathcal{M}_{10}^{\mu\nu} =& -ig_s^2 \frac{y_t}{\sqrt{2}} D_t^{-1}(q_2+k) D_t^{-1}(p_2+q_1)\overline{u}(q_1)\gamma^\nu[(\not{p}_2+\not{q}_1+m_t]\gamma^\mu[-(\not{q}_2+\not{k})+m_t]v(q_2)\cdot \\
& [t^a t^b]^{i_1 i_2}
\end{aligned}
\tag{B.2}
$$

Now as we said we are interested in is the cross section $\sigma(gg \to t\bar{t}H)$ so we need $|\sum_i \mathcal{M}_i|^2 = \sum_i |\mathcal{M}_i|^2 + 2\sum_{i,j>i} Re(\mathcal{M}_i^* \mathcal{M}_j)$, for i starting at 3. We start by writing the complex conjugates of the amplitudes (B.2) by making use of the same identities we used before. This gives

$$
\begin{aligned}
\mathcal{M}_3^{*\mu\nu} =& g_s^2 \frac{y_t}{\sqrt{2}} D_t^{-1}(q_1+k) D_g^{-1}(p_1+p_2)\overline{v}(q2)\gamma_\beta[\not{q}_1+\not{k}+m_t]u(q1)[t_c]^{i_1 i_2}\cdot \\
& f^{abc}[\eta^{\rho\sigma}(p_1-p_2)^\beta + \eta^{\sigma\beta}(2p_2+p_1)^\rho - \eta^{\beta\rho}(2p_1+p_2)^\sigma] \\
\mathcal{M}_4^{*\mu\nu} =& g_s^2 \frac{y_t}{\sqrt{2}} D_t^{-1}(q_2+k) D_g^{-1}(p_1+p_2)\overline{v}(q2)[-(\not{q}_2+\not{k})+m_t]\gamma_\beta u(q1)[t_c]^{i_1 i_2}\cdot \\
& f^{abc}[\eta^{\rho\sigma}(p_1-p_2)^\beta + \eta^{\sigma\beta}(2p_2+p_1)^\rho - \eta^{\beta\rho}(2p_1+p_2)^\sigma] \\
\mathcal{M}_5^{*\mu\nu} =& -ig_s^2 \frac{y_t}{\sqrt{2}} D_t^{-1}(p_2-q_2) D_t^{-1}(q_1+k)\overline{v}(q2)\gamma^\sigma[\not{p}_2-\not{q}_2+m_t]\gamma^\rho[\not{q}_1+\not{k}+m_t]u(q1)\cdot \\
& [t^a t^b]^{i_1 i_2} \\
\mathcal{M}_6^{*\mu\nu} =& -ig_s^2 \frac{y_t}{\sqrt{2}} D_t^{-1}(q_1-p_1) D_t^{-1}(p_2-q_2)\overline{v}(q2)\gamma^\sigma[\not{p}_2-\not{q}_2+m_t][\not{q}_1-\not{p}_1+m_t]\gamma^\rho u(q1)\cdot \\
& [t^a t^b]^{i_1 i_2}
\end{aligned}
$$

$$\mathcal{M}_7^{*\mu\nu} = -ig_s^2\frac{y_t}{\sqrt{2}}D_t^{-1}(p_1-q_1)D_t^{-1}(q_2+k)\overline{v}(q2)[-(\not{q}_2+\not{k})+m_t]\gamma^\sigma[\not{q}_1-\not{p}_1+m_t]\gamma^\rho u(q1)\cdot$$
$$[t^a t^b]^{i_1 i_2}$$
$$\mathcal{M}_8^{*\mu\nu} = -ig_s^2\frac{y_t}{\sqrt{2}}D_t^{-1}(q_1+k)D_t^{-1}(p_1-q_2)\overline{v}(q2)\gamma^\rho[(\not{p}1-\not{q}_2+m_t)]\gamma^\sigma[(\not{q}_1+\not{k})+m_t]u(q1)\cdot$$
$$[t^a t^b]^{i_1 i_2}$$
$$\mathcal{M}_9^{*\mu\nu} = -ig_s^2\frac{y_t}{\sqrt{2}}D_t^{-1}(p_2-q_1)D_t^{-1}(p_1-q_2)\overline{v}(q2)\gamma^\rho[(\not{p}1-\not{q}_2+m_t)][\not{q}_1-\not{p}_2+m_t]\gamma^\sigma u(q1)\cdot$$
$$[t^a t^b]^{i_1 i_2}$$
$$\mathcal{M}_{10}^{*\mu\nu} = -ig_s^2\frac{y_t}{\sqrt{2}}D_t^{-1}(q_2+k)D_t^{-1}(p_2+q_1)\overline{v}(q2)[-(\not{q}_2+\not{k})+m_t)]\gamma^\rho[\not{p}_2+\not{q}_1+m_t]\gamma^\sigma u(q1)\cdot$$
$$[t^a t^b]^{i_1 i_2} \tag{B.3}$$

So now we are able to obtain $|\sum_i \mathcal{M}_i|^2$

$$|\mathcal{M}_3|^2 = \left(-\frac{1}{2}\right) f^{abc}f_{abc}\left(g_s^2\frac{y_t}{\sqrt{2}}\right) D_t^{-2}(q_1+k)D_g^{-2}(p_1+p_2)Tr\left[(\not{q}_2-mt)\gamma_\beta\right.$$
$$\left.[\not{q}_1+\not{k}+m_t](\not{q}_1+m_t)[(\not{q}_1+\not{k})+m_t]\gamma_\alpha\right][\eta^{\rho\sigma}(p_1-p_2)^\beta+\eta^{\sigma\beta}(2p_2+p_1)^\rho-\eta^{\beta\rho}(2p_1+p_2)^\sigma]$$
$$[\eta^{\mu\nu}(p_1-p_2)^\alpha+\eta^{\nu\alpha}(2p_2+p_1)^\mu-\eta^{\alpha\mu}(2p_1+p_2)^\nu]$$

$$|\mathcal{M}_4|^2 = \left(-\frac{1}{2}\right) f^{abc}f_{abc}\left(g_s^2\frac{y_t}{\sqrt{2}}\right) D_t^{-2}(q_2+k)D_g^{-2}(p_1+p_2)Tr\left[(\not{q}_2-m_t)[-(\not{q}_2+\not{k})+m_t]\gamma_\beta(\not{q}_1+m_t)\right.$$
$$\left.\gamma_\alpha[-(\not{q}_2+\not{k})+m_t]\right][\eta^{\rho\sigma}(p_1-p_2)^\beta+\eta^{\sigma\beta}(2p_2+p_1)^\rho-\eta^{\beta\rho}(2p_1+p_2)^\sigma]$$
$$[\eta^{\mu\nu}(p_1-p_2)^\alpha+\eta^{\nu\alpha}(2p_2+p_1)^\mu-\eta^{\alpha\mu}(2p_1+p_2)^\nu]$$

$$|\mathcal{M}_5|^2 = \left(-\frac{2}{3}g_s^2\frac{y_t}{\sqrt{2}}\right) D_t^{-2}(p_2-q_2)D_t^{-2}(q_1+k)Tr\left[(\not{q}_2-m_t)\gamma^\sigma[\not{p}_2-\not{q}_2+m_t]\gamma^\rho[\not{q}_1+\not{k}+m_t]\right.$$
$$\left.(\not{q}_1+m_t)[\not{q}_1+\not{k}+m_t]\gamma^\mu[(\not{p}_2-\not{q}_2)+m_t]\gamma^\nu\right]P_{\mu\nu\rho\sigma}$$

$$|\mathcal{M}_6|^2 = \left(-\frac{2}{3}g_s^2\frac{y_t}{\sqrt{2}}\right) D_t^{-2}(q_1-p_1)D_t^{-2}(p_2-q_2)Tr\left[(\not{q}_2-mt)\gamma^\sigma[\not{q}_1-\not{p}_1+m_t][(\not{p}_2-\not{q}_2)+m_t]\gamma^\rho\right.$$
$$\left.(\not{q}_1+m_t)\gamma^\mu[\not{q}_1-\not{p}_1+m_t][(\not{p}_2-\not{q}_2)+m_t]\gamma^\nu\right]P_{\mu\nu\rho\sigma}$$

$$|\mathcal{M}_7|^2 = \left(-\frac{2}{3}g_s^2\frac{y_t}{\sqrt{2}}\right) D_t^{-2}(q_2+k)D_t^{-2}(q_1-p_1)Tr\left[(\not{q}_2-mt)[-(\not{q}_2+\not{k})+m_t]\gamma^\sigma[\not{q}_1-\not{p}_1+m_t]\gamma^\rho\right.$$
$$\left.(\not{q}_1+m_t)\gamma^\mu[\not{q}_1-\not{p}_1+m_t]\gamma^\nu[-(\not{q}_2+\not{k})+m_t]\right]P_{\mu\nu\rho\sigma}$$

$$|\mathcal{M}_8|^2 = \left(-\frac{2}{3}g_s^2\frac{y_t}{\sqrt{2}}\right) D_t^{-2}(p_1-q_2)D_t^{-2}(q_1+k)Tr\left[(\not{q}_2-mt)\gamma^\rho[(\not{p}_1-\not{q}_2+m_t)]\gamma^\sigma[(\not{q}_1+\not{k})+m_t]\right.$$
$$\left.(\not{q}_1+m_t)]\right] P_{\mu\nu\rho\sigma}$$

$$|\mathcal{M}_9|^2 = \left(-\frac{2}{3}g_s^2\frac{y_t}{\sqrt{2}}\right) D_t^{-2}(p_1-q_2)D_t^{-2}(q_1-p_2)Tr\left[(\not{q}_2-mt)\gamma^\rho[(\not{p}_1-\not{q}_2+m_t)][\not{q}_1-\not{p}_2+m_t]\gamma^\sigma\right.$$
$$\left.(\not{q}_1+m_t)\gamma^\nu[\not{q}_1-\not{p}_2+m_t][(\not{p}_1-\not{q}_2)+m_t]\gamma^\mu\right] P_{\mu\nu\rho\sigma}$$

$$|\mathcal{M}_{10}|^2 = \left(-\frac{2}{3}g_s^2\frac{y_t}{\sqrt{2}}\right) D_t^{-2}(p_2+q_1)D_t^{-2}(q_2+k)Tr\left[(\not{q}_2-mt)[-(\not{q}_2+\not{k})+m_t)]\gamma^\rho[\not{p}_2+\not{q}_1+m_t]\gamma^\sigma\right.$$
$$\left.(\not{q}_1+m_t)\gamma^\nu[(\not{p}_2+\not{q}_1+m_t]\gamma^\mu[-(\not{q}_2+\not{k})+m_t]\right] P_{\mu\nu\rho\sigma}$$

$$Re(\mathcal{M}_3^*\mathcal{M}_4) = \left(-\frac{1}{2}\right) f^{abc}f_{abc}\left(g_s^2\frac{y_t}{\sqrt{2}}\right) D_t^{-1}(q_1+k)D_t^{-1}(q_1+k)D_g^{-2}(p_1+p_2)Tr\left[(\not{q}_2-mt)\gamma_\beta\right.$$
$$[\not{q}_1+\not{k}+m_t](\not{q}_1+m_t)\gamma_\alpha[-(\not{q}_2+\not{k})+m_t]\gamma_\alpha]\left[\eta^{\rho\sigma}(p_1-p_2)^\beta+\eta^{\sigma\beta}(2p_2+p_1)^\rho\right.$$
$$\left.-\eta^{\beta\rho}(2p_1+p_2)^\sigma][\eta^{\mu\nu}(p_1-p_2)^\alpha+\eta^{\nu\alpha}(2p_2+p_1)^\mu-\eta^{\alpha\mu}(2p_1+p_2)^\nu]\right.$$

$$Re(\mathcal{M}_5^*\mathcal{M}_6) = \left(-\frac{2}{3}g_s^2\frac{y_t}{\sqrt{2}}\right) D_t^{-2}(p_2-q_2)D_t^{-1}(q_1+k)D_t^{-1}(q_1-p_1)Tr\left[(\not{q}_2-mt)\gamma^\sigma[\not{p}_2-\not{q}_2+m_t]\gamma^\rho\right.$$
$$\left.[\not{q}_1+\not{k}+m_t](\not{q}_1+m_t)\gamma^\mu[\not{q}_1-\not{p}_1+m_t][(\not{p}_2-\not{q}_2)+m_t]\gamma^\nu\right] P_{\mu\nu\rho\sigma}$$

$$Re(\mathcal{M}_5^*\mathcal{M}_7) = \left(-\frac{2}{3}g_s^2\frac{y_t}{\sqrt{2}}\right) D_t^{-1}(p_2-q_2)D_t^{-1}(q_1+k)D_t^{-1}(p_1-q_1)D_t^{-1}(q_2+k)Tr\left[(\not{q}_2-mt)\gamma^\sigma\right.$$
$$\left.[\not{p}_2-\not{q}_2+m_t]\gamma^\rho[\not{q}_1+\not{k}+m_t](\not{q}_1+m_t)\gamma^\mu[\not{q}_1-\not{p}_1+m_t]\gamma^\nu[-(\not{q}_2+\not{k})+m_t]\right] P_{\mu\nu\rho\sigma}$$

$$Re(\mathcal{M}_5^*\mathcal{M}_8) = \left(-\frac{2}{3}g_s^2\frac{y_t}{\sqrt{2}}\right) D_t^{-1}(p_2-q_2)D_t^{-2}(q_1+k)D_t^{-1}(p_1-q_2)Tr\left[(\not{q}_2-mt)\gamma^\sigma[\not{p}_2-\not{q}_2+m_t]\gamma^\rho\right.$$
$$\left.[\not{q}_1+\not{k}+m_t](\not{q}_1+m_t)\ \gamma^\rho[(\not{p}_1-\not{q}_2+m_t)]\gamma^\sigma[(\not{q}_1+\not{k})+m_t]\right] P_{\mu\nu\rho\sigma}$$

$$Re(\mathcal{M}_5^*\mathcal{M}_9) = \left(-\frac{2}{3}g_s^2\frac{y_t}{\sqrt{2}}\right) D_t^{-1}(p_2-q_2)D_t^{-1}(q_1+k)D_t^{-1}(p_2-q_1)D_t^{-1}(p_1-q_2)Tr\left[(\not{q}_2-mt)\gamma^\sigma\right.$$
$$\left.[\not{p}_2-\not{q}_2+m_t]\gamma^\rho[\not{q}_1+\not{k}+m_t](\not{q}_1+m_t)\gamma^\nu[\not{q}_1-\not{p}_2+m_t][(\not{p}_1-\not{q}_2)+m_t]\gamma^\mu\right] P_{\mu\nu\rho\sigma}$$

$$Re(\mathcal{M}_5^*\mathcal{M}_{10}) = \left(-\frac{2}{3}g_s^2\frac{y_t}{\sqrt{2}}\right) D_t^{-1}(p_2-q_2)D_t^{-1}(q_1+k)D_t^{-1}(q_2+k)D_t^{-1}(p_2+q_1)Tr\left[(\not{q}_2-mt)\gamma^\sigma\right.$$
$$\left.[\not{p}_2-\not{q}_2+m_t]\gamma^\rho[\not{q}_1+\not{k}+m_t](\not{q}_1+m_t)\gamma^\nu[(\not{p}_2+\not{q}_1+m_t]\gamma^\mu[-(\not{q}_2+\not{k})+m_t]\right] P_{\mu\nu\rho\sigma}$$

$$Re(\mathcal{M}_6^*\mathcal{M}_7) = \left(-\frac{2}{3}g_s^2\frac{y_t}{\sqrt{2}}\right) D_t^{-2}(q_1-p_1)D_t^{-1}(p_2-q_2)D_t^{-1}(q_1+k)Tr\left[(q\!\!\!/_2-mt)\gamma^\mu[q\!\!\!/_1-p\!\!\!/_1+m_t]\right.$$
$$\left.[(p\!\!\!/_2-q\!\!\!/_2)+m_t]\gamma^\nu(q\!\!\!/_1+m_t)\gamma^\mu[q\!\!\!/_1-p\!\!\!/_1+m_t]\gamma^\nu[-(q\!\!\!/_2+k\!\!\!/)+m_t]\right]P_{\mu\nu\rho\sigma}$$

$$Re(\mathcal{M}_6^*\mathcal{M}_8) = \left(-\frac{2}{3}g_s^2\frac{y_t}{\sqrt{2}}\right) D_t^{-1}(q_1-p_1)D_t^{-1}(p_2-q_2)D_t^{-1}(q_1+k)D_t^{-1}(p_1-q_2)Tr\left[(q\!\!\!/_2-mt)\gamma^\mu\right.$$
$$\left.[q\!\!\!/_1-p\!\!\!/_1+m_t][(p\!\!\!/_2-q\!\!\!/_2)+m_t]\gamma^\nu(q\!\!\!/_1+m_t)\gamma^\rho[(p\!\!\!/1-q\!\!\!/_2+m_t)]\gamma^\sigma[(q\!\!\!/_1+k\!\!\!/)+m_t]\right]P_{\mu\nu\rho\sigma}$$

$$Re(\mathcal{M}_6^*\mathcal{M}_9) = \left(-\frac{2}{3}g_s^2\frac{y_t}{\sqrt{2}}\right) D_t^{-1}(q_1-p_1)D_t^{-1}(q_2-p_2)D_t^{-1}(p_2-q_1)D_t^{-1}(p_1-q_2)Tr\left[(q\!\!\!/_2-mt)\gamma^\mu\right.$$
$$\left.[q\!\!\!/_1-p\!\!\!/_1+m_t][(p\!\!\!/_2-q\!\!\!/_2)+m_t]\gamma^\nu(q\!\!\!/_1+m_t)\gamma^\nu[q\!\!\!/_1-p\!\!\!/_2+m_t][(p\!\!\!/_1-q\!\!\!/_2)+m_t]\gamma^\mu\right]P_{\mu\nu\rho\sigma}$$

$$Re(\mathcal{M}_6^*\mathcal{M}_{10}) = \left(-\frac{2}{3}g_s^2\frac{y_t}{\sqrt{2}}\right) D_t^{-1}(q_1-p_1)D_t^{-1}(q_2-p_2)D_t^{-1}(q_2+k)D_t^{-1}(p_2+q_1)Tr\left[(q\!\!\!/_2-mt)\gamma^\mu\right.$$
$$\left.[q\!\!\!/_1-p\!\!\!/_1+m_t][(p\!\!\!/_2-q\!\!\!/_2)+m_t]\gamma^\nu(q\!\!\!/_1+m_t)\gamma^\nu[(p\!\!\!/_2+q\!\!\!/_1+m_t]\gamma^\mu[-(q\!\!\!/_2+k\!\!\!/)+m_t]\right]P_{\mu\nu\rho\sigma}$$

$$Re(\mathcal{M}_7^*\mathcal{M}_8) = \left(-\frac{2}{3}g_s^2\frac{y_t}{\sqrt{2}}\right) D_t^{-2}(p_1-q_1)D_t^{-1}(q_2+k)D_t^{-1}(q_1+k)Tr\left[(q\!\!\!/_2-mt)[-(q\!\!\!/_2+k\!\!\!/)+m_t]\gamma^\sigma\right.$$
$$\left.[q\!\!\!/_1-p\!\!\!/_1+m_t]\gamma^\rho(q\!\!\!/_1+m_t)\gamma^\rho[(p\!\!\!/1-q\!\!\!/_2+m_t)]\gamma^\sigma[(q\!\!\!/_1+k\!\!\!/)+m_t]\right]P_{\mu\nu\rho\sigma}$$

$$Re(\mathcal{M}_7^*\mathcal{M}_9) = \left(-\frac{2}{3}g_s^2\frac{y_t}{\sqrt{2}}\right) D_t^{-1}(p_1-q_1)D_t^{-1}(q_2+k)D_t^{-1}(p_2-q_1)D_t^{-1}(q_2+p_1)Tr\left[(q\!\!\!/_2-mt)\right.$$
$$\left.[-(q\!\!\!/_2+k\!\!\!/)+m_t]\gamma^\sigma[q\!\!\!/_1-p\!\!\!/_1+m_t]\gamma^\rho(q\!\!\!/_1+m_t)\gamma^\nu[q\!\!\!/_1-p\!\!\!/_2+m_t][(p\!\!\!/_1-q\!\!\!/_2)+m_t]\gamma^\mu\right]P_{\mu\nu\rho\sigma}$$

$$Re(\mathcal{M}_7^*\mathcal{M}_{10}) = \left(-\frac{2}{3}g_s^2\frac{y_t}{\sqrt{2}}\right) D_t^{-1}(p_1-q_1)D_t^{-2}(q_2+k)D_t^{-1}(p_2+q_1)Tr\left[(q\!\!\!/_2-mt)[-(q\!\!\!/_2+k\!\!\!/)+m_t]\right.$$
$$\left.\gamma^\sigma[q\!\!\!/_1-p\!\!\!/_1+m_t]\gamma^\rho(q\!\!\!/_1+m_t)\gamma^\nu[(p\!\!\!/_2+q\!\!\!/_1+m_t]\gamma^\mu[-(q\!\!\!/_2+k\!\!\!/)+m_t]\right]P_{\mu\nu\rho\sigma}$$

$$Re(\mathcal{M}_8^*\mathcal{M}_9) = \left(-\frac{2}{3}g_s^2\frac{y_t}{\sqrt{2}}\right) D_t^{-1}(q_1+k)D_t^{-2}(p_1-q_2)D_t^{-1}(p_2-q_1)Tr\left[(q\!\!\!/_2-mt)(q\!\!\!/_1+m_t)\right.$$
$$\left.\gamma^\nu[q\!\!\!/_1-p\!\!\!/_2+m_t][(p\!\!\!/_1-q\!\!\!/_2)+m_t]\gamma^\mu\right]P_{\mu\nu\rho\sigma}$$

$$Re(\mathcal{M}_8^*\mathcal{M}_{10}) = \left(-\frac{2}{3}g_s^2\frac{y_t}{\sqrt{2}}\right) D_t^{-1}(q_1+k)D_t^{-1}(p_1-q_2)D_t^{-1}(q_2+k)D_t^{-1}(p_2+q_1)Tr\left[(q\!\!\!/_2-mt)(q\!\!\!/_1+m_t)\right.$$
$$\left.\gamma^\nu[(p\!\!\!/_2+q\!\!\!/_1+m_t]\gamma^\mu[-(q\!\!\!/_2+k\!\!\!/)+m_t]\right]P_{\mu\nu\rho\sigma}$$

$$Re(\mathcal{M}_9^*\mathcal{M}_{10}) = \left(-\frac{2}{3}g_s^2\frac{y_t}{\sqrt{2}}\right) D_t^{-1}(p_2-q_1)D_t^{-1}(p_1-q_2)D_t^{-1}(q_2+k)D_t^{-1}(p_2+q_1)Tr\left[(\not{q}_2 - mt)\gamma^\rho \right.$$
$$\left.[(\not{p}_1 - \not{q}_2 + m_t)][\not{q}_1 - \not{p}_2 + m_t]\gamma^\sigma(\not{q}_1 + m_t)\gamma^\nu[(\not{p}_2 + \not{q}_1 + m_t]\gamma^\mu[-(\not{q}_2 + \not{k}) + m_t]\right] P_{\mu\nu\rho\sigma}$$

(B.4)

where we used that $Tr[t^a t^b t_a t_b] = -\frac{2}{3}$ and defined $P_{\mu\nu\rho\sigma} = \sum_{\lambda_1\lambda_2}\epsilon_\mu(\lambda_1,p)\epsilon_\nu(\lambda_2,q)\bar{\epsilon}_\rho(\lambda_1,p)\bar{\epsilon}_\sigma(\lambda_2,q)$. In order to obtain the cross section one can now perform the traces in FORM and use a simple generalization of the code in appendix C.2 . For the integration over the parton distribution functions one can install the LHAPDF package and obtain the PDFs from there. In principle all the conditions are met for constructing an event generator that computes the hadronic cross-section $\sigma(pp \to t\bar{t}H)$.

C Codes

C.1. Higgs decay to two photons through W-loop

C.1.1 Calculation of $\mathcal{M}^{\rho}_{\rho}$

```
*---------------------------------------------------------
* Calculation of H->2*photons via W boson loop
* Result using the algebraic manipulation program FORM
*
*--------------------Declarations-----------------------------
Symbol m, d, D1, D2, D3, mh, n, A0;
Symbol P2, P3, P12, P13, P23, P123;
Vector p q k;
Index mu=n nu=n, a1=n, a2=n, a3=n, b1=n, b2=n, b3=n;
T prop1, prop2, prop3, V3mu, V3nu, V4munu,VH;
*---------------------------------------------------------------


Off statistics;


***Amplitude***

Local diag1=d_(mu,nu)*(prop2(a1,b1)*V3mu(b1,a2,mu)*prop1(a2,b2)*V3nu(b2,a3,nu)
    *p
rop3(a3,b3)*VH(b3,a1));

Local diag2= d_(mu,nu)*(prop2(a1,b1)*V4munu(b1,a2,mu,nu)*prop3(a2,b2)*VH(b2,a1
    ))
;


Local Tot=2*diag1-diag2;
```

```
***Feynman Rules***

**Propagators**
id prop1(mu?,nu?) = (d_(mu,nu)-(k(mu)*k(nu)/m^2))/D1;
id prop2(mu?,nu?) = (d_(mu,nu)-(k(mu)+p(mu))*(k(nu)+p(nu))/m^2)/D2;
id prop3(mu?,nu?) =(d_(mu,nu)-(k(mu)-q(mu))*(k(nu)-q(nu))/m^2)/D3;


**Vertices**
id V3mu(a1?,a2?,mu?)=(d_(a1,a2)*(2*k(mu)+p(mu))+ d_(a2,mu)*(p(a1)-k(a1))-d_(mu
    ,a
1)*(2*p(a2)+k(a2)));

id V3nu(a1?,a2?,mu?)=(d_(a1,a2)*(2*k(mu)-q(mu))+ d_(a2,mu)*(2*q(a1)-k(a1))-d_(
    mu
,a1)*(q(a2)+k(a2)));

id V4munu(a1?,a2?,mu?,nu?)=(2*d_(a1,a2)*d_(mu,nu)-d_(a1,mu)*d_(a2,nu)-d_(a1,nu
    )*
d_(a2,mu));

id VH(a1?,a2?)=d_(a1,a2);


**On shell momenta**
id p.p=0;
id q.q=0;


**Express the momenta as a function of the denominators**
id k.p= (D2-D1)/2;
id k.q= -(D3-D1)/2;
id p.q= (mh^2)/2;
id k.k= D1+m^2;



**Rewriting of factors**

*Placeholder for D1^-1*D2^-1*D3^-1*
id D1^-1*D2^-1*D3^-1=P123;
```

```
**Placeholder for the D2^2 and D3^2 terms**
id D2^2*D1^-1*D3^-1=P2;
id D3^2*D1^-1*D2^-1=P3;


**simplify D3, D2 and D1 factors**

id D1*D2^-1*D3^-1 = A0 - mh^2/2 * D2^-1*D3^-1;
id D2*D1^-1*D3^-1=  A0 + mh^2/2 * D1^-1*D3^-1;
id D3*D1^-1*D2^-1=  A0 + mh^2/2 * D1^-1*D2^-1;


** Placeholder **
id D1^-1*D2^-1       = P12;
id D1^-1*D3^-1       = P13;
id D2^-1*D3^-1       = P23;

*Simplify remaining factors*

id D2*D1^-1=D1*D2^-1;
id D1*D2^-1=0;

id D3*D1^-1= D1*D3^-1;
id D1*D3^-1=0;


id D3*D2^-1=D2*D3^-1;
id D2*D3^-1=mh^2*D1^-1;


id D1^-1=A0;
id D2^-1=A0;
id D3^-1=A0;


*Revert all the Placeholders*

id P2=D2^2*D1^-1*D3^-1;
id P3=D3^2*D1^-1*D2^-1;

id P123 = D1^-1*D2^-1*D3^-1;
id P12  = D1^-1*D2^-1;
```

```
  id P13  = D1^-1*D3^-1;
  id P23  = D2^-1*D3^-1;



  b D1 D2 D3 A0;

  Print  Tot;
  .end

 Tot =
     + D1^-1*D2^-1*D3^-1 * (  - 1/4*m^-4*mh^6 + 1/2*m^-2*mh^4 + 13*mh^2 - 9*
       mh^2*n - 8*m^2 + 8*m^2*n )

     + D1^-1*D2^-1 * (  - 2 + 5/8*m^-4*mh^4 + m^-2*mh^2 + 2*n )

     + D1^-1*D2^-1*D3^2 * (  - 1/2*m^-4 )

     + D1^-1*D3^-1 * (  - 2 + 5/8*m^-4*mh^4 + m^-2*mh^2 + 2*n )

     + D1^-1*D2^2*D3^-1 * (  - 1/2*m^-4 )

     + D2^-1*D3^-1 * (  - 4 + 1/16*m^-6*mh^6 - 3/8*m^-4*mh^4 + 2*m^-2*mh^2
        - m^-2*mh^2*n + 6*n - 2*n^2 )

     + A0 * (  - 1/4*m^-6*mh^4 + 2*m^-4*mh^2 )

     - 1/4*m^-6*mh^2 + m^-4 - m^-4*n;

0.12 sec out of 0.13 sec
```

C.1.2 Calculation of $q^\lambda \mathcal{M}_{\lambda\tau} p^\tau$

```
*---------------------------------------------------------------
* Calculation of H->2*photons via W boson loop
* Result using the algebraic manipulation program FORM
*
*--------------------Declarations-------------------------------
Symbol m, d, D1, D2, D3, mh, n, A0;
Symbol P2, P3, P12, P13, P23, P123;
Vector p q k;
Index mu=n nu=n, a1=n, a2=n, a3=n, b1=n, b2=n, b3=n;
T prop1, prop2, prop3, V3mu, V3nu, V4munu,VH;
*---------------------------------------------------------------

Off statistics;


***Amplitude***

Local diag1=d_(mu,nu)*(prop2(a1,b1)*V3mu(b1,a2,mu)*prop1(a2,b2)*V3nu(b2,a3,nu)
    *p
rop3(a3,b3)*VH(b3,a1));

Local diag2= d_(mu,nu)*(prop2(a1,b1)*V4munu(b1,a2,mu,nu)*prop3(a2,b2)*VH(b2,a1
    ))
;


Local Tot=2*diag1-diag2;



***Feynman Rules***

**Propagators**
id prop1(mu?,nu?) = (d_(mu,nu)-(k(mu)*k(nu)/m^2))/D1;
id prop2(mu?,nu?) = (d_(mu,nu)-(k(mu)+p(mu))*(k(nu)+p(nu))/m^2)/D2;
id prop3(mu?,nu?) =(d_(mu,nu)-(k(mu)-q(mu))*(k(nu)-q(nu))/m^2)/D3;


**Vertices**
id V3mu(a1?,a2?,mu?)=(d_(a1,a2)*(2*k(mu)+p(mu))+ d_(a2,mu)*(p(a1)-k(a1))-d_(mu
    ,a
```

```
1)*(2*p(a2)+k(a2)));

id V3nu(a1?,a2?,mu?)=(d_(a1,a2)*(2*k(mu)-q(mu))+ d_(a2,mu)*(2*q(a1)-k(a1))-d_(
    mu
,a1)*(q(a2)+k(a2)));

id V4munu(a1?,a2?,mu?,nu?)=(2*d_(a1,a2)*d_(mu,nu)-d_(a1,mu)*d_(a2,nu)-d_(a1,nu
    )*
d_(a2,mu));

id VH(a1?,a2?)=d_(a1,a2);


**On shell momenta**
id p.p=0;
id q.q=0;


**Express the momenta as a function of the denominators**
id k.p= (D2-D1)/2;
id k.q= -(D3-D1)/2;
id p.q= (mh^2)/2;
id k.k= D1+m^2;



**Rewriting of factors**

*Placeholder for D1^-1*D2^-1*D3^-1*
id D1^-1*D2^-1*D3^-1=P123;

**Placeholder for the D2^2 and D3^2 terms**
id D2^2*D1^-1*D3^-1=P2;
id D3^2*D1^-1*D2^-1=P3;


**simplify D3, D2 and D1 factors**

id D1*D2^-1*D3^-1 = A0 - mh^2/2 * D2^-1*D3^-1;
id D2*D1^-1*D3^-1=  A0 + mh^2/2 * D1^-1*D3^-1;
id D3*D1^-1*D2^-1=  A0 + mh^2/2 * D1^-1*D2^-1;
```

```
** Placeholder **
id D1^-1*D2^-1       = P12;
id D1^-1*D3^-1       = P13;
id D2^-1*D3^-1       = P23;

*Simplify remaining factors*

id D2*D1^-1=D1*D2^-1;
id D1*D2^-1=0;

id D3*D1^-1= D1*D3^-1;
id D1*D3^-1=0;


id D3*D2^-1=D2*D3^-1;
id D2*D3^-1=mh^2*D1^-1;


id D1^-1=A0;
id D2^-1=A0;
id D3^-1=A0;


*Revert all the Placeholders*

id P2=D2^2*D1^-1*D3^-1;
id P3=D3^2*D1^-1*D2^-1;

id P123 = D1^-1*D2^-1*D3^-1;
id P12  = D1^-1*D2^-1;
id P13  = D1^-1*D3^-1;
id P23  = D2^-1*D3^-1;



b D1 D2 D3 A0;

Print  Tot;
.end

Tot =
```

```
      + D1^-1*D2^-1*D3^-1 * (  - 1/4*m^-4*mh^6 + 1/2*m^-2*mh^4 + 13*mh^2 - 9*
        mh^2*n - 8*m^2 + 8*m^2*n )

      + D1^-1*D2^-1 * (  - 2 + 5/8*m^-4*mh^4 + m^-2*mh^2 + 2*n )

      + D1^-1*D2^-1*D3^2 * (  - 1/2*m^-4 )

      + D1^-1*D3^-1 * (  - 2 + 5/8*m^-4*mh^4 + m^-2*mh^2 + 2*n )

      + D1^-1*D2^2*D3^-1 * (  - 1/2*m^-4 )

      + D2^-1*D3^-1 * (  - 4 + 1/16*m^-6*mh^6 - 3/8*m^-4*mh^4 + 2*m^-2*mh^2
         - m^-2*mh^2*n + 6*n - 2*n^2 )

      + A0 * (  - 1/4*m^-6*mh^4 + 2*m^-4*mh^2 )

      - 1/4*m^-6*mh^2 + m^-4 - m^-4*n;

0.12 sec out of 0.13 sec
```

C.1.3 Dimensional Regularization

```
*---------------------------------------------------------------
* Calculation of H->2*photons via W boson loop
* Result using the algebraic manipulation program FORM
*
*--------------------Declarations-------------------------------
Symbol m, D1, D2, D3, mh, n;
Symbol [B0(1,2)] [B0(1,3)] [B0(2,3)];
Symbol C0, B0, A0;
Symbol epsi;
Symbol pi;

Vector p q k;
Index mu=n nu=n, a1=n, a2=n, a3=n, b1=n, b2=n, b3=n;
*---------------------------------------------------------------

Off statistics;



**Ampi are the Mi including the factor and polarizations**

g Amptrace= + D1^-1*D2^-1*D3^-1 * (  - 1/4*m^-4*mh^6 + 1/2*m^-2*mh^4 + 13*mh^2
     -
 9*
        mh^2*n - 8*m^2 + 8*m^2*n )

       + D1^-1*D2^-1 * (  - 2 + 5/8*m^-4*mh^4 + m^-2*mh^2 + 2*n )

       + D1^-1*D2^-1*D3^2 * (  - 1/2*m^-4 )

       + D1^-1*D3^-1 * (  - 2 + 5/8*m^-4*mh^4 + m^-2*mh^2 + 2*n )

       + D1^-1*D2^2*D3^-1 * (  - 1/2*m^-4 )

       + D2^-1*D3^-1 * (  - 4 + 1/16*m^-6*mh^6 - 3/8*m^-4*mh^4 + 2*m^-2*mh^2
          - m^-2*mh^2*n + 6*n - 2*n^2 )

       + A0 * (  - 1/4*m^-6*mh^4 + 2*m^-4*mh^2 );
```

```
g Ampmomenta=  + D1^-1*D2^-1*D3^-1 * (  - 1/8*m^-4*mh^8 + 1/4*m^-2*mh^6 - 7/2*
    mh
^4 - 1/
         2*mh^4*n )

       + D1^-1*D2^-1 * ( 5/16*m^-4*mh^6 + 1/2*m^-2*mh^4 - mh^2 + mh^2*n )

       + D1^-1*D2^-1*D3^2 * (  - 1/4*m^-4*mh^2 )

       + D1^-1*D3^-1 * ( 5/16*m^-4*mh^6 + 1/2*m^-2*mh^4 - mh^2 + mh^2*n )

       + D1^-1*D2^2*D3^-1 * (  - 1/4*m^-4*mh^2 )

       + D2^-1*D3^-1 * ( 1/32*m^-6*mh^8 - 3/16*m^-4*mh^6 - m^-2*mh^4 + 2*mh^2
          - 2*mh^2*n )

       + A0 * (  - 1/8*m^-6*mh^6 + m^-4*mh^4 );


g Sum = (Amptrace-2/mh^2 *Ampmomenta);
g Total=  (1+epsi+epsi^2)/mh^2 *Sum;

b D1, D2, D3;
Print Sum;

.sort

Sum =
   + D1^-1*D2^-1*D3^-1 * ( 20*mh^2 - 8*mh^2*n - 8*m^2 + 8*m^2*n )

   + D2^-1*D3^-1 * (  - 8 + 4*m^-2*mh^2 - m^-2*mh^2*n + 10*n - 2*n^2 );


**Dimensional Regularization**

***Scalar Integrals***

**C0**
id D1^-1*D2^-1*D3^-1=C0;
```

```
** D2^2*D1^-1*D3^-1 integral**
*id D2^2*D1^-1*D3^-1= 2*mh^2*A0+i_*mh^2/(48*pi^2)*epsi^-1;

**D3^2*D1^-1*D2^-1 integral**
*id D3^2*D1^-1*D2^-1= 2*mh^2*A0+i_*mh^2/(48*pi^2)*epsi^-1;

**B0(1,2)**
id D1^-1*D2^-1=[B0(1,2)];

**B0(1,3)**
id D1^-1*D3^-1=[B0(1,3)];

**B0(2,3)**
id D2^-1*D3^-1=[B0(2,3)];

** Kinematic relations**
id p.p=0;
id q.q=0;
id p.q=(mh^2) /2;



**Dimensional regularization**
id n=4-2*epsi;

**C0 is finite**
id epsi*C0=0;

**B0 have a first order pole**

id epsi*[B0(1,2)]=i_/(16*pi^2);
id epsi*[B0(1,3)]=i_/(16*pi^2);
id epsi*[B0(2,3)]=i_/(16*pi^2);



**set epsilon to 0**
id epsi=0;


b C0, D2, D3, D1;
```

```
 Print +s Total;


Total =

    + C0 * (
       - 12
       + 24*m^2*mh^-2
       )

    + 1/8*i_*m^-2*pi^-2
    + 3/4*i_*mh^-2*pi^-2
      ;

  .end
0.00 sec out of 0.00 sec
```

C.2. Monte Carlo integration: $q\bar{q} \to t\bar{t}H$

```
#include <iostream>
#include <cstdlib>
#include <ctime>
#include <vector>
#include <math.h>

using namespace std;

//Define energy of the CM squared
long double shat=14000*14000;


//Define parameters for this process
long double mt=173;
long double mh=125;
long double alphas=0.118;
long double v=246;
long double GF=1.16639*0.00001;
long double m1=mt;
long double m2=mt;
long double m3=mh;
long double modk2old;
long double modk3old;

//Define auxilliary variables to compute the uncertainty
long double var;
long double var1=0;
long double var2=0;


//Define external momenta as global variables
vector<long double> k1 (4);
vector<long double> k2 (4);
vector<long double> k3 (4);

vector<long double> p1 (4);
vector<long double> p2 (4);

// Lambda function
long double lambda (long double x, long double y, long double z )
```

```
{
  return x*x+y*y+z*z-2.*x*y-2.*x*z-2.*y*z;
}

//Function that returns a random number between 0 and 1
long double random_number()
{
  return ((long double) rand() / ((long double)RAND_MAX));
}

//Define a dot product function
long double dot(vector<long double> a, vector<long double> b)
{
  return a[0]*b[0]-a[1]*b[1]-a[2]*b[2]-a[3]*b[3];
}


//Define denominator of top propagator
long double top_denominator(vector<long double> a, vector<long double> b, int sign
    ){

  long double x;

  if(sign==1)
   x= dot(a,a)+dot(b,b)+2.*dot(a,b)-mt*mt;
 else if (sign==-1)
   x= dot(a,a)+dot(b,b)-2.*dot(a,b)-mt*mt;
 else cout<<"Error in the code"<<endl;

 return 1./x;
}

long double gluon_denominator(vector<long double> a, vector<long double> b)
{

  long double x= dot(a,a)+dot(b,b) +2.*dot(a,b);
  return 1./x;
}

//qq->tt~h amplitude squared
long double incoming_quark_amp_squared(vector<long double> q1, vector<long double>
     q2, vector<long double> k )
```

```
{
  long double m1squared;
  long double m2squared;
  long double m1m2;
  long double ampsquared;

  m1squared= mt*mt*mh*mh*shat
  + 4.*mt*mt*mt*mt*shat
  - 2.*dot(p1,q1)*dot(p2,q2)*mh*mh
  + 8.*dot(p1,q1)*dot(p2,q2)*mt*mt
  - 2.*dot(p1,q2)*dot(p2,q1)*mh*mh
  + 8.*dot(p1,q2)*dot(p2,q1)*mt*mt
  + 4.*dot(p1,q2)*dot(p2,k)*dot(q1,k)
  + 8.*dot(p1,q2)*dot(p2,k)*mt*mt
  + 4.*dot(p1,k)*dot(p2,q2)*dot(q1,k)
  + 8.*dot(p1,k)*dot(p2,q2)*mt*mt
  + 4.*dot(q1,k)*mt*mt*shat;

  m2squared=  mt*mt*mh*mh*shat
  + 4.*mt*mt*mt*mt*shat
  - 2.*dot(p1,q1)*dot(p2,q2)*mh*mh
  + 8.*dot(p1,q1)*dot(p2,q2)*mt*mt
  + 4.*dot(p1,q1)*dot(p2,k)*dot(q2,k)
  + 8.*dot(p1,q1)*dot(p2,k)*mt*mt
  - 2.*dot(p1,q2)*dot(p2,q1)*mh*mh
  + 8.*dot(p1,q2)*dot(p2,q1)*mt*mt
  + 4.*dot(p1,k)*dot(p2,q1)*dot(q2,k)
  + 8.*dot(p1,k)*dot(p2,q1)*mt*mt
  + 4.*dot(q2,k)*mt*mt*shat;

  m1m2= + 4.*mt*mt*mt*mt*shat
  - 2.*dot(p1,q1)*dot(p2,q2)*mh*mh
  + 8.*dot(p1,q1)*dot(p2,q2)*mt*mt
  + 2.*dot(p1,q1)*dot(p2,k)*dot(q2,k)
  + 4.*dot(p1,q1)*dot(p2,k)*mt*mt
  - 2.*dot(p1,q2)*dot(p2,q1)*mh*mh
  + 8.*dot(p1,q2)*dot(p2,q1)*mt*mt
  + 2.*dot(p1,q2)*dot(p2,k)*dot(q1,k)
  + 4.*dot(p1,q2)*dot(p2,k)*mt*mt
  + 2.*dot(p1,k)*dot(p2,q1)*dot(q2,k)
  + 4.*dot(p1,k)*dot(p2,q1)*mt*mt
  + 2.*dot(p1,k)*dot(p2,q2)*dot(q1,k)
```

```
  + 4.*dot(p1,k)*dot(p2,q2)*mt*mt
  - 4.*dot(p1,k)*dot(p2,k)*dot(q1,q2)
  + 4.*dot(p1,k)*dot(p2,k)*mt*mt
  + dot(q1,q2)*mh*mh*shat
  + 2.*dot(q1,k)*mt*mt*shat
  + 2.*dot(q2,k)*mt*mt*shat;

  ampsquared= 8./9. * M_PI*M_PI *alphas*alphas*mt*mt*sqrt(2)*GF*gluon_denominator(
      p1,p2)*gluon_denominator(p1,p2)* (

    16.*top_denominator(q1,k,1)*top_denominator(q1,k,1)*m1squared +
    16.*top_denominator(q2,k,1)*top_denominator(q2,k,1)*m2squared +
    2.*16.*top_denominator(q1,k,1)*top_denominator(q2,k,1)*m1m2
    );

  return ampsquared;
}

//Function that generates an event k1, k2 and k3
void generate_event()
{

    //Define auxilliary virtual momenta
  vector<long double> Q1 (4);
  vector<long double> Q2 (4);
  vector<long double> Q3 (4);

//Define and initialize array of 3 random numbers for each particle
  vector<long double> x1 (3);
  vector<long double> x2 (3);
  vector<long double> x3 (3);

  for(int i=0; i<3; ++i)
  {
    x1[i]=random_number();
    x2[i]=random_number();
    x3[i]=random_number();
  }


//Define auxiliary mass variables
  long double s1= m1+m2+m3;
```

```
  long double s2= m2+m3;
  long double s3= m3;
  long double mQ1=sqrt(shat);
  long double mQ2;
  long double mQ3;

//Define boost variables - from Q2 to CM frame
  long double gamma;
  long double beta;
  long double modn;
  vector<long double> n (3);

//Define auxiliary variable for boost
  long double kpara;
  long double k2Eold;
  long double k3Eold;
  vector<long double> kperp (3);

//Define the module of spatial momenta

  long double modk1;
  long double modk2;
  long double modk3;

//Define phi and cosine theta for the three particles
  long double phi1=2.*M_PI*x1[0];
  long double phi2=2.*M_PI*x2[0];
  long double phi3=2.*M_PI*x3[0];

  long double costheta1 =1.- 2.*x1[1];
  long double costheta2 =1.- 2.*x2[1];
  long double costheta3 =1.- 2.*x3[1];

//Initialize labframe momentum Q1
  Q1[0]=sqrt(shat);
  for(int i=1; i<4; ++i) Q1[i]=0;


/*** Start computing momenta  ***/

//  Determine module of spatial vector k1
```

```
    mQ2= s2 + x1[2]*(mQ1-s1);

  modk1= sqrt( lambda(mQ1*mQ1, m1*m1, mQ2*mQ2) )/(2.*mQ1);

//Obtain the energy of k1

  k1[0]=sqrt( modk1*modk1 + m1*m1  );

// Obtain the spatial components of k1

  k1[1]= modk1*sqrt(1.-costheta1*costheta1)*cos(phi1);
  k1[2]= modk1*sqrt(1.-costheta1*costheta1)*sin(phi1);
  k1[3]= modk1*costheta1;

//No boost necessary for this step - we are in Q1's reference frame

//Obtain Q2 by momentum conservation
  for(int i=0; i<4 ; ++i) Q2[i]=Q1[i]-k1[i];

//Now we obtain k2 and k3, in Q2's reference frame

//Compute mQ2 by squaring Q2
    mQ2= sqrt( Q2[0]*Q2[0]-(Q2[1]*Q2[1]+Q2[2]*Q2[2]+Q2[3]*Q2[3]) );

//Compute modk2 and modk3

  modk2=sqrt( lambda(mQ2*mQ2, m2*m2, m3*m3) )/(2.*mQ2);
  modk3=modk2;

  modk2old=modk2;
  modk3old=modk3;

//Obtain energy of k2 and k3
  k2[0]=sqrt( modk2*modk2 + m2*m2  );
  k3[0]=sqrt( modk3*modk3 + m3*m3  );


//Obtain spatial components of k2 and k3

  k2[1]= modk2*sqrt(1.-costheta2*costheta2)*cos(phi2);
  k2[2]= modk2*sqrt(1.-costheta2*costheta2)*sin(phi2);
  k2[3]= modk2*costheta2;
```

```
//In the restframe of Q2 spatial vector k3= - spatial vector k2
  for (int i=1; i<4; ++i) k3[i]=-k2[i];


//Boost k2 back to the CM frame

//Initialize boost parameters
    gamma=Q2[0]/mQ2;
  beta=sqrt(Q2[1]*Q2[1]+Q2[2]*Q2[2]+Q2[3]*Q2[3])/Q2[0];


//Define unit vector in the direction of boost

  long double modQ2=sqrt(Q2[1]*Q2[1]+Q2[2]*Q2[2]+Q2[3]*Q2[3]);
  for(int i=0; i<3; ++i) n[i]=Q2[i+1]/modQ2;

    modn=0;
  for (int i = 0; i < 3; ++i) modn+=n[i]*n[i];

    modn=sqrt(modn);

//Evaluate kparallel

  kpara=0;

  for (int i = 0; i < 3; ++i)
    kpara+= n[i]*k2[i+1];

//Define kperp, which will remain invariant
  for(int i=0; i<3; ++i) kperp[i]=k2[i+1]-kpara*n[i];

//Store energy of k2 in current frame
    k2Eold=k2[0];

//Energy of k2 in CM frame
  k2[0]=gamma*(k2[0]+beta*kpara);

//Boost kpara
  kpara=gamma*(kpara+beta*k2Eold);

//Get k2 in the lab frame
```

```
  for(int i=0; i<3; ++i)
    k2[i+1]=kpara*n[i]+kperp[i];

//Repeat the procedure for k3
//Evaluate kparallel
  kpara=0;

  for (int i = 0; i < 3; ++i)
    kpara+= n[i]*k3[i+1];

//Define kperp, which will remain invariant
  for(int i=0; i<3; ++i) kperp[i]=k3[i+1]-kpara*n[i];

//Store energy of k3 in current frame
    k3Eold=k3[0];

//Energy of k2 in CM frame
  k3[0]=gamma*(k3[0]+beta*kpara);

//Boost kpara
  kpara=gamma*(kpara+beta*k3Eold);

//Get k3 in the lab frame
  for(int i=0; i<3; ++i)
    k3[i+1]=kpara*n[i]+kperp[i];
/** End of the generation of events**/
}

long double monte_carlo_point()
{
  long double modk1=sqrt(k1[1]*k1[1]+k1[2]*k1[2]+k1[3]*k1[3]);

  long double sqrtshat= sqrt(shat);

  long double factor=1./(16.*M_PI*M_PI*M_PI)*modk1*modk2old*(sqrtshat-m1-m2-m3)/
     sqrtshat;

  long double contribution;

  contribution=  factor*incoming_quark_amp_squared(k1,k2,k3);

  var1+=contribution*contribution;
```

```
  return contribution;
}


int main()
{

//time seed for random numbers
  srand(time(NULL));

//Number of events to compute the integral
  long double nevents=100000;
  long double integral=0;
  long double crosssection;

//initialize incoming momenta
  p1[0]=sqrt(shat)/2.;
  p1[3]=sqrt(shat)/2.;

  p2[0]=sqrt(shat)/2.;
  p2[3]=-sqrt(shat)/2.;

//Cycle that computes the integral
  for(int i=0; i<nevents; ++i)
  {
    generate_event();

    integral+=monte_carlo_point();
    if(i%1000==0) cout<<"i: "<<i<<"  INTEGRAL:"<<integral<<endl;
  }

//Estimation of the integral
  integral=integral/nevents;

    //Error of the Monte Carlo integration
  var1=var1/nevents;
  var2=integral*integral;
  var=var1-var2;
  var=sqrt(var/nevents);
```

```
//Conversion factor from GeV to pb
  double convfactor=3.894*100000000.;

//Obtain and print value of the cross section and corresponding error
  crosssection= convfactor*integral/(2.*shat);
  var*=convfactor/(2.*shat);
  cout<<"The value of the integral for "<<nevents<<" events was "<< integral<<endl
      ;
  cout<<"The cross section is: "<<crosssection<<"+FFF"<<var<<" pb"<<endl;

  return 0;
}
```

Bibliography

[1] B. De Wit, E. Laenen, and J. Smith, *Field Theory in Particle Physics*. 2015.

[2] M. Peskin and D. Schroeder, *An introduction To Quantum Field Theory*. 1995.

[3] M. D. Schwartz, *Quantum field theory and the Standard Model*. 2010.

[4] M. Thomson, *Modern Particle Physics*. 2013.

[5] M. Srednicki, *Quantum Field Theory*. 2006.

[6] H. W. Merk, M and I. Vulpen, *Particle Physics 1 Lecture Notes*. 2016.

[7] C. F. Uhlemann and N. Kauer, "Narrow-width approximation accuracy," *Nuclear Physics B*, vol. 814, no. 1-2, pp. 195–211, 2009.

[8] A. Denner and S. Dittmaier, "The complex-mass scheme for perturbative calculations with unstable particles," *Nuclear Physics B - Proceedings Supplements*, vol. 160, pp. 22–26, 2006.

[9] A. Denner, "Techniques for calculation of electroweak radiative corrections at the one loop level and results for W physics at," *LEP200, Fortschr. Phys.*, vol. 41, pp. 307–420, 1993.

[10] A. Denner, S. Dittmaier, M. Roth, and D. Wackeroth, "Predictions for all processes e^+e^- -> 4 fermions + gamma," no. April 1999, p. 32, 1999.

[11] A. Denner, S. Heinemeyer, I. Puljak, D. Rebuzzi, and M. Spira, "Standard model Higgs-boson branching ratios with uncertainties," *European Physical Journal C*, vol. 71, no. 9, pp. 1–29, 2011.

[12] A. Denner and J.-N. Lang, "The Complex-Mass Scheme and Unitarity in perturbative Quantum Field Theory," no. April, 2014.

[13] U. Baur and D. Zeppenfeld, "Finite width effects and gauge invariance in radiative W production and decay," no. March, 1995.

[14] J. Alwall, M. F. Herquet, M., O. Mattelaer, and T. Stelzer, *MadGraph 5 : Going Beyond*. 2011.

[15] J. Vermaseren, J. Kuipers, B. Ruijl, M. Tentyukov, T. Ueda, and J. Vollinga, *FORM version 2.4 Reference manual*. 2017.

[16] M. Carena, C. Grojean, M. Kado, and V. Sharma, "Status of Higgs Boson Physics - Particle Data Group," vol. 100001, no. May, p. 136, 2016.

[17] K. e. a. Nakamura, "Review of Particle Physics - Particle Data Group," *J. Physics G*, no. 37.

[18] J. Ellis, "Higgs Physics," *arXiv.org*, vol. hep-ph, no. 3, p. 52, 2013.

[19] T. Plehn, *Lectures on LHC physics*, vol. 886. 2015.

[20] S. Bentvelsen, E. Laenen, and P. Motylinski, "Higgs production through gluon fusion at leading order," 2005.

[21] Z. C. Marciano, W. J. and S. Willenbrock, "Higgs Decay to Two Photons," *Physics*, 2011.

[22] B. P. Kersevan and E. Richter-Was, "Improved Phase Space Treatment of Massive Multi-Particle Final States," pp. 1–17, 2004.

[23] A. Papaefstathiou, *How to write your own Monte Carlo event generator*. 2015.